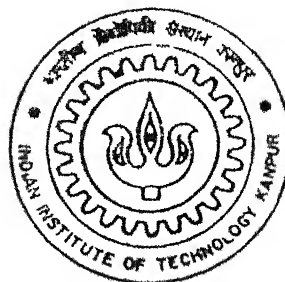


Y110604.

ACTIVE BRAZING OF STAINLESS STEEL AND CERAMIC

By

Devraj Chattaraj



DEPARTMENT OF MATERIALS AND METALLURGICAL ENGINEERING

Indian Institute of Technology Kanpur

FEBRUARY, 2003

TH
mmf/2003/m
C392a

ACTIVE BRAZING OF STAINLESS STEEL AND CERAMIC

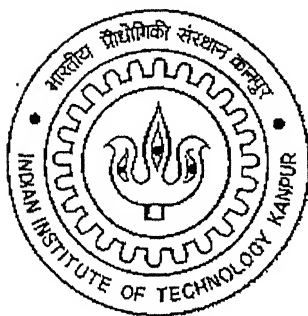
A Thesis Submitted

In Partial Fulfillment of the Requirements
for the Degree of

MASTER OF TECHNOLOGY

by

DEVRAJ CHATTARAJ



to the

**DEPARTMENT OF MATERIALS AND METALLURGICAL ENGINEERING
INDIAN INSTITUTE OF TECHNOLOGY KANPUR**

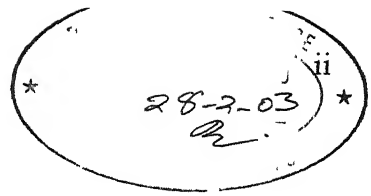
February, 2003

3 JUN 2003

पुरुषोत्तम काशी हिन्दू विश्वविद्यालय
भारतीय प्रौद्योगिकी विभाग, बनारस
अवधि क्र० A ... 143516



CERTIFICATE



It is certified that the work contained in the thesis entitled "*Active Brazing of Stainless Steel and Ceramic*", by Devraj Chattaraj has been carried out under my supervision and that this work has not been submitted elsewhere for a degree

28/2/03

February, 2003

NKS ~

(Dr. N. K. Batra)

Department of Materials & Metallurgical Engineering
I.I.T. Kanpur.

ACKNOWLEDGEMENT

I gratefully acknowledge my indebtedness and sincere thanks to Dr. N. K. Batra, Professor, Department of Materials and Metallurgical Engineering, for his valuable guidance, timely suggestions and painstaking efforts during the course of my work. I will always be thankful to him for providing me the opportunity to work with him. It was indeed, a great pleasure and privilege to have worked with him. Without his constant encouragement, warmth and affection this work would not have been possible.

I also extend my thanks and gratitude to Mr. K. S. Tripathi and Mr. Surendra Agnihotri, for providing with me valuable information and extending their kind cooperation at every stage of my work.

I take this opportunity to thank other faculty and staff of Department of materials and metallurgical engineering, especially Dr. S. P. Gupta, Dr. M. N. Mungole, for their in time help and support in carrying out this work.

I am obliged to all my friends for making the ambient so congenial that it was pleasure staying at campus and for giving necessary help in my work. I pay my special thanks to Gopi and Sankar. I also express my acknowledgement to all, who directly or indirectly helped me.

(DEVRAJ CHATTARAJ)

dedicated to my parents.....

ABSTRACT

The advancement in technology has led to lot of interest in ceramic to ceramic as well as ceramic to metal joining to derive advantages of specific properties of ceramics such as high wear resistance, high melting point and low electrical conductivity etc. By far, the simplest method is to use an activated brazing alloy. It cuts out several processing steps when compared with the premetallizing process. Alumina, silicon carbide, silicon nitride, graphite, diamond and many other ceramic materials can be successfully brazed using active braze alloys. More and more filler metals, which can operate above 1050°C , are increasingly being sought after to make ceramic – metal seals in various applications such as advanced engines, electronic tubes etc.

The present work concerns with the study of wetting and bonding behavior of different types of brazing alloys in joining of metal to metal, metal to ceramic and ceramic to ceramic. In this work, an attempt has been made to study the mechanical testing of the brazing alloys and the brazed test samples. Seven types of brazing alloys, namely, Ag – 28 Cu, Ag – 27.4 Cu – 2 Ti, Ag – 26.6 Cu – 5 Ti, Ag – 1 Ti, Ag – 2 Ti, Cu – 1 Ti and Cu – 2 Ti were prepared. Ti was used as an active element. Wetting and bonding experiments were carried out above 1000°C in air as well as in vacuum of 0.013 atmosphere. It could be demonstrated that by increasing the Ti content of the brazing alloy, the wetting behavior of stainless steel and alumina could be enhanced. Presence of Ti in the braze filler metal resulted in an improvement in the strength of the filler metal as well as that of bonded stainless steel rods.

CONTENTS

| | |
|-----------------------------------|-----|
| Certificate. | ii |
| Acknowledgement. | iii |
| Abstract. | v |
| List of Figures | ix |
| List of Tables. | xii |
| Chapter 1: Introduction. | 1 |
| Chapter 2: Literature Review. | 5 |
| 2.1: Brazing. | |
| 2.1.1: Definition of Brazing. | |
| 2.1.2: Key Parameters of Brazing. | |
| Contact Angle and Wetting. | |
| Wettability Index. | |
| Capillary Attraction. | |
| 2.1.3: Brazing Considerations. | |
| Joining Atmosphere. | |
| Vacuum Brazing. | |
| Temperature and Time. | |
| Joint Design and Clearance. | |
| Heating Rate. | |
| Braze Fixturing. | |
| Braze Interlayer. | |

2.1.4: High Temperature Brazing.

2.1.5: Filler Metal – Parent Metal Interaction.

2.2. Ceramic Joining.

2.2.1: Structural Ceramics.

Aluminum Oxide.

Zirconium Oxide.

Silicon Carbide.

Silicon Nitride.

Sialons.

2.2.2: Active Soldering.

Active Solder Technology.

Applications.

2.2.3: Ceramic Brazing.

The Moly-Manganese Process
or the Sintered Metal Powder Process.

Vapor Coating Process.

The Active Brazing Alloy Process.

2.3: Stainless Steel Brazing.

Brazeability.

Filler Metals.

Process and Equipment.

Precleaning and Surface Preparation.

Fluxes and Atmospheres.

2.4: Mechanical Testing of Joints.

Chapter 4: Experimental Procedures.

47

4.1: Materials and Equipments.

4.1.1: Materials.

4.1.2: Equipments.

4.2: Procedures.

4.2.1: Fabrication of the Master Eutectic Alloy and Active Braze Alloys.

4.2.2: Melting Range Determination.

4.2.3: Fabrication of Green Alumina Ceramic Pellets.

4.2.4: Sintering of Green Pellets.

4.2.5: Dipping and Bonding Experiments.

4.2.6: Mechanical Testing of the Brazing Alloys and Vacuum Brazed and Torch Brazed Stainless Steel Rods.

Chapter 5: Results.

69

5.1: Fabrication and Melting Range Determination of Brazing Alloys and Fabrication and Sintering of Ceramic Pellets.

Sintering Analysis.

5.2: Results of Dipping and Bonding Experiments.

5.3: Results of Mechanical Testing of the Brazing Alloys and the Brazed Stainless Steel Rods.

Chapter 6: Discussions.

97

Summary and Conclusions.

100

Recommendations for Further Work.

102

List of References.

103

LIST OF FIGURES

| Fig. No. | Title | Page No. |
|----------|--|----------|
| 2.1 | Surface tension forces acting on the liquid droplet on the solid surface. | 7 |
| 2.2 | Influence of brazing temperature on the wetting of Si_3N_4 by the Ag – 27 Cu – 2 Ti alloy, as measured by the contact angle. | 11 |
| 2.3 | Variation in contact angle with brazing time for Ag – 27 Cu – 2 Ti on Si_3N_4 . | 11 |
| 2.4 | Ni – P constitutional diagram. | 15 |
| 2.5 | Schematic illustration of active solder under mechanical agitation. | 23 |
| 2.6 | Microstructure of an aluminium / active solder (Sn – Ag – Ti) joint interface showing metallurgical interface reactions. | 25 |
| 2.7 | Microstructure of a titanium / titanium joint with an active solder (Sn – Ag – Ti) filler metal. | 25 |
| 2.8 | Graphite foam joined to aluminium base using active solder (Sn – Ag – Ti). | 25 |
| 2.9 | Al: SiC joined with active solder filler metal. | 25 |
| 2.10 | Schematic diagram of Moly – Manganese process. | 28 |
| 2.11 | Schematic representation of two techniques for brazing ceramics: the Mo – Mn process, and active filler metal brazing. | 35 |
| 2.12 | Wetting angle of Ag – Cu brazing metal with or without Ti addition for various ceramics. | 36 |
| 2.13 | SEM micrograph of the brazing layer. | 36 |
| 2.14 | Flow chart of active brazing of ceramic. | 37 |
| 2.15 | Flow chart of brazing of stainless steel. | 42 |
| 2.16 | Test piece configurations based on simple butt and lap joints. | 44 |

| | |
|--|----|
| 4.1 Silicon carbide tube furnace. | 50 |
| 4.2 Stainless steel pipe used for creating vacuum. | 52 |
| 4.3 The sample holder assembly with sample. | 54 |
| 4.4 Formation of master eutectic alloy. | 57 |
| 4.5 Experimental set up for active braze alloy fabrication. | 57 |
| 4.6 Experimental set up for measuring melting range of the alloys. | 58 |
| 4.7 Experimental set up for dipping of stainless steel. | 60 |
| 4.8 Experimental set up for dipping of alumina ceramic pellet. | 61 |
| 4.9 Experimental set up for brazing experiments. | 63 |
| 4.10 The line along which the brazed joint was cut to expose the interface. | 64 |
| 4.11 Two stainless steel rods, before and after brazing. | 68 |
| 5.1 Photomicrograph of Ag – 28 Cu at 3000 X. | 71 |
| 5.2 Photomicrograph of Ag – 27.4 Cu – 2 Ti at 3000 X. | 71 |
| 5.3 Photomicrograph of Ag – 26.6 Cu – 5 Ti at 3000 X. | 72 |
| 5.4 Photomicrograph of Cu – 1 Ti at 2000 X. | 72 |
| 5.5 Photomicrograph of Cu – 2 Ti at 2000 X. | 73 |
| 5.6 Temperature-time plots of Ag – 28 Cu and Ag – 26.6 Cu – 5 Ti during cooling. | 73 |
| 5.7 Temperature-time plot of Cu – 2 Ti during cooling. | 74 |
| 5.8 Temperature-time plot of Ag – 2 Ti during cooling. | 75 |
| 5.9 Photomicrograph of the sintered ceramic pellet at 5000 X. | 76 |
| 5.10 Photomicrograph of the as received stainless steel at 500 X. | 86 |
| 5.11 Photomicrograph of the interface of stainless steel and Ag – 28 Cu at 500 X. | 86 |

| | |
|---|----|
| 5.12 Photomicrograph of stainless steel to stainless steel brazed joint by Ag – Cu – 2 Ti at 50 X. | 87 |
| 5.13 Photomicrograph of the interface of stainless steel and Ag – Cu – 2 Ti at 1500 X. | 87 |
| 5.14 Photomicrograph of the interface of stainless steel and Ag – Cu – 5 Ti at 3000 X. | 88 |
| 5.15 Photomicrograph of the interface of stainless steel and Ag – 1 Ti at 1000 X. | 88 |
| 5.16 Photomicrograph of the stainless steel to stainless steel brazed joint by Ag – 2 Ti at 100 X. | 89 |
| 5.17 Photomicrograph of the interface of stainless steel and Ag – 2 Ti at 500 X. | 89 |
| 5.18 Photomicrograph of the interface of stainless steel and Cu – 1 Ti at 500 X. | 90 |
| 5.19 Photomicrograph of the interface of stainless steel and Cu – 2 Ti at 2000 X. | 90 |
| 5.20 Photomicrograph showing wetting as well as bonding of two stainless steel plates by Ag – Cu – 5 Ti at 50 X. | 91 |
| 5.21 Photomicrograph showing bonding of two stainless steel plates by Ag – Cu – 5 Ti at 50 X. | 91 |
| 5.22 Photograph showing wetting of alumina ceramic surface by the active braze filler metal Ag – Cu – 5 Ti. | 92 |
| 5.23 Photomicrograph showing wetting of alumina ceramic surface by the active braze filler metal Ag – Cu – 5 Ti at 100 X. | 92 |
| 5.24 Comparison of the strength values of the brazing alloys and the vacuum brazed stainless steel rods. | 95 |
| 5.25 Strength values of the torch brazed stainless steel rods. | 96 |

LIST OF TABLES

| Table No. | Title | Page No. |
|-----------|---|----------|
| 1.1 | Selected properties of some pure metals and structural ceramics. | 4 |
| 2.1 | Mechanical properties of some selected ceramics. | 18 |
| 2.2 | Thermal properties of some selected ceramics. | 19 |
| 2.3 | Selected data on contact angles for various liquid metals and alloys on Al_2O_3 and Si_3N_4 substrates. | 32 |
| 2.4 | Literature at a glance on active brazing of ceramics. | 33 |
| 2.5 | Commercial active braze alloys (ABA). | 34 |
| 2.6 | Experimental active braze alloys (ABA). | 34 |
| 4.1 | Dipping experiments with stainless steel plates (in air). | 65 |
| 4.2 | Bonding experiments with stainless steel plates by dipping in molten alloy (in air). | 65 |
| 4.3 | Dipping experiments with sintered alumina ceramic pellets (in air). | 65 |
| 4.4 | Bonding experiments with stainless steel plates (in vacuum, without flux). | 66 |
| 4.5 | Bonding experiments with sintered alumina ceramic pellets and stainless steel plates (in vacuum). | 66 |
| 4.6 | Bonding experiments with sintered alumina ceramic pellets (in vacuum). | 66 |
| 5.1 | Results of preparation of eutectic alloy and active braze alloys. | 70 |
| 5.2 | Data analysis of green pellets before sintering at 1600°C for 9 hours. | 77 – 78 |
| 5.3 | Data analysis of pellets after sintering at 1600°C for 9 hours. | 79 – 80 |

| | |
|--|----|
| 5.4 Results of dipping experiments with stainless steel plates (in air atmosphere) | 82 |
| 5.5 Results of bonding experiments with stainless steel plates by dipping in molten alloys (in air atmosphere). | 83 |
| 5.6 Results of dipping experiments with sintered alumina ceramic pellets (in air atmosphere). | 83 |
| 5.7 Results of bonding experiments with stainless steel plates (in vacuum atmosphere, without flux). | 84 |
| 5.8 Results of bonding experiments with sintered alumina ceramic pellets and stainless steel plates (in vacuum atmosphere). | 85 |
| 5.9 Results of bonding experiments with sintered alumina ceramic pellets (in vacuum atmosphere). | 85 |
| 5.10 Strength values of the brazing alloys and the vacuum brazed stainless steel rods. | 94 |
| 5.11 Strength values of the torch brazed stainless steel rods. | 94 |

CHAPTER 1

INTRODUCTION

The ability to produce reliable brazed ceramic/metal joints is a key enabling technology for many production, prototype and advanced developmental items and assemblies. The increasing use of ceramic-to-ceramic and ceramic-to-metal joints in industrial and developmental applications is due to the unique combination of properties of ceramic materials. Selected properties of some important ceramics with metals are included in Table 1. ^[1] The large usage of ceramic – to – metal joints in vacuum tubes compared to glass tubing in the electronics industry stems from the following properties. (a) ceramic tubes can be outgassed at higher temperatures than glass tubes; (b) ceramic tubes can withstand higher temperatures than glass tubes of similar dimensions; (c) ceramic tubes are mechanically stronger and less sensitive to thermal shock than glass tubes; (d) ceramic components can be ground to the precise tolerances required for vacuum-tube construction; and (e) ceramic materials have very low electrical losses at high frequencies. Another major application of ceramic-to-metal joints occurs in the electrical industry, where they are used in lead-through devices in which electrical leads are insulated from another metal.

Because of their inertness in many corrosive environments, ceramics are used as seals in fuel cells and other devices that convert chemical, nuclear, or thermionic energy to electricity. Structural ceramics are also used as friction materials for brakes, clutches, and other energy-absorbing devices; coatings for nuclear fuel particles; constituents in high-temperature adhesives; radomes used to enclose antennae; and ablative materials.

Ceramic materials are inherently difficult to wet with conventional brazing filler metals. Most of these filler metals merely ball up at the joint, and little or no wetting occurs. When bonding does occur, it can be either mechanical or chemical. The strength of a mechanical bond can be attributed to interlocking particles or penetration into surface pores and voids, whereas a chemical bond derives strength from material transfer between the filler metal and the base material. ^[2] Cannon et al. ^[3] showed that the contact angle between the mullite ceramic ($3\text{Al}_2\text{O}_3 \cdot 2\text{SiO}_2$) surface with pure silver, pure copper and with silver copper eutectic (Ag – 28 wt. pct. Cu) was more than 90° even at temperature more than 1000°C .

They also found that the contact angle drastically falls even to zero by addition of 1 to 5 at. pct. of Ti or Zr in liquid Ag – 28 Cu alloy.

Stainless steels are also difficult to wet because of their high chromium contents. The high quantities of chromium that are present in stainless steels cause the chromium oxide films that are on the surfaces of all stainless steels, as well as the films of titanium oxide that form on the surfaces of titanium-stabilized stainless steels, such as type 321. If these oxides, which are both refractory and strongly adherent, are inadequately removed, they will prevent the molten filler metal from wetting the base metal, and thus will prevent a capillary joint from being formed between the metals being joined.

The formation of chromium oxide is accelerated when stainless steel is heated in air. Although the oxide may have been removed from the surface by chemical cleaning at room temperature, a new oxide layer that seriously interferes with wetting will rapidly form when the steel is heated in air to the brazing temperature. ^[4] Brazing of these alloys is best accomplished in a purified (dry) hydrogen atmosphere or in a vacuum. Dew points of -50°C or lower must be maintained. In torch brazing of these base metals, fluxes are required to reduce any chromium oxides present. ^[2]

Another basic problem in brazing of ceramics may result from the differences in thermal expansion between the base material and the brazing filler metal and, in the case of ceramic-to-metal joints, between the two base materials. In addition, ceramics are poor conductors of heat, which means that it takes them longer to reach equilibrium temperature than it does metals. Both of these factors may lead to cracking in the joint. Because ceramics generally have lower tensile and shear strengths than metals, crack propagation occurs at lower stresses in ceramics than in metals. In addition, the low ductilities permit very little distribution of the stresses set up by stress raisers. ^[2]

Suganuma et al. ^[5] showed that the insertion of soft interlayer between ceramic and metal decreases the residual stresses. They developed a new concept in the ceramic-metal joint design like ceramic/soft metal interlayer/metal layer, which has similar thermal expansion coefficient as that of ceramic/metal. Subsequently, Xian and Si ^[6] used Cu, Ta,

Mo, Kovar (Fe – 32 wt% Ni – 5 wt% Co) and Ni alloy as interface between ceramic/metal to decrease the residual stresses.

The present work was aimed at joining of stainless steel to stainless steel, stainless steel to alumina and alumina to alumina by using seven types of brazing filler metals. Ti was used as an active element. The interface microstructures of the brazed specimens were seen under the EPMA or SEM. This work was also aimed at studying the mechanical strength of the brazed joints as well as the brazing filler metals.

Table 1.1: Selected properties of some pure metals and structural ceramics¹

| Material | Strength ² (MPa) | Modulus of Elasticity (GPa) | Coefficient of Linear Thermal Expansion, $\mu\text{m}/\text{m}^{\circ}\text{C}$ | Electrical Resistivity, $\mu\Omega \cdot \text{cm}$ | Thermal Conductivity, $\text{W}/\text{m} \cdot \text{K}$ |
|-------------------------|--------------------------------|-----------------------------------|---|---|--|
| Al | 34 | 62 | 23.6 | 2.6548 | 221.75 |
| Cu | 69 | 110 | 16.5 | 1.6730 | 393.71 |
| Fe | 130 | 196 | 11.7 | 9.71 | 75.31 |
| Mo | 345 | 324 | 4.9 | 5.2 | 142.26 |
| Ni | 152 | 207 | 13.3 | 6.84 | 92.05 |
| Ti | 207 | 116 | 8.41 | 42 | 21.9 |
| Al_2O_3 | 300 | 380 | 6.8 | $> 10^{20}$ | 27.2 |
| SiC | 500 | 480 | 4.2 | 10^7 | 62.8 |
| Si_3N_4 | 1000 | 304 | 3.2 | $> 10^{20}$ | 10 |
| ZrO_2 | 700 | 205 | 9.7 | 10^6 | 2 |

1. Values given are typical values for each material at or near room temperature. The property values for the strength, electrical resistivity, and thermal conductivity of metals vary significantly with composition

2. Yield strengths are given for metals; modulus of rupture strengths is given for ceramics.

CHAPTER 2

LITERATURE REVIEW

The literature related to present work can be divided in four parts, first part regarding the general definition of brazing and its key parameters, second part dealing with the joining processes for ceramics, third part regarding the brazing of stainless steels and the last part consisting of the mechanical testing of the brazed joints.

2.1 Brazing.

2.1.1 Definition of Brazing.

The American Welding Society defines brazing as “a group of welding processes which produces coalescence of materials by heating them to a suitable temperature and by using a filler metal having a liquidus temperature above 450°C and below the solidus temperature of the base materials. The filler metal is distributed between the closely fitted surfaces of the joint by capillary attraction”.^[1] Since there is no melting of base materials the bond formed is metallurgical bond. The joint, in general, will be heterogeneous in nature as it is composed of different phases with differing physical and chemical properties. The partial dissolution of base materials, combined with diffusion process, can change the composition and therefore, physical and chemical properties at the interface of the entire joint.^[7, 8]

To achieve a good joint, the parts must be properly cleaned and must be protected by either liquid flux, gaseous or vacuum atmosphere during the heating process to prevent excessive oxidation. The parts must be designed to afford a capillary for the filler metal when properly aligned, and a heating process must be selected that will provide the proper brazing temperature and heat distribution.

Applications of brazing cover the entire manufacturing arena from inexpensive toys to highest quality aircraft engines and aerospace vehicles. Brazing is used because it can produce results which are not always available with other joining processes.^[1, 2]

2.1.2 Key Parameters of Brazing.

Contact Angle and Wetting.

Contact angle or wetting angle is the angle included between the tangent plane to the surface of the liquid and the tangent plane to the surface of the solid, at any point along their line of contact.

Surface tension forces acting on a spherical droplet is shown schematically in Fig. 2.1 ^[9] From the principal of minimum surface energy of the system or by the balance of forces, one may derive the following expression:

$$\cos \theta = (\gamma_{SV} - \gamma_{SL}) / \gamma_{LV}$$

Where,

γ_{SL} = interfacial tension between the solid and liquid,

γ_{SV} = interfacial tension between the solid and vapor,

γ_{LV} = interfacial tension between the liquid and vapor, and

θ = contact angle of the liquid droplet on the solid surface.

This equation is known as “**WETTING EQUATION**”.

The contact angle θ provides a measure of quality of wetting. Thus, if $90^\circ < \theta < 180^\circ$, liquid will not be spread on the contacting surface. On the other hand, if $\theta < 90^\circ$, liquid will wet the substrate and also spread. Therefore it is clear that the area of spreading will increase with decrease in contact angle. Wetting is improved by decreasing θ , which can be achieved by increasing γ_{SV} and decreasing γ_{SL} and γ_{LV} . Cleaning the solid surface can maximize the γ_{SV} but γ_{SL} is highly temperature dependent and usually decreases rapidly with increasing temperature for a particular liquid-solid combination. Similarly altering the composition and pressure of an atmosphere used for the joining operation can vary γ_{LV} . ^[9, 10, 11]

Wettability Index (WI).

Wettability Index developed by Feduska ^[12] is used as the measure of the wettability. Wettability Index is defined as the area covered by the filler braze metal times the cosine of the contact angle between the braze and the base metals. So for high value of WI, there is a

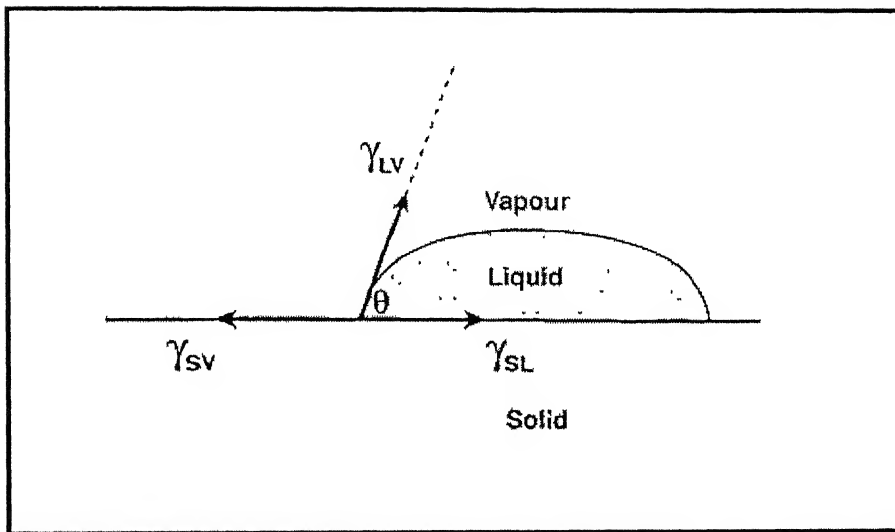


Fig. 2.1: Surface tension forces acting on the liquid droplet on the solid surface.^[2]

good wettability. WI depends on the volume of the filler metal used. WI greater than 0.05 is indicative of good performance during brazing, however, when it is greater than 0.1, it is an indication of excellent performance during brazing.^[12] In some cases, the wetting of a surface is much more complex and use of the above classical model, i.e., the theory of wettability with respect to contact angle, is not so simple when chemical reaction between the filler metal and solid surface takes place. The effect of metallurgical interaction between the filler metal and the component material in promoting wetting is exploited in active filler metals. The addition of a small fraction of a reactive metal such as Ti or Zr to filler metal enables them to wet and spread over ceramic materials. In this instance wetting of and reaction with the ceramic are inextricably linked.^[14]

Capillary Attraction.

Capillary attraction is the physical force that governs the action of a liquid against solid surfaces in small confined areas. Capillary flow is the dominant physical principle that ensures good brazements. When the joint gap at brazing temperature is proper, capillary force will be stronger than gravity and enable a liquid brazing filler metal, to be drawn between the faying surfaces of the joint in any direction, regardless of the orientation of the assembly (horizontal or vertical). The capillarity is a result of surface tension between the base metal(s), brazing filler metal, flux or atmosphere, and the contact angle between the base and filler metals.

The vertical height to which a liquid rises between two parallel plates separated by a distance d is given by^[13]:

$$H = (2 \gamma_{LV} \cos \theta) / (6 \rho d)$$

Where, ρ = density of the liquid.

The velocity v of the liquid into the space between two parallel surfaces of separation d is given by^[13]: $v = (d^2 H) / (8 \eta h)$

Where, h is the height, to which the liquid has risen, η is the kinematic viscosity given by (μ/ρ) . The parameter μ is the viscosity of the liquid. It may be deduced that, other things being equal, the height to which a liquid rises in a capillary space increases as the separation

of the surface is reduced and the rate of flow into the joint decreases as the separation of the surface is reduced.

In actual practice, brazing filler metal flow characteristics are also influenced by dynamic consideration involving fluidity, viscosity, vapor pressure, gravity and metallurgical reactions between brazing filler metal and base metal. ^[14] For capillary force to work, the base metal and the braze filler metal must be compatible, i.e., they must be able to alloy with each other. The braze filler metal will then be able to “wet” or spread out along the surface of the base metal. The extent of alloying does not have to be much, but it must occur.

2.1.3 Brazing Considerations.

Joining Atmosphere.

Mizuhara et al. ^[15] have suggested that Ti readily reacts with oxygen, nitrogen, and water vapor in the brazing process. Consumption of Ti by interaction with the above depletes the amount of Ti available to wet the ceramic surface, and the reaction product can also form on the surface of the brazing filler metal, which may prevent physical contact between Ti and ceramic part of the assembly. As a result, bonding with the ceramic will be poor. It has also been indicated that one of the best atmospheres for active brazing is a vacuum of level 10^{-5} torr and leak rate of the vacuum furnace should be less than 0.67 Pa per hour.

Vacuum Brazing. Vacuum brazing is economical for flux less brazing of many similar and dissimilar base metal combinations, especially for brazing very large, continuous area or complex assemblies where removal of solid or liquid flux is difficult and where there is inability of providing proper gaseous mixture. Vacuum is also suitable for brazing ceramics and reactive and refractory base metals such as Ti, Zr, Mo, Ta etc. Vacuum brazing has the following advantages and disadvantages compared with high-purity brazing atmospheres.

Vacuum removes essentially all gases from the brazing area, thereby eliminating the necessity of purifying the supplied atmosphere. Commercial vacuum brazing generally is accomplished at pressure varying from 10^{-6} to 0.5 torr (10^{-4} to 67.5 Pa) and above, depending upon the materials to be brazed, the filler metal being used, the area of the brazing interfaces and the degree to which gases are expelled by the base metals during brazing cycle.

Certain oxides of the base metal will dissociate in vacuum at brazing temperatures. Vacuum is widely used to braze stainless steel, superalloys, aluminium alloys, and with special techniques, refractory materials and ceramics.

Difficulties sometimes experienced with contamination of brazing interfaces due to base metal expulsion of gases are minimized in vacuum brazing. Occluded gases are removed from the interfaces immediately upon evolution from the metal. ^[11]

Temperature and Time.

The temperature of brazing of course must be above the melting point of the brazing filler metal and below the melting point of the parent metal. This temperature plays an important role with regard to the wetting action and flow of the filler metal, the wetting and alloying action improves as the temperature increases (Fig. 2.2). ^[16] Braze filler metals can be fairly complex alloys and their melting can take place over a range of temperature. Lower brazing temperatures are preferred to minimize heat effect on the base metal, increase the life of the fixture, jigs or other tools, minimize base metal / filler metal interaction etc. Higher brazing temperatures may be preferred to promote base – metal interaction in order to modify the brazing filler metal, permit subsequent processing at elevated temperatures, and use a higher melting but more economical brazing filler metal.

There are two opposing factors in determining the maximum brazing temperature. The higher the temperature, the more active the active brazing alloys (ABAs), and therefore, the better the wettability. Conversely, the higher the temperature, the more alloying occurs with the metal member, and the braze alloy has a lower viscosity. In very general terms, a temperature between 20 – 25⁰C above the braze alloy liquidus nearly always gives good results. The time at the brazing temperature also affects the wetting action (Fig. 2.3) ^[16], particularly with respect to the creep of the brazing filler metal.

Joint Design and Clearance.

Mizuhara et al. ^[15] have investigated the effect of Ti concentration in the Cu – Ag filler alloy on the peel strength. Peel strength was observed to be maximum at a Ti concentration of about 1.5 wt%. However, both below and above 1.5 wt% Ti the peel strength was lower. According to them, plastic deformation of the brazing filler metal during

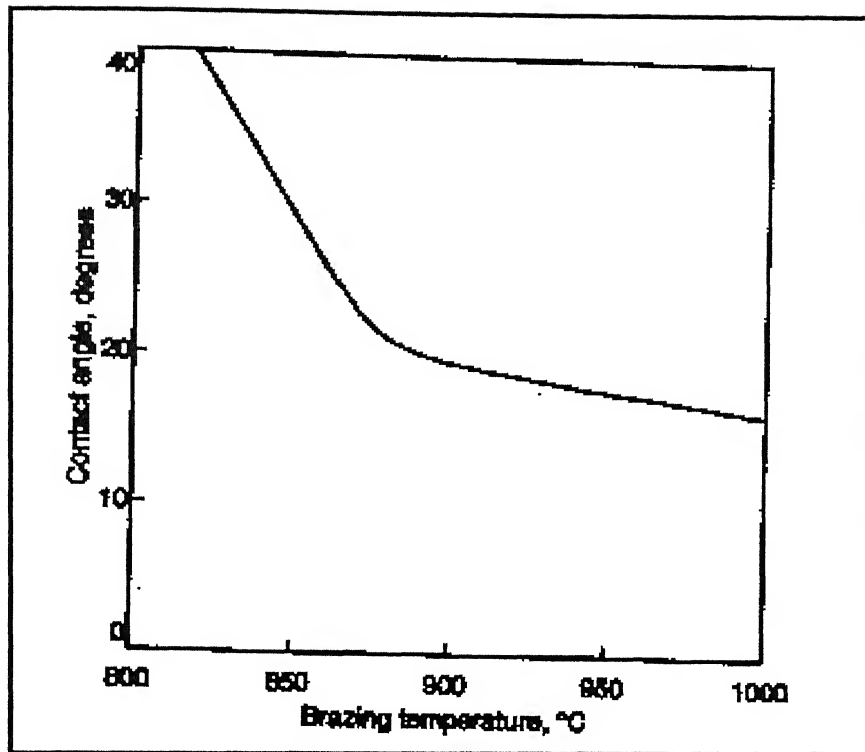


Fig. 2.2: Influence of brazing temperature on the wetting of Si_3N_4 by the Ag – 27 Cu – 2 Ti alloy, as measured by the contact angle^[16].

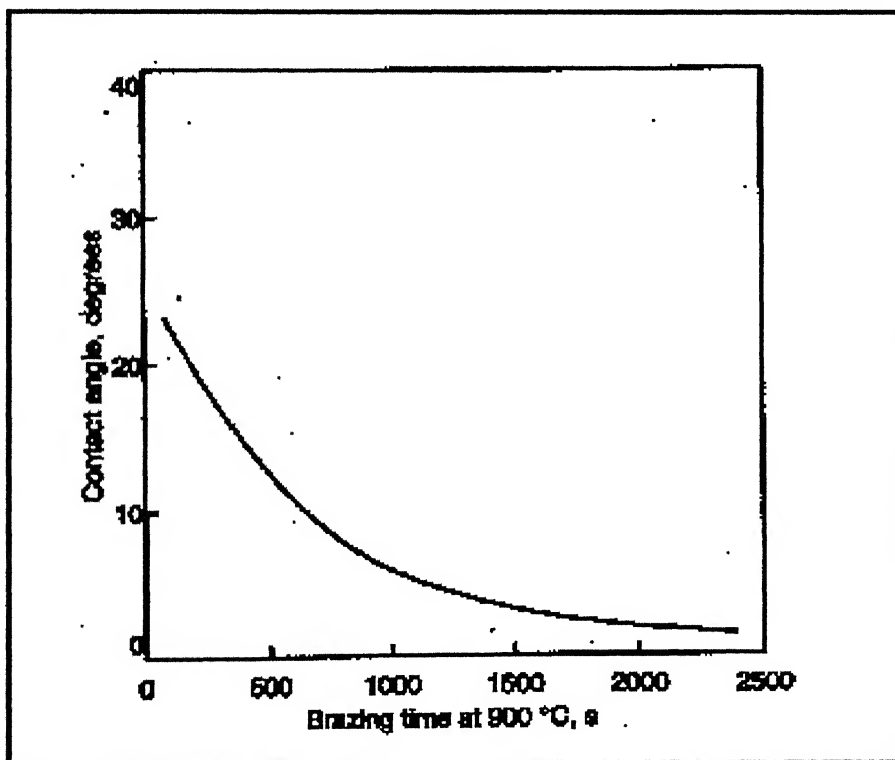


Fig. 2.3: Variation in contact angle with brazing time for Ag – 27 Cu – 2 Ti on Si_3N_4 .^[16]

cooling from the brazing temperature accommodates thermal expansion mismatch. Therefore, the increase in strength of brazing filler metal, which is due to excess Ti content, leads to poor accommodation of thermal expansion mismatch and results in high residual stress and hence, low joint strength.

Heating Rate.

The heating rate is a critical parameter in any brazing operation, but becomes even more so when joining ceramics to metals. There are two opposing factors. The heating rate of metals is much higher due to the excellent thermal conductivity of metals as opposed to the insulating properties of ceramics. Therefore, the metal member reaches temperature before the ceramic. Often, the ceramic is much more bulky than the metal, which compounds this problem. A slow heating rate ensures that the temperature differential is minimized. However, if the metal member has a strong alloying tendency with the filler metal, such as a copper member with copper-silver eutectic ABA filler, the copper dissolves into the filler, elevating the liquidus temperature of the filler, which can lead to a partial or totally missed braze. In this case, a rapid heating rate is required. A hold for 30 minutes in the heating rate 30-50°C below the solidus of the braze filler is always advisable to ensure uniformity. ^[9]

Braze Fixturing.

For active brazing to be effective, the main criteria are that pressure (about 5 psi is ample) must be applied to the joint during brazing, and that the fixture does not come into contact at any point with the ABA as it will nearly braze itself to *anything*, including graphite and boron nitride. ^[9]

Braze Interlayer.

If the parts are large, and there is a big difference in the thermal coefficients of expansion, then a braze interlayer can help to reduce the residual stresses in the joint. The thickness of the interlayer is important; it should be thick enough so as not to be totally affected by diffusion from the braze alloy so that the ductile layer is embrittled, and thin enough so as not to destroy the bulk properties of the configuration. 0.008" (0.2mm) to 0.016" (0.4mm) interlayers have been found to be the most effective. ^[9] Metals such as Copper, Nickel, Niobium, Molybdenum, Aluminium and Titanium have all been tried as interlayers.

2.1.4 High Temperature Brazing.

As yet, there is only one braze alloy commercially available that brazes over 1050°C, and that is the new Gold-ABA-V from Wesgo. This alloy has a solidus of 1045°C and a liquidus of 1090°C. However, it is only intended for operating temperatures in usage of around 950°C.

There is a very pressing need to braze ceramics to metals, oxide dispersion strengthened materials and to other ceramics at much higher temperatures. Already, there are Gas Turbine Engines, which have seal requirements to withstand 1100°C continuous operating temperatures.

The main problem with developing higher temperature ABA type brazes are that the alloying systems are not available. Nickel ABA type alloys have been unsuccessful. Work is currently being done on both Palladium and Platinum based alloys. ^[9]

2.1.5 Filler Metal – Parent Metal Interaction.

When stainless steels and the Ni – and Co – base alloys are brazed at temperatures of 1000 – 1200°C, interaction between the molten filler metal and solid parent metal occurs. This is especially the case when Ni – and Co – based filler metals are used.

A simple system, for example, brazing of Ni with the eutectic alloy (89/11 Ni/P) at 1000°C, can be used to explain the principles. From the constitutional diagram for Ni – P (Fig. 2.4), ^[17] it can be seen that no equilibrium is possible between the molten filler metal of composition A and the parent metal (Ni) of composition E. The joint will consist of two solid nickel masses with eutectic Ni / P liquid in-between. At each phase there will be a layer of composition C in-between the eutectic and the Ni after a short time, for diffusion of Ni into the liquid and P into the solid. This will lower the P content of the liquid from A to B and raise the melting point to 1000°C under the joint making conditions. After heat treatment at 1000°C and assuming there is much more Ni available than P, the surface of the parent metal will achieve composition D and will start to melt at T (the solidus), while the liquidus will be at C, and it will start to solidify at T.

Subsequent to the heat treatment, the interface will not start to melt until heated to T and the filler, which will start to melt at 875°C, will not be completely liquid until T. Both of these changes will raise the failure temperature above what it was previously, perhaps

1000°C with no load. The amount of eutectic will diminish during the heat treatment and if it is long enough, none will be left and no melting will occur below T. Similar, but more complicated mechanisms takes place during brazing when B and S1 temperature depressants are used.

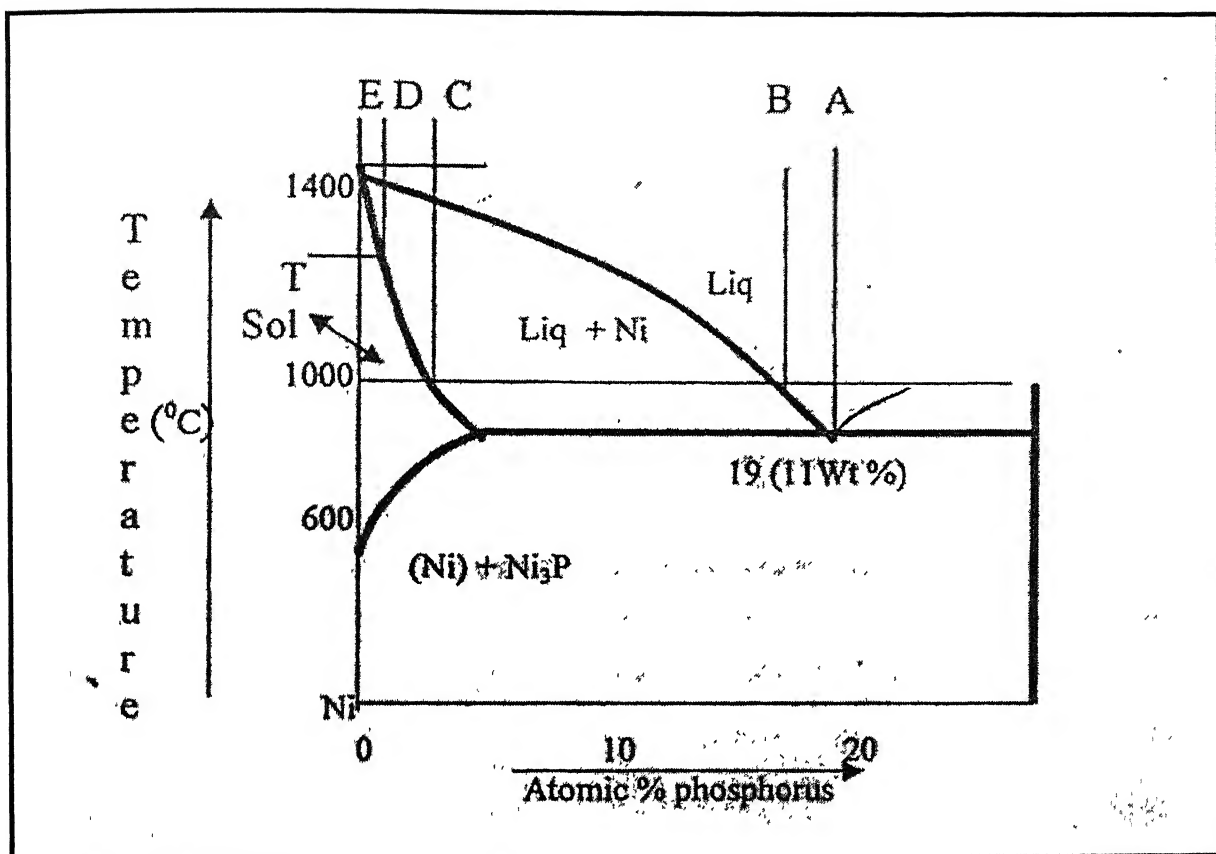


Fig. 2.4: Ni – P constitutional diagram (E. Lugscheido).^[11]

2.2 Ceramic Joining.

2.2.1 Structural Ceramics.

Aluminium Oxide: ^[1]

Aluminium oxide (or alumina or Al_2O_3) is generally extracted from the mineral ore bauxite with world production around 35 million metric tons annually. About 90% of this alumina is reduced to produce aluminium metal, and about 3% is used for alumina speciality products including structural ceramic grades of Al_2O_3 . The ceramics market for Al_2O_3 encompasses a wide range of applications from glass and chinaware to spark plugs, biomedical ceramics, and integrated circuitry. Some of these applications require an insulating material having high mechanical strength (e.g., for rectifier housings), high volume resistivity, low dielectric losses (e.g., for transmitter tubes), high density, and translucency (e.g., for sodium vapor discharge lamps). Most of these requirements can be met by high-purity structural grades of Al_2O_3 . Mechanical and thermal properties of alumina and a few other ceramic materials are included in Table 2.1 and Table 2.2. ^[9]

Zirconium Oxide: ^[1]

Zirconium oxide (or zirconia or ZrO_2) occurs in the nature as the mineral zircon, ZrSiO_4 , and less frequently as free zirconia. Annual production of zirconia ore reportedly has been as high as 650 000 tons, with most of it being used as refractory material and only a relatively small portion in structural ceramics. Zirconia can exist in three different crystal structures: cubic, tetragonal and monoclinic. The structure or combination of structures that exists in ZrO_2 ceramics can be controlled by alloying and heat treatment to produce materials with high strength and relatively high toughness. The good mechanical properties are a result of stress-induced phase changes that can occur between the different crystal structures. Several distinct types of toughened ZrO_2 have been developed: partially stabilized zirconia, PSZ; tetragonal polycrystalline zirconia, TZP; and composites of zirconia with other ceramics such as Al_2O_3 containing ZrO_2 particles, a material which is referred to as zirconia-toughened Al_2O_3 , or ZTA.

Excellent resistance to thermal shock and mechanical impact damage has led to the use of PSZ materials as extrusion die materials. Superior wear properties and low susceptibility to stress corrosion has led to the use of PSZ as a structural biomedical material. Wear properties, high strength, low thermal conductivity, and relatively high thermal expansion have resulted in the application of PSZ in a variety of internal combustion engine components. An important use of zirconia-toughened Al_2O_3 is for metal cutting tool bits where dramatic improvements in bit life can be achieved.

Silicon Carbide: ^[1]

Silicon carbide (SiC) occurs naturally, but not in quantities large enough to be of significant commercial value. In the western countries, about 500 000 tons/year of SiC are produced by reacting silica, SiO_2 with carbon at high temperatures (2200°C). Major uses of SiC are for abrasives where it is commonly used as loose or bonded grits, as a siliconizing agent in steel making, and as a structural ceramic material. Structural grades of SiC are most commonly made by two processes. In one case, a porous body of SiC and carbon are infiltrated with liquid silicon metal, and then heat treated (reaction sintered) to produce further reaction of the carbon and silicon to form more SiC. SiC parts produced by this technique are known as *reaction-bonded SiC*, and typically have very high densities and contain about 10 – 15 % of free, unreacted silicon. The other process commonly used to produce SiC parts is pressureless sintering. SiC produced by the method is known as sintered SiC, and it is routinely densified to near its theoretical value.

One of first important engineering applications of SiC was for rotating mechanical seals where reaction-bonded SiC was found to outperform hard metals and Al_2O_3 by a wide margin. Sintered SiC has become an important material for the fabrication of sliding seals in hermetically sealed pumps particularly where hazardous, corrosive, or abrasive media must be pumped. The corrosion resistance and mechanical properties of sintered SiC make it an attractive candidate material for many high-temperature applications. Automotive applications are an area of intense interest in SiC, where this material is being used to make critical components of advanced design turbine engines.

Table 2.1: Mechanical properties of some selected ceramics.^[9]

| | Density gm/cm ³ | Flexure strength MPa | Hardness HV _{0.1} kp/mm ³ | Fracture Toughness MPam ^{1/2} | Young's modulus GPa |
|---|-------------------------------|----------------------------|---|--|---------------------------|
| Non-oxide Ceramics | | | | | |
| Aluminium nitride | 3.3 | 350 | 2200 | - | 310 |
| Silicon carbide Sintered | 3.2 | 400-600 | 2500 | 3 | 430 |
| Silicon carbide Recrystallized | 2.65 | 120 | - | - | 240 |
| Silicon carbide Silicon infiltrated | 3.1 | 300-350 | 2000 | 4 | 350 |
| Silicon nitride Sintered | 3.2 | 500-1000 | 1600 | 5-8 | 310-330 |
| Titanium diboride | 4.4 | 600 | 2200 | - | 570 |
| Oxides | | | | | |
| Alumina 99.9% | 3.80-3.99 | 200-700 | 1900 | 3-6 | 400 |
| Zirconia PSZ Y ₂ O ₃ | 6.05 | 1000-1300 | - | 7-70 | 205 |
| Zirconia PSZ-MgO | 5.60 | 500 | - | 9 | 205 |

Table 2.2: Thermal properties of some selected ceramics.^[9]

| | Thermal expansion 1/°C 10 ⁻⁶ | Thermal Conductivity 20 C W/mK | Maximum use temperature °C | Maximum loaded temperature °C |
|---|---|--------------------------------------|----------------------------------|-------------------------------------|
| Non- oxide Ceramics | | | | |
| Aluminium nitride | 4.5 | 150 | - | - |
| Silicon carbide Sintered | 4 | 60-80 | 1500 | 1600 |
| Silicon carbide Recrystallized | 4 | - | 1500 | - |
| Silicon carbide Silicon infiltrated | 4 | 150 | 1400 | - |
| Silicon nitride Sintered | 3 | 20-40 | 1200 | 1350 |
| Titanium diboride | 7.2 | 110 | - | - |
| Oxides | | | | |
| Alumina 99.9% | 8 | 20-30 | 1000 | 1800 |
| Zirconia PSZ-Y ₂ O ₃ | 10.5 | 2.1 | 300 | 950 |
| Zirconia PSZ-MgO | 8.9-10-1 | 2.1 | 500 | 950 |

Silicon Nitride: ^[1]

Silicon nitride (Si_3N_4) does not occur in nature, and the high-quality Si_3N_4 powders required for making structural material must be derived. Common processes for producing Si_3N_4 powders include the reaction of silicon metal with nitrogen gas, the decomposition of silicon diimide, the reaction of silicon chloride and ammonia, and by the carbothermic reaction of silica, carbon and nitrogen gas. Si_3N_4 parts also can be made by a technique referred to as *reaction bonding*. Reaction bonded Si_3N_4 is relatively porous and of low strength. The production of high-density, high-strength Si_3N_4 requires the use of hot-temperature processing, as well as the use of small quantities of liquid phase "sintering aids".

Widespread use of Si_3N_4 parts has been hampered by the difficulties of producing high-quality, low-cost Si_3N_4 powders, and densifying them into flaw-free articles. Nevertheless, Si_3N_4 figures prominently in all of the advanced engine concepts currently under development. Silicon nitride is considered to be one of the toughest and strongest of ceramics at temperatures above 1000°C . It is also a prime candidate for lightweight engine components requiring good wear resistance. Potential applications for Si_3N_4 include valves, valve train parts, and turbocharger rotors for internal combustion engines, and power turbine rotors and shafts for gas turbine engines.

Sialons: ^[1]

Silicon-aluminium oxynitrides (or sialons) do not occur in nature, but because the elements used to produce sialons are among the most abundant on earth there is no possibility of a raw materials shortage for their production. Sialons powders can be produced by a number of techniques including the heating of clay and coal mixtures, or sand and aluminium mixtures, in nitrogen. Sialons are a solid solution of Si-Al-O-N and are described by the chemical formula, $\text{Si}_{x-6}\text{Al}_x\text{O}_x\text{N}_{8-x}$, where X can vary from 0-4. The most common form of sialon used in industry is β' -sialons: one which contains a small amount of glassy phase used to promote densification during sintering, and another in which heat treatment causes the glassy phase to crystallize. The material containing the glassy phase has very high strength at low temperatures, but its strength quickly decreases with increasing temperature. The heat treated version has lower strength but retains it to higher temperatures, and it has better creep resistance than the glass-containing materials.

One of the most successful applications of sialons has been in cutting tools for machining cast irons, hardened steels and nickel-based alloys where because of superior strength, wear resistance, and thermal shock resistance, it outperforms both tungsten carbide and alumina tools. Sialons are also being used as extrusion die inserts in the production of ferrous and nonferrous metals, and as die inserts and mandrels in the production of stainless and high-alloy steel tubing. The excellent strength and thermal shock resistance of sialons also makes them preferred materials for gas shrouds for automatic welding operations. Sialons are also well suited for many seal and bearing applications.

2.2.2 Active Soldering.

Active soldering is an emerging technology that is based on soldering alloys with active elements such as Ti and Al. These active solders which are mostly lead-free alloy melt at temperatures less than 450°C, need no fluxes, and require no premetallization. Active solders may join the most of inorganic materials in an economic, one-step joining process. Applications include joining thermal management devices because of the filler metal's high thermal conductivity; joining electronic packages that utilize new ceramics and composite materials; and a host of other joining applications where adhesives or conventional solders have not worked.

Active Solder Technology.^[18]

Active solder implies that a reaction occurs between elements in the solder filler metal with compounds on surfaces being joined, such as the surfaces of titanium, stainless steel or ceramics. The surface oxides and nitrides of these materials typically disrupt wetting, thus fluxes or premetallization are normally used to provide a layer of fresh metal. Xien et al.^[19] reported that addition of active element, such as In, Ti, Hf, and Zr to the soldering alloys reduce surface compounds and form insitu fresh metal surfaces. Smith^[18] has reported that active solders had to be processed at brazing temperatures in protective atmospheres. These active solder alloys may not flow well at lower temperatures, therefore, techniques to distribute them in the capillary joint were developed by the investigators.

Currently, two alloy-based systems have been developed. One is based on Sn – Ag – Ti and the other on Zn – Ag – Al. Both alloys have rare earth elemental additions that catalyze wetting and surface reactions at normal soldering temperatures (below 450°C). Once the

active solders are molten, their active elements migrate to the joint interface and react with the joint surface compounds. Rare earth element (lanthanides) additions are believed to lower the energy of reaction with oxides, nitrides, and other surface compounds during heating in air, allowing the active elements in the solders to interact with the joint metal surfaces and diffuse into the surface of two opposing joint materials to form metallic, or atomic, bonds.

Since no chemical fluxes are used, the oxides that naturally form on base metals must be mechanically disrupted. Activation implies that the active elements in the solders are “released” to permit wetting and joining to the faying surfaces. The schematic in Fig. 2.5 ^[18] illustrates how a molten active solder’s surface oxide is disrupted by mechanical agitation, thus permitting the molten active solder to be spread.

Mechanical agitation has been accomplished by metal edge abrasion, brushing, vibration, or a combination of these methods. Once an active solder layer is melted on to a heated surface, ultrasonic polishing / spreader tools and / or ultrasonic soldering irons can be used to mechanically vibrate the molten alloy layer and initiate wetting. More aggressive wetting is produced through ultrasonic-induced cavitation of molten active solder pulls as they are spread across a surface for wetting, employing either ultrasonic soldering irons or an other type of ultrasonic vibrating tool tip.

Other means of spreading include wire brushes, metal edge, spatulas, or abrasive porous metals. Assemblies are made after the active solder has been preapplied or preplaced in the joint. Assemblies must be agitated when the active solders are molten (assembled molten or preheated after assembling) after the joints are assembled. This can be done by relative spinning, oscillation, or vibration of the components. One specific joining technique incorporates the use of ultrasonic “plastic” welding equipment.

It is important to note that active solders do not flow and therefore, they must be preplaced and mechanically activated. This method may be limiting for some joint configurations, but in applications where the flow of excess solder needs to be controlled, such as in closed passages or in large joint clearances, active solders are advantageous. Supplemental solder filling with conventional solders (Sn - and Pb – based) can be used since all conventional solders will wet any preplaced molten active solder layer without any flux.

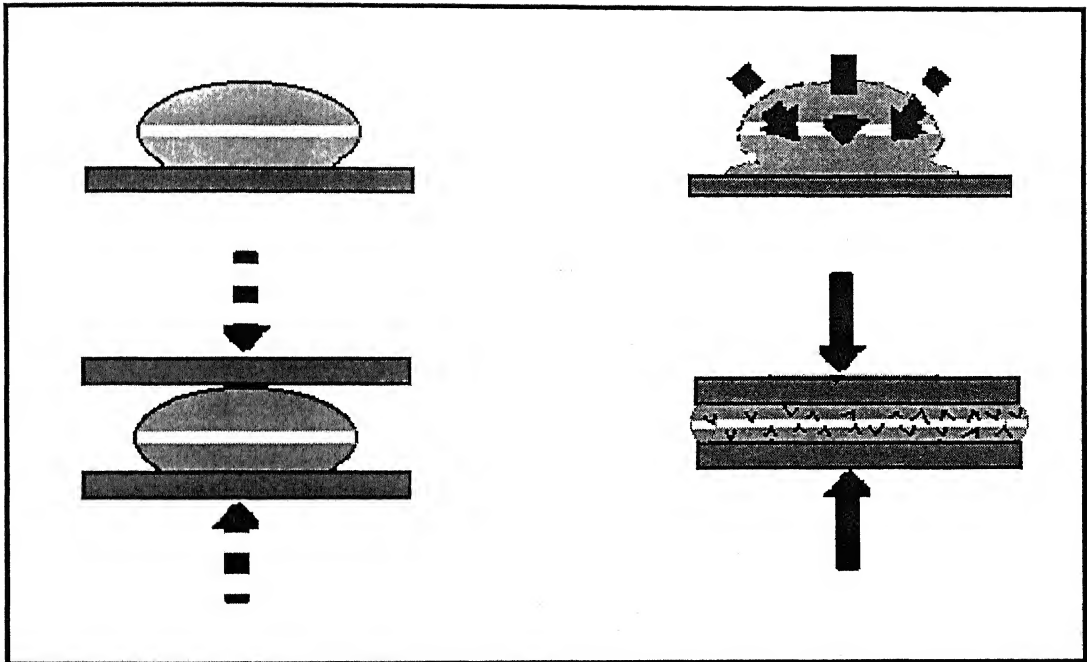


Fig. 2.5 – Schematic illustration of active solder under mechanical agitation.^[18]

The microstructures of solder joints are shown in Figs. 2.6 – 2.9 ^[18]. One can identify the following features: (a) active Sn – based solder filler metals (b) dispersed intermetallic (Sn – Ti) phases (c) a Sn – Ag eutectic structure.

Aluminium, copper, and materials with tenacious oxide surface compounds such as titanium and stainless steel, have been joined using active solders. In electronic and electrical applications, metals, ceramics, semiconductors, and metal matrix composites (MMCs) need to be joined. Research on active solders, ^[18, 19] such as the Sn – Ag – Ti alloy, showed a capability to join this range of electronic materials, using essentially the same active soldering process used in other metal joining.

Active solder joints have been shown to be hermetic when used for ceramic, metal, and metal – ceramic seals. Such joints have been accomplished without gold, silver, or nickel metallizing the ceramic surfaces. These metal – ceramic joints, although initially hermetic, can fail under thermal cycling if the thermal expansion mismatch between the opposing faces results in interface stresses that shear the active solder bond.

Applications.

Active solders provide metallic, thermally and electrically conductive joints that are tough but have sufficient ductility to effectively join many dissimilar material combinations. Its low - temperature joining, compared to brazing (for example in joining aluminium alloys, metal – to – glass, or ceramic joints), offers advantages when joining mismatched materials with large coefficients of thermal expansion (CTE). With these advantages, active joining is finding applications in electronics, heat exchangers, magnets, aluminium tooling, aluminium matrix composites, glass – metal seals, house wares, sports equipment, and satellite components. ^[18]

2.2.3 Ceramic Brazing.

Brazing is often the preferred method for joining ceramics to metals because it can provide hermetic seals and the plasticity of the braze to accommodate the differential expansion between the ceramic and metal. But several important problems such as the poor wettability, residual stresses due to thermal expansion mismatch between ceramics and metals still remain unsolved. Generally, ceramics have covalent or ionic bonding, but metals have metallic bonding in terms of atomic structures concerned with free electrons. Thus, the creation of a metal/ceramic interface causes an electron discontinuity and can require more

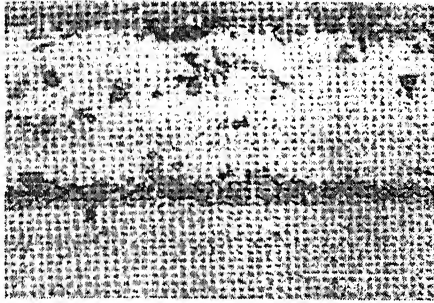


Fig. 2.6 – Microstructure of an aluminium / active solder (Sn – Ag – Ti) joint interface showing metallurgical interface reactions. ^[18]

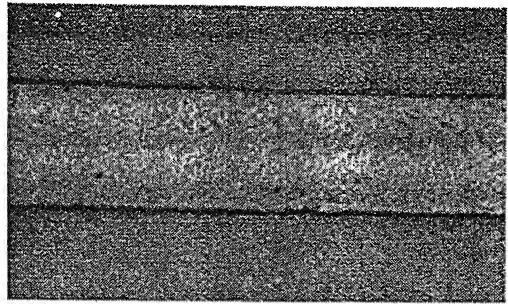


Fig. 2.7 – Microstructure of a titanium / titanium joint with an active solder (Sn – Ag – Ti) filler metal. ^[18]

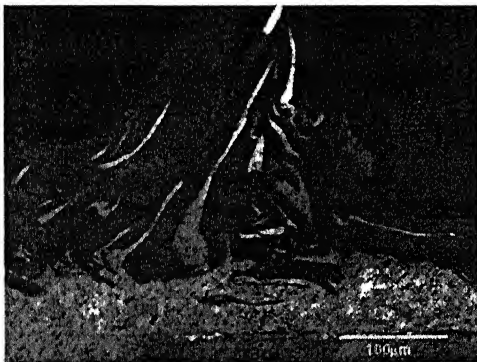


Fig. 2.8 – Graphite foam joined to aluminium base using active solder (Sn – Ag – Ti). ^[18]

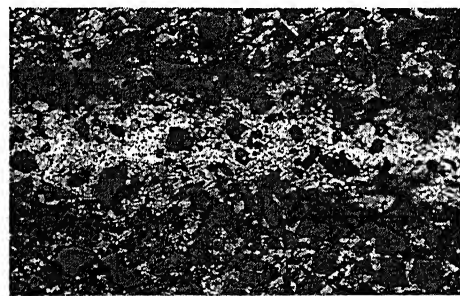


Fig. 2.9 – Al: SiC joined with active solder filler metal. ^[18]

energy than the formation of a ceramic surface and hence result in poor wettability.

Brazing has many advantages over welding and in most cases; the cost is very competitive with welding. The advantages of brazing include cosmetic appearance, cleanliness and baked-out surfaces. Wetting of ceramic surfaces is a prerequisite for brazing and it can be obtained by two general methods: (1) applying coatings that promote wetting to the ceramic surfaces prior to brazing; and, (2) alloying braze filler metals with elements that activate wetting.

The Moly – Manganese Process or Sintered – Metal – Powder Process.

Moly-Manganese paint is applied by brushing or screen-printing onto the ceramic surface to be brazed to form a 25 μm (0.001") metallic layer after sintering at around 1400°C in wet hydrogen (dew point around 30°C). The process is shown schematically in Fig. 2.10. ^[9]

The mechanism that makes this metal to ceramic bond work is that during the sintering process, the glass phase in the ceramic is drawn into the interstices of the Molybdenum layer. The effect of the Manganese is two-fold:

1. On heating during the sintering, the manganese is oxidized to form manganese oxide, which, at temperature, enhances the permeation of the glass phase into the molybdenum layer.

2. It penetrates down the ceramic grain boundaries and changes the properties of the glass phase in the ceramic. This change decreases both the thermal expansion mismatch between the Molybdenum layer and the ceramic, and also alters the glass transition temperature. As a result, there is less residual stress at the metallized interface, which leads to a stronger bond than had previously been achieved with the refractory metals alone. Once a defect free Moly-Manganese layer has been successfully applied, a thin layer of Nickel or Copper is usually applied to prevent oxidation of the Mo-Mn layer and promote wetting of the braze alloy. Usually, Nickel around 5 μm is deposited either by electroplating, electro-less plating or by the reduction in hydrogen of nickel oxide paint.

The ceramic now has a surface suitable for brazing with conventional braze alloys such as Silver 72% / Copper 28% Eutectic or the range of Gold / Copper alloys. A hard vacuum of better than 10-5 torr and a leak rate of better than 5 Microns / Hour is

recommended for the brazing, but successful joints can be obtained when necessary using a high purity inert gas such as Argon or Helium, or a dry reducing atmosphere of hydrogen with a dew point of -70°C . ^[1, 9]

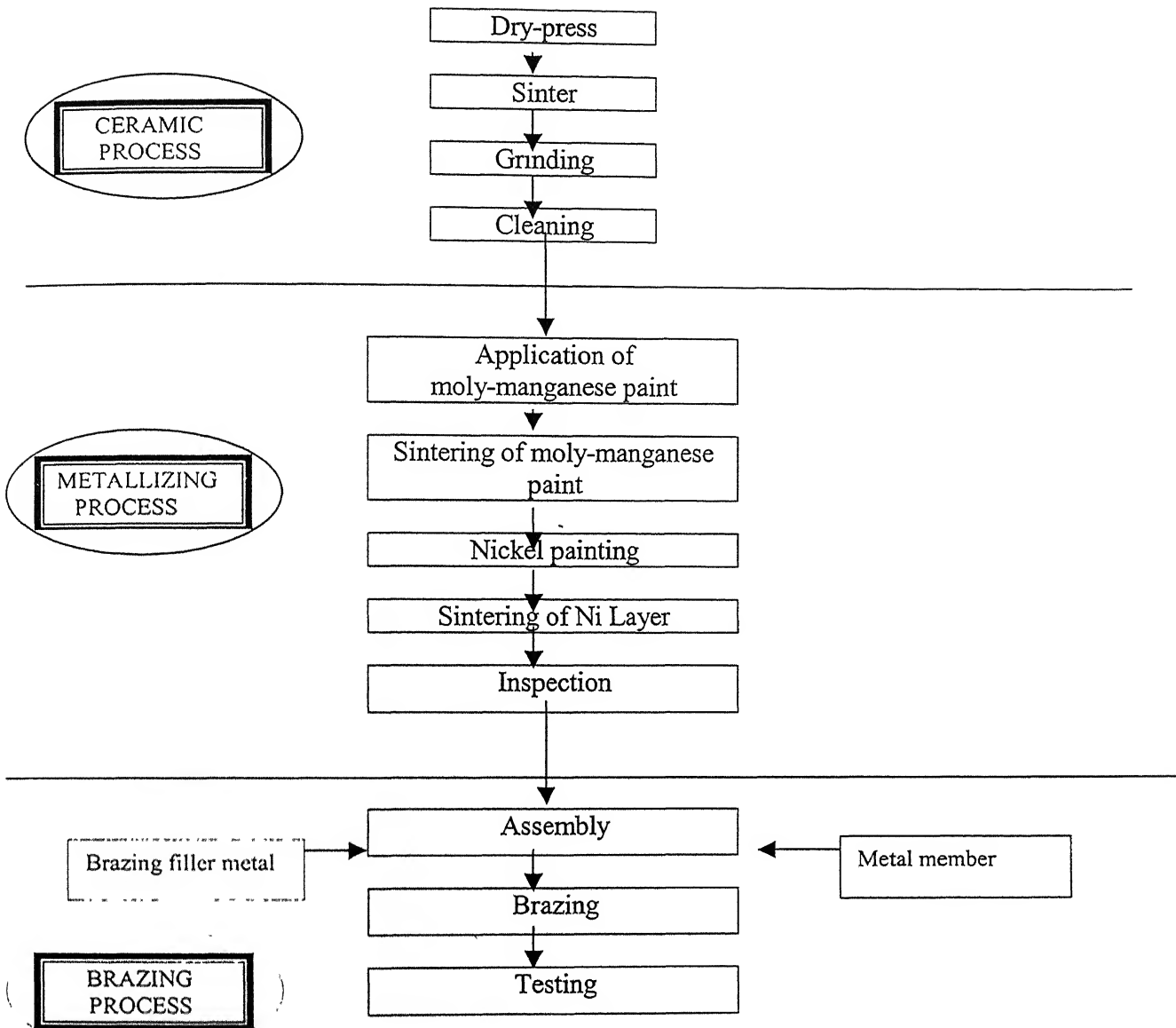


Fig. 2.10 - Schematic diagram of Moly-Manganese process. ^[9]

Vapor Coating Process.

Another variation of the metallizing approach is the use of vapor deposited coatings of metals to promote the wetting of ceramics. The ability of metallic vapor coatings to enhance the brazing characteristics of ceramics has been known for some time, but has only been exploited for practical purposes in recent years. The key element of the process is the deposition of a thin coating, generally of a reactive metal such as Ti, onto ceramic surfaces prior to brazing. These coatings either isolate the ceramic from directly contacting the liquid filler metals, or they react with the ceramic during the brazing process. The coatings typically are made by the sputter coating process or the electron beam vapor coating process, and coating thicknesses of a few microns or less appear to be satisfactory for promoting wetting. Some examples of the use of this technique include: ^[1]

- (a) Sputter – deposited coatings of Ti were used to enhance the wetting of partially stabilized zirconia (PSZ) and alumina by Ag – 30 Cu – 10 Sn (B_{Ag} – 18) filler metal. For brazing PSZ to cast iron or Ti, joint shear strengths in the range of 30 Ksi (200 Mpa) were obtained.
- (b) Vapor – deposited coatings of Hf, Ta, Ti, and Zr have been used to promote the wetting of SiC and Si₃N₄ by a wide variety of filler metals including Ag – 28 Cu (B_{Ag} – 8), Au – 18 Ni (B_{Au} – 4), and Au – 25 Ni – 25 Pd (B_VAu – 7).

The Active Brazing Alloy Process.

In active brazing, the ceramic and metal components are brazed directly onto the surface of the component using an active braze alloy [ABA].

ABAs contain elements such as Titanium or Vanadium which react chemically with the ceramic component, and enhance the wetting ability of the braze alloy onto the ceramic.

The process mechanism that enables the ABA to wet the ceramic is a chemical reaction between the active element (Ti, Zr, Hf or V etc.) in the braze alloy with the ceramic. The exact reaction products, however, are not so well understood. In all cases reported, the reaction products with Ti are many and varied, with many complex reactions taking place in the same series of experiments. Active Braze Alloys are available commercially in different forms such as wire, sheet, bar, powder etc.

Mixed Powders: Titanium or Titanium Hydride powder can be mixed with conventional braze alloy powders to form slurry with a binder. Titanium Hydride decomposes at around 500°C into metallic Titanium to form the active element.

Coated Ceramics A simple method is to deposit a titanium layer onto the ceramic, and braze using a conventional braze alloy system. Deposition methods can be sputter coating, thin foils, titanium brush or screen paints, etc.

Clad Filler Metals. Titanium cored wires or a titanium "sandwich" foil are also made commercially. These products have the additional advantage over the previous two types because the Titanium is protected from the out-gassing products during furnace heating by the conventional braze alloy cladding. The disadvantage is that the active metal is not exposed to the ceramic surface until melting has taken place, which gives a poor initial wetting contact angle, and can sometimes lead to a complete failure in the technique. ^[9]

Most noble metals exhibit contact angle more than 110° on refractory oxides or graphite surface. On adding active element like Cr, Ti, V, Hf, Zr, Nb, Th etc. to the filler metals, wettability is improved. The contact angle of pure silver, pure copper or Ag – Cu on mullite ($3\text{Al}_2\text{O}_3 \cdot 2\text{SiO}_2$), alumina, silicon nitride, aluminium nitride or graphite is more than 90° even at temperature of 1100°C . But addition of 1 to 5 at. pct. of Ti or Zr decreases the contact angle to zero. This is due to the fact that the Ti or Zr has high affinity with oxygen, which is adsorbed, on the ceramic – metal interface. ^[3, 11] Selected data on contact angles for various liquid metals and alloys on Al_2O_3 and Si_3N_4 substrates are given in Table 2.3 ^[28].

In general Ti was used as an active element by Mizuhara and Oyama. ^[15] Valentine et al. ^[20] showed that 8 at. pct. of Ti in copper is sufficient for the wetting of Al_2O_3 . The Ti percentage was decreased if the third element like Sn, In, Ag, Au was added. Particularly, the addition of Sn or In decreased the surface energy of copper and enhanced the activity of Ti. Subsequently, Nicholas ^[21] also showed that the addition of 2 at. pct. of Ti in Ag – 28 wt pct. Cu is equivalent to that of Cu – 12 Ag – 22 Ti, with the help of the phase diagram. Previous work also showed that the addition of 1 to 5 at. pct. of Ti or Zr in Ag – Cu eutectic drastically decreased the contact angle and increases its wettability on ceramic surface. The addition of 10 to 15 at. pct. of

In in Ag – Cu eutectic required 1 at. pct. Ti for sufficient wetting. Loehman et al. ^[22, 23] have reported that Ag – Cu – In – Ti was more effective than Ag – Cu – Ti.

The reaction products of Ti with different ceramics are different. In the case of oxide ceramics such as alumina, Ti forms TiO, TiO₂ and Ti₂O₃ with oxygen, due to its high affinity with oxygen. Nicholus ^[21] has reported that metallically bonded TiO was responsible for the wettability of ceramics. In Ti – Cu – Ag filler metals Ti₂Cu, TiCu, TiCu₂, Ti₃Cu₄, Ti₂Cu₃ and TiCu₄ are the binary phases of Ti and Cu, as reported by Murray. ^[24]

Samandi et al. ^[25] showed that if Ti is implanted on alumina ceramic, TiO₂ metallic like compound formed. This changes the nature of bonding of alumina and enhances its degree of wetting. The Ti – implanted ceramic can be brazed with copper by using non-reactive filler metals, which was not possible for non-implanted alumina. Xien et al. ^[26] have found that Ag – Cu eutectic with 5 at. pct. Ti brazing alloy has very low oxidation resistance. This can be improved by using the addition of 5 at. pct. of aluminium to the filler metal, without affecting its wettability. This was due to the formation of adherent protective CuAl₂O₄ film. The addition of Cr, Ni or Re did not improve its oxidation resistance. The Ti₃Al and TiAl₃ intermetallic compound were formed with Ti near alumina ceramic.

Table 2.3: Selected data on contact angles for various liquid metals and alloys on Al_2O_3 and Si_3N_4 substrates. ^[28]

| Metal | Al_2O_3 | | Si_3N_4 | |
|-------------------|--------------------------------|----------------------------|--------------------------------|----------------------------|
| | Temperature ($^{\circ}C$) | Contact Angle (Degrees) | Temperature ($^{\circ}C$) | Contact Angle (Degrees) |
| Sn | 1050 | 145 | 1100 | 144 |
| Ag | 1000 | 159 | 1100 | 155 |
| Au | 1100 | 138 | 1100 | 157 |
| Cu | 1100 | 148 | 1100 | 131 |
| Ni | 1500 | 120 | ----- | ----- |
| Fe | 1550 | 128 | ----- | ----- |
| Cr | 1900 | 85 | ----- | ----- |
| Cu – 2 Ti | 1100 | 142 | ----- | ----- |
| Cu – 3 Ti | ----- | ----- | 1200 | 64 |
| Cu – 25 Ti | 1100 | 15 | ----- | ----- |
| Ag – 28 Cu | ----- | ----- | 900 | 167 |
| Ag – 28 Cu – 2 Ti | ----- | ----- | 900 | 50 |
| Ag – 28 Cu – 5 Si | ----- | ----- | 900 | 129 |

Table 2.4: Literature at a glance on active brazing of ceramics. ^[27]

| Investigators | Year | Ceramic Substrate | Active Braze Alloy |
|---|-------|--------------------------------|--|
| Valentine, Nicholus & Waite | 1980 | Al ₂ O ₃ | Cu – 8 Ti |
| Nicholus | 1989 | Al ₂ O ₃ | Ag – 2 Cu – 2 Ti |
| Xian, Si, Zhou, Shen & Li | 1991 | Al ₂ O ₃ | Ag – 28 Cu – 5 Al – 5 Ti |
| Loehman, Tomsia, Pask & Johnson | 1990 | Si ₃ N ₄ | Ag – Cu – Ti |
| Peteves, Paulasto, Ceccone & Stamos | 1998 | Si ₃ N ₄ | Au – 36 Ni – 5 V – 1 Mo |
| Tillman, Lugscheider, Schlumbach, Manter & Indacochea | 1998 | Si ₃ N ₄ | Ag – Cu – Ti, Pd – Ni – Ti, Pd – Cu – Ti, Pd – Cu – Pt – Ti |
| Loehman | ----- | Al ₂ O ₃ | Ag – 28 Cu – 10 Ni – 1 Ti |
| Timley, Huddleston & Lacey | 1998 | SIALON | Ag – Cu – Ti |
| Santella & Pak | 1993 | ZrO ₂ | Ti Coating |
| Hao, Wang, Jin & Wang | 1995 | ZrO ₂ | Ag ₅₇ Cu ₃₈ Ti ₅ |
| Yano & Suematsa | 1988 | SiC | Ag – Cu – Ti |
| Lee & Lee | 1992 | SiC | Cu – Ti |
| Iwamoto & Tanaka | 1998 | SiC | Ag- Cu – Ti |

Table 2.5: Commercial active braze alloys (ABAs). ^[28]

| Alloy Composition (wt. %) | Trade Name | Solidus Temp. (°C) | Liquidus Temp (°C) | Brazing Temp. (°C) | Manufacturer |
|----------------------------------|-------------|--------------------|--------------------|--------------------|------------------|
| Ag - 19.5 Cu -5 In - 3Ti | CB1 | 730 | 760 | 850-950 | Degussa |
| Ag - 4 Ti | CB2 | 970 | 970 | 1000-1050 | Degussa |
| Ag - 26.5 Cu - 3 Ti | CB4 | 830 | 850 | 810-900 | Degussa |
| Sn - 10 Ag - 4 Ti | CS1 | 221 | 300 | 850-950 | Degussa |
| Pb - 4 In - 4 Ti | CS2 | 320 | 325 | 850-950 | Degussa |
| Ag - 24 Cu -14.5 In - Ti | Lucanex616 | 605 | 715 | 700-750 | Lucas - Milhaupt |
| Ag - 28 Cu -0.5 Ni - Ti | Lucanex715 | 780 | 795 | 850-950 | Lucas - Milhaupt |
| Ag - 42 Cu - 2 Ni - Ti | Lucanex559 | 770 | 895 | 954 | Lucas - Milhaupt |
| Ag - 27 Cu - 4.5 Ti | Ticusil | 830 | 850 | 850-950 | WESGO |
| Ag - 27.5 Cu - 2 Ti | Cusil-ABA | 830 | 850 | 810-950 | WESGO |
| Ag - 23.5 Cu - 14.5 In - 1.25 Ti | Incusil-ABA | 620 | 710 | 845 | WESGO |
| Ti - 33 Ni | TiNi | 900 | 970 | 970-1000 | WESGO |
| Ti - 15 Cu - 15 Ni | TiCuNi | 910 | 960 | 960-1000 | WESGO |
| Au -3 Ni - 0.6 Ti | Gold-ABA | 1003 | 1030 | 1025-1030 | WESGO |

Table 2.6: Experimental active braze alloys (ABAs). ^[28]

| |
|--------------------|
| Ti - 48 Zr - 4 Be |
| Ti - 49 Cu - 2 Be |
| Ti - 25 Zr - 2 V |
| Cu - 26 Ag - 29 Ti |
| Cu - 20 Au - 18 Ti |
| Ti - 25 Cr - 21 V |
| Cu - 43 Ti |
| Ti - 30 Ni |

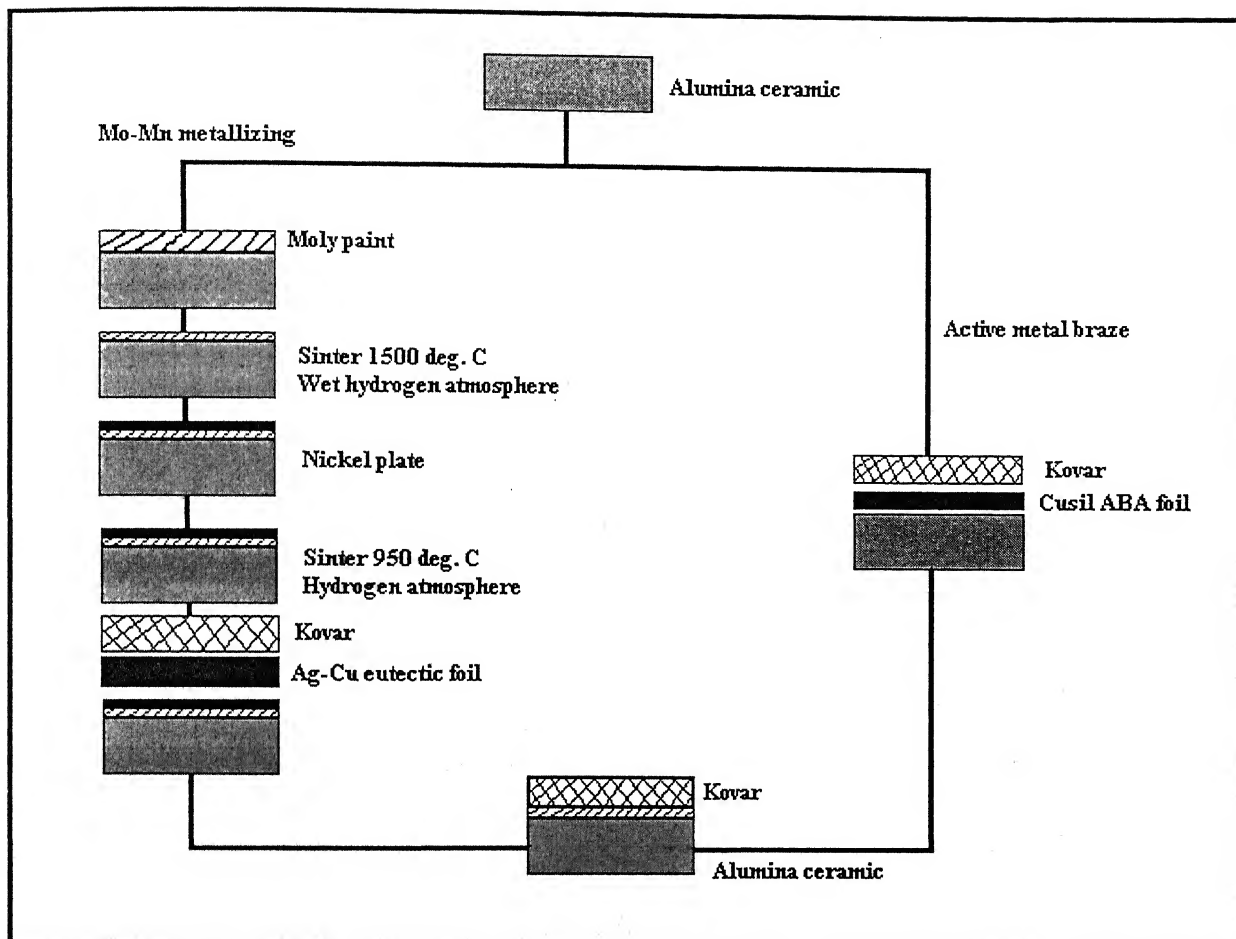


Fig. 2.11 – Schematic representation of two techniques for brazing ceramics: the Mo – Mn process, and active filler metal brazing.^[16]

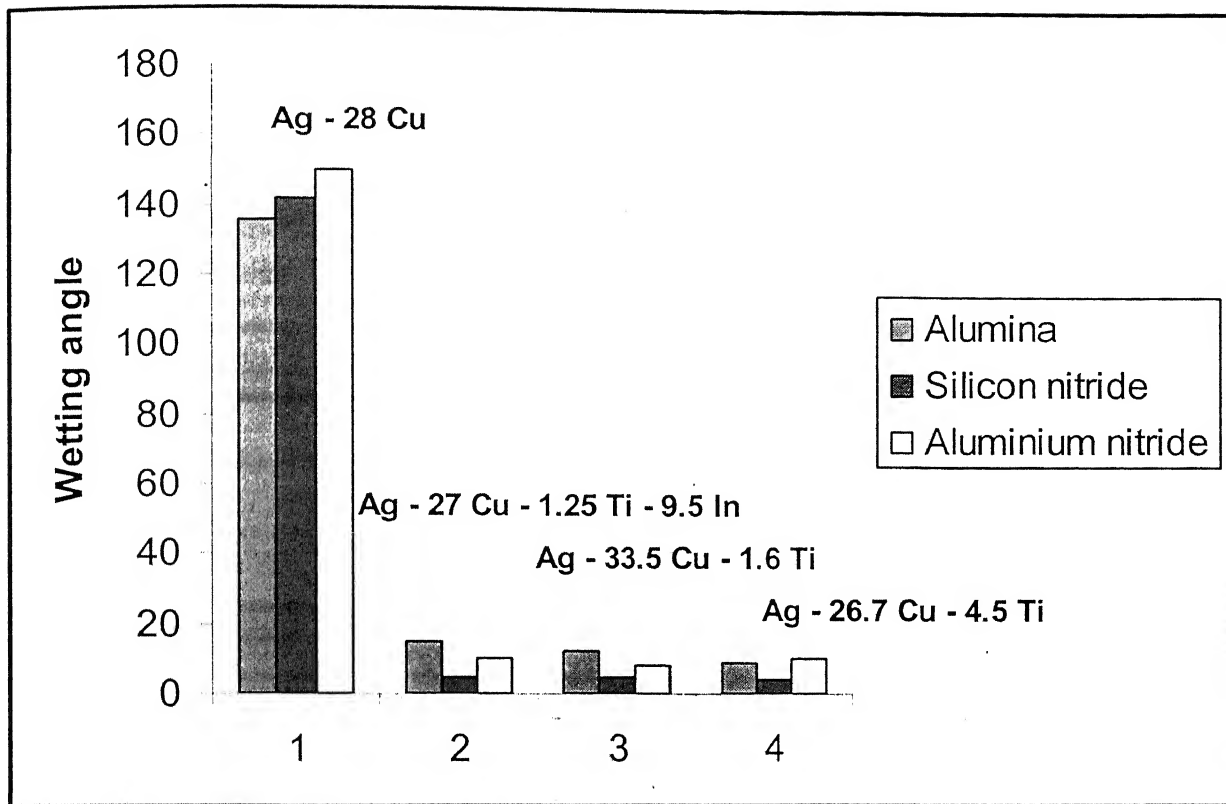


Fig. 2.12 – Wetting angle of Ag – Cu brazing metal with and without Ti addition for various ceramics. ^[13]

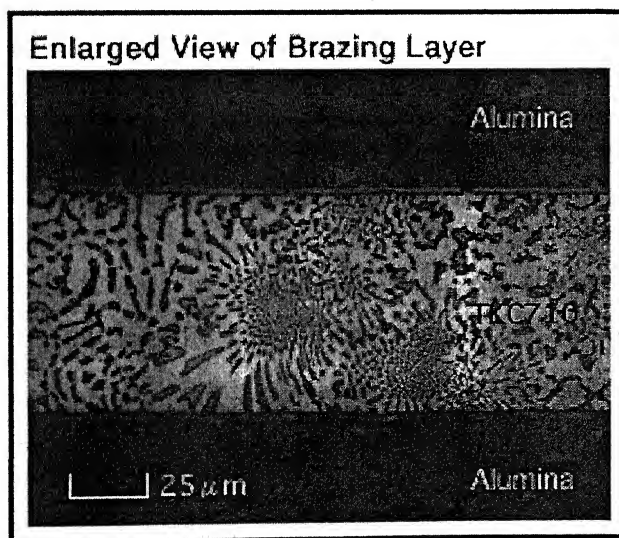


Fig. 2.13 – SEM micrograph of the brazing layer. ^[2]

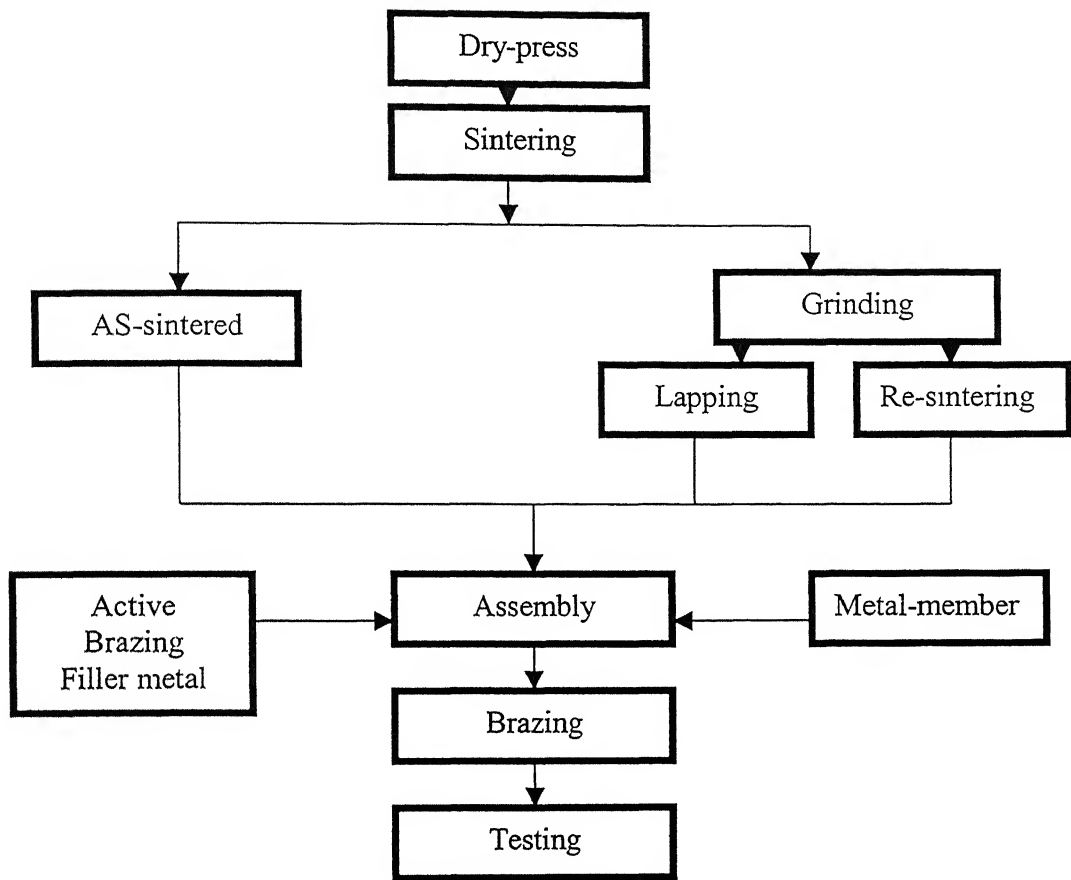


Fig. 2.14 – Flow chart of active brazing of ceramic. ^[9]

2.3 Stainless Steel Brazing.

Stainless steel alloys as a group are not difficult to braze, but those alloys that also contain Ti or Al require additional precautions to prevent alloy oxidation during the brazing cycle. Excellent results can be obtained when standard wrought stainless steels are brazed.

The brazeability and weldability of these steels do vary with composition. The quality of brazed joints depends on the selection of the brazing process, process temperature, filler metal and the type of protective atmosphere or flux that is used. These choices must be compatible with the intended performance of the brazed item. ^[1]

Brazeability.

High content of chromium that is present in stainless steels results in formation of chromium oxide film on the surface of all stainless steels. Film of titanium oxide may be formed on the surfaces of titanium-stabilized stainless steels, such as type 321. If these oxides, which are both refractory and strongly adherent, are inadequately removed, they will retard wetting of the base metal by the molten filler metal.

The formation of chromium oxide is accelerated when stainless steels are heated in air. Although the oxide may have been removed from the surface by chemical cleaning at room temperature, a new oxide layer that seriously interferes with wetting will rapidly form when the steel is heated in air to the brazing temperature.

Filler Metals.

A wide variety of filler metals is available commercially for the brazing of stainless steel. The factors to consider in selecting a filler metal for a particular application include the following:

- (a) Service conditions, including operating temperature, stress, and environment
- (b) Heat treatment requirements for martensitic or precipitation hardening steels
- (c) Brazing process
- (d) Cost

(e) Special precautions, such as sensitization of unstabilized austenitic stainless steels at certain temperatures.

Commercially available brazing filler metals used for joining stainless steels are commonly the copper, silver, nickel, cobalt, platinum, palladium, and gold-based alloys.

A number of silver and copper based braze filler metals (such as BAg-1, BAg-1a, BAg-2, BAg-3, BAg-5, BAg-6, BAg-8, BAg-8a, BAg-18, BAg-19, BAg-24, BAg-29, BVAg-86 and RBCuZn, BCuP etc.) are used for brazing different grades of stainless steels.

Nickel base filler metals are used primarily where extreme heat and corrosion resistance are required. They are commonly used in the manufacture of components for jet and rocket engines, chemical processing equipment, and nuclear reactors. BNi filler metals commonly are used on stainless steels for oxidation resistance to temperatures up to 982 – 1093°C. Filler metals BNi-1, BNi-2, BNi-3, and BNi-4, which contain boron, tend to erode thin sheet metal because of their reaction with many base metal compositions. Therefore, time at braze temperature and the quantity of filler metal should be carefully controlled when these filler metals are used.

Filler metals based on gold, platinum, palladium, and their alloys, such as gold-nickel, gold-nickel-chromium, gold-nickel-palladium, copper-platinum, and silver-palladium-manganese, are useful for brazing heat and corrosion resistant components. BAu-4 is used where maximum corrosion resistance is necessary, such as resistance to sulphur bearing gases and compounds.

Process and Equipment.

Stainless steels can be brazed with any brazing process. Much controlled atmosphere brazing is performed on stainless steels, and the acceptability of this technique is attributed to the ready availability of reliable atmospheres and vacuum furnaces. The primary requirements are that the furnaces have good temperature control at brazing temperature (plus or minus 8°C is desirable) and be capable of fast heating and cooling. All gases used in atmosphere furnaces must be of high purity (>99.995 percent pure). Commercial vacuum brazing equipment operates at pressures varying from 10^{-5} to 10^{-1} torr. The necessary vacuum

level depends upon the particular grade of stainless steel, with those containing titanium or aluminium requiring better vacuums.

Precleaning and Surface Preparation.

Stainless steels require more stringent precleaning than do carbon steels. During the heating cycle, residual contaminants often form tenacious films which are difficult to remove by fluxes or reducing atmospheres. These films form as a direct reaction between the contaminant and stainless steel surface.

Precleaning of stainless steels for brazing should include a degreasing operation to remove any grease or oil films. The joint surfaces to be brazed also should be cleaned mechanically or with an acid pickling solution. Wire brushing should be avoided, but if necessary, stainless steel brushes should be used. Cleaned surfaces should be protected to prevent soiling by dirt, oil, or fingerprints. For best results, parts to be brazed should be brazed immediately after cleaning. When this is not practical, the cleaned parts should be enclosed in containers such as sealed polyethylene bags or dessicator jars to exclude moisture and other contaminants until the part can be brazed.

Fluxes and Atmospheres.

Stainless steel assemblies are routinely furnace brazed in atmospheres of dry hydrogen, argon, helium, dissociated ammonia, or vacuum, without the aid of flux. When fluxes are required, there are a number of special compositions available for use with stainless steels.

Dissociated ammonia atmospheres should be used with caution. Certain stainless steels can be nitrided at some brazing temperatures. Nitriding produces a hard surface that can be either beneficial or detrimental depending on the service requirements of the component. Nitriding can be detected by an increase in surface hardness or by metallographic examination.

Oxides of aluminium and titanium can not be reduced in atmosphere furnaces at ordinary brazing temperatures. If these oxides are present in small amounts, satisfactory brazes can be obtained by the use of high purity gas atmospheres and vaporizing flux. When these elements are present in quantities exceeding one or two percent by weight, the metal

surface should be cleaned and nickel-plated instead of using fluxes or vacuum atmospheres. Nickel plating will prevent the formation of harmful oxides and can be an effective means of limiting embrittlement or erosion of base metals. Thickness of the electrolytic nickel plating should be kept in the range of 0.005 to 0.05 mm. The thickness of plating should be controlled so that it is dissolved into the brazing filler metal, preventing the possibility of failure occurring in the remaining plating layer. ^[1]

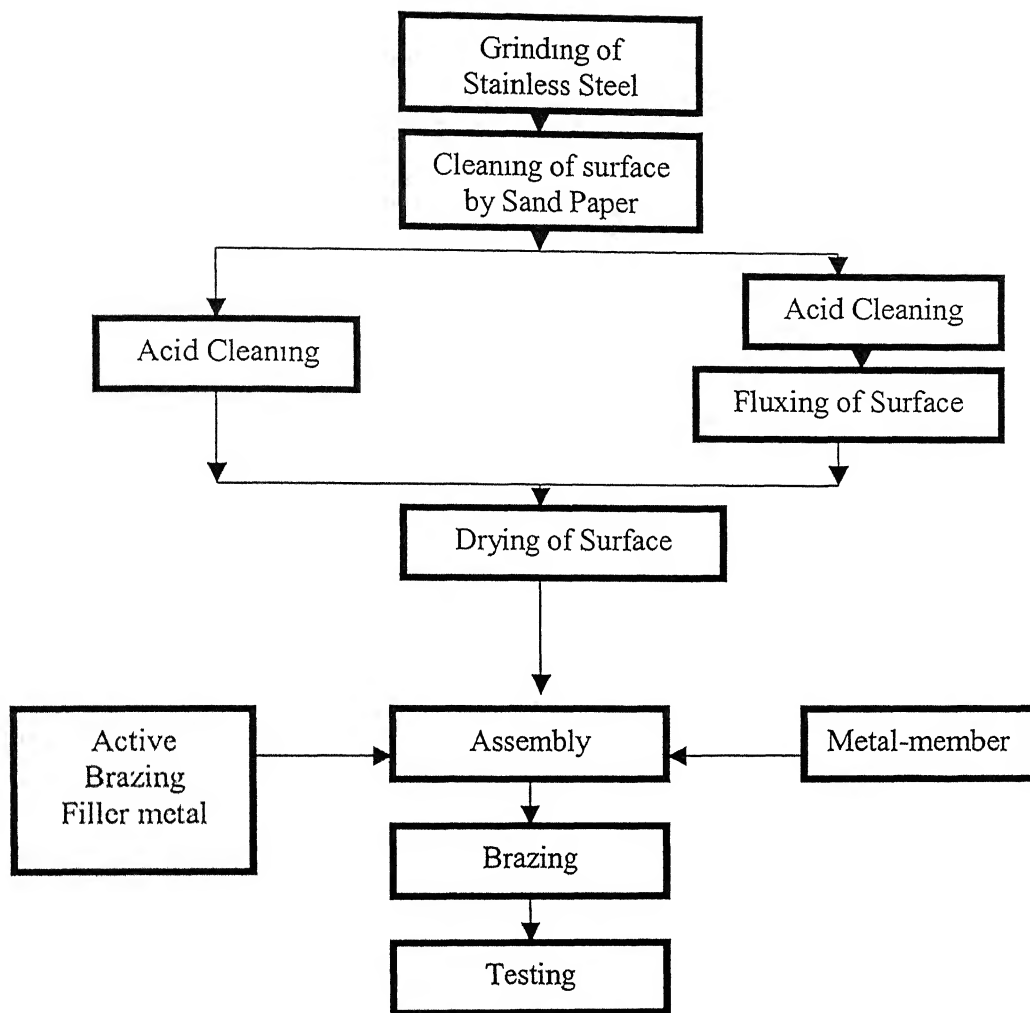


Fig. 2.15 – Flow chart of brazing of stainless steel. ^[9]

2.4 Mechanical Testing of Joints.

The most usual requirement of soldered and brazed joints is to provide bonds between components that are sufficiently strong and durable for meeting the design life of the assembly. For this reason, the strength of joints is frequently measured in various stressing modes – typically tensile, shear, peel, and cyclic fatigue, depending on the intended application. Mechanical testing should also encompass the effects of corrosion on the mechanical properties of the brazed components.

The set of properties that are of importance tend to be application specific and will depend on the stress, temperature, and chemical conditions that the assembly will experience in service. This environmental regime is usually complex and interactive, and a testing schedule for quality control and assessment purposes can only approximate the set of conditions that apply in practice and thus will be necessarily selective. For practical and economic reasons, the testing is often limited to scaled-down specimens of simplified geometry. Despite the apparent remoteness of the idealized test pieces from products in the field, it is frequently possible to develop test procedures that can offer a high degree of confidence regarding the adequacy of the product for the intended application environment.

Measurement of the joint strength provides the most direct indication of whether a soldered or brazed joint has achieved the rudimentary level of mechanical integrity necessary to satisfy the function of an assembly. Assessment of mechanical properties usually involves destructive tests in which representative or simplified assemblies are stressed until failure occurs. There is a benefit in carrying out the testing on a given parent/filler combination using different stressing modes in as much as this is more likely to furnish a clearer picture of the mechanism of failure and the critical flaws that are responsible than if a single test configuration is employed. Several difficulties are associated with the mechanical testing of joined assemblies for quality control and assurance purposes.

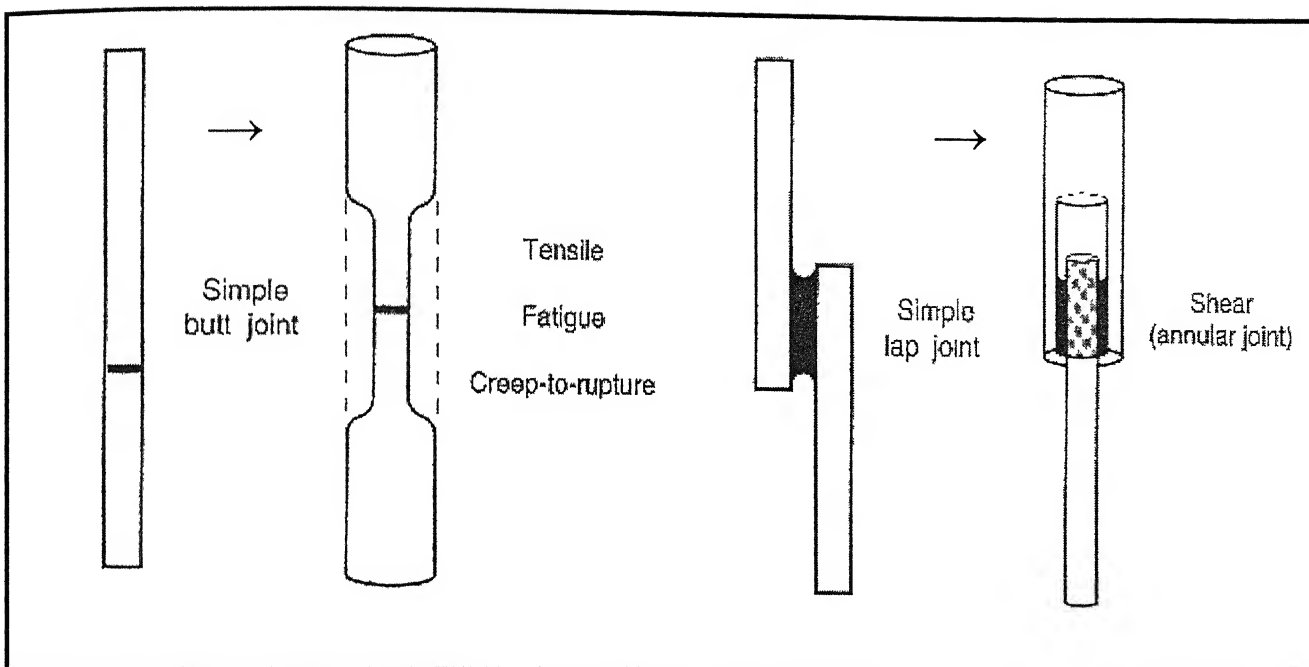


Fig. 2.16 – Test piece configurations based on simple butt and lap joints. ^[16]

Devising mechanical tests that will furnish usable data. Assuming that the conditions which operate during the service life of an assembly are known, tests that reproduce these conditions often are too complicated to be practical. In such circumstances it is common practice to carry out simplified tests, designed to provide a high degree of semi quantitative discrimination of joints. One sort of simplification that is widely applied is to test under resolved stresses, for example, pure tensile or pure shear. For this purpose joints of simplified geometry are used, notably butt and lap joint configurations (Fig. 1). Resolution of the actual applied stresses that develop in the test pieces is usually difficult, because a test intended to measure tensile strength, for example, may inadvertently subject the joint to shear or peel forces.

The test conditions will generally have a significant influence on the results obtained. Associated parameters that need to be closely defined include strain rate, test temperature, test environment, and size and shape of any fillets.

CHAPTER 3

PLAN OF WORK

The aim of this work is to study the wetting behavior of different types of brazing alloys in joining of stainless steel to stainless steel, stainless steel to ceramic and ceramic to ceramic. The present work also deals with the study of mechanical testing of the brazing alloys as well as the brazed stainless steel rods. This chapter gives in brief the plan of complete work.

3.1 Fabrication of Brazing Alloys and Ceramic Pellets.

Arrangements are made to prepare brazing alloys, such as, Ag – 28 Cu, Ag – 27.4 Cu – 2 Ti, Ag – 26.6 Cu – 5 Ti, Ag – 1 Ti, Ag – 2 Ti, Cu – 1 Ti and Cu – 2 Ti are prepared in the laboratory. Ceramic pellets of 99.99 % pure alumina powder are prepared using a 20 T hydraulic press and then, these pellets are sintered in a box furnace at 1600°C for 9 hours. Melting range of the prepared alloys is determined by measuring the temperature responses during cooling cycles.

3.2 Joining Experiments.

A system is developed to heat pieces of stainless steel and ceramic together in vacuum by preplacing the brazing alloy between the two.

3.3 Mechanical Testing.

Strength measurements of the brazing alloys as well as the industrially and vacuum brazed stainless steel rod samples are carried out by using a testing machine.

3.4 Microstructural Characterization.

Prepared brazing alloys are subjected to normal metallographic studies. The interface of the brazed test sample is seen under the optical microscope and scanning electron microscope to study the metallurgical changes that may occur during brazing.

3.5 Analysis of Results.

Attempts are made to analyze the results obtained from the microstructural characterization as well as from the mechanical testing experiments.

CHAPTER 4

EXPERIMENTAL PROCEDURES

This chapter describes the experiments carried out in the work. The chapter basically consists of two sections. In first section of the chapter the material, sample details and the equipments used in the study are introduced in brief. Other section gives details of the experiments and tests carried out.

4.1 Materials and Equipments.

4.1.1 Materials.

(1) Stainless Steel Sheet –

The variety of stainless steel that was used as one of the base material was commercial austenitic stainless steel sheet of thickness 2 mm, purchased from local market. The austenitic stainless steel was analyzed to contain 0.075% Carbon, 8.49% Nickel and 17.43% Chromium and 0.06% Titanium. Around 40 numbers of test specimens were made in workshop. Dimensions of the stainless steel test specimens were 10 mm × 5 mm × 2 mm for joining of stainless steel to stainless steel and 10 mm × 10 mm × 2 mm for joining of stainless steel to ceramic. In addition to this, small samples of approximate dimension 5 mm × 5 mm × 2 mm were cut for observing the microstructure of the as-received specimen.

(2) Alumina Powder –

Alumina was used as the ceramic member in this work. For making alumina ceramic pellets, 99.99% pure alumina powder of size 99% of total less than 96.14 μm and 50% of total less than 39.74 μm was used.

(3) Silver –

99.9% pure silver rod of diameter 15 mm was used for fabrication of brazing alloys.

(4) Copper –

99.9% pure copper sheet was used for fabrication of brazing alloys.

(5) Titanium –

99.99% pure titanium rod of diameter 15 mm was used for fabrication of brazing alloys. Semi-elements, inc , USA supplied the material.

(6) Binder –

Polyvinyl Alcohol (PVA) $(-C_2H_4O)_n$, and Dextrine Weiß $(C_6H_{10}O_5)_n \cdot x H_2O$ were used as binder for fabrication of alumina ceramic pellets. 4 - 5 wt% of binder was used for cold compaction. Loba Chemie Pvt. Ltd., Mumbai, supplied the binder.

(7) Sand Paper –

Sand Papers of grades 1/0, 2/0, 3/0 and 4/0 were used for paper polishing.

(8) Graphite Blocks –

The graphite sleeves were used to minimize oxidation of the alloys in furnace during fabrication of brazing alloys. Graphite India Limited supplied the graphite rods.

(9) Ceramic Tube –

Ceramic tubes made up of mullite, having inside diameter 25mm, length 300 mm and wall thickness 5mm were used for fabrication of brazing alloys. Kumar Refractory & Co. supplied the tubes.

(10) Quartz Tube –

Quartz tubes, having inside diameter 14mm, length 300 mm and wall thickness 2mm were also used for fabrication of brazing alloys.

(11) Sampling Tube –

6 mm diameter quartz tubes were used for drawing metal samples using an aspirator.

(12) Molybdenum Rod and Wire –

Pure molybdenum rod and wire was used for stirring the melt and to hold the titanium sheet inside the melt.

(13) Refractory Cap –

One refractory cap was used to minimize the heat loss at the top of the furnace tube during fabrication of brazing alloys.

(14) Etching Reagents –

Aqueous FeCl_3 and freshly Marble's reagent (4 gm. CuSO_4 , 20 ml. Conc. HCl , 20 ml water).

(15) Dead Weight –

High C high Cr steel block was used as dead weight for applying pressure during the brazing experiments.

(16) Acid Solutions –

Acid solutions of HNO_3 , H_2SO_4 , HF , and HCl were used for precleaning of Cu, Ti etc.

(17) Potassium Chloride –

Potassium chloride was used as flux for stainless steel during the dipping experiments.

4.1.2 Equipments.

(1) Silicon Carbide Tube Furnace –

Fabrication of brazing alloys and the brazing experiments were carried out in a vertical silicon carbide tube furnace (outer diameter of the furnace 600 mm and length 400 mm), with silicon carbide heating element and Platinum – Platinum, 10% Rhodium alloy thermocouple. The furnace tube consisted of a one-end closed alumina tube having internal diameter 50mm and length 450 mm. It rested on a refractory base at the bottom. The tube was filled with alumina powder at bottom up to the level of high temperature zone in the furnace. The power of the furnace was supplied using a 40 A single phase oil-cooled auto-transformer with 220 V input and 0-240 V output. The maximum working temperature of the furnace was 1400°C with accuracy of temperature controller being $\pm 5^\circ\text{C}$. One on-off temperature controller and magnetic relay switch were used to keep the temperature of the furnace in a narrow range. The schematic of furnace is shown in Fig. 4.1.

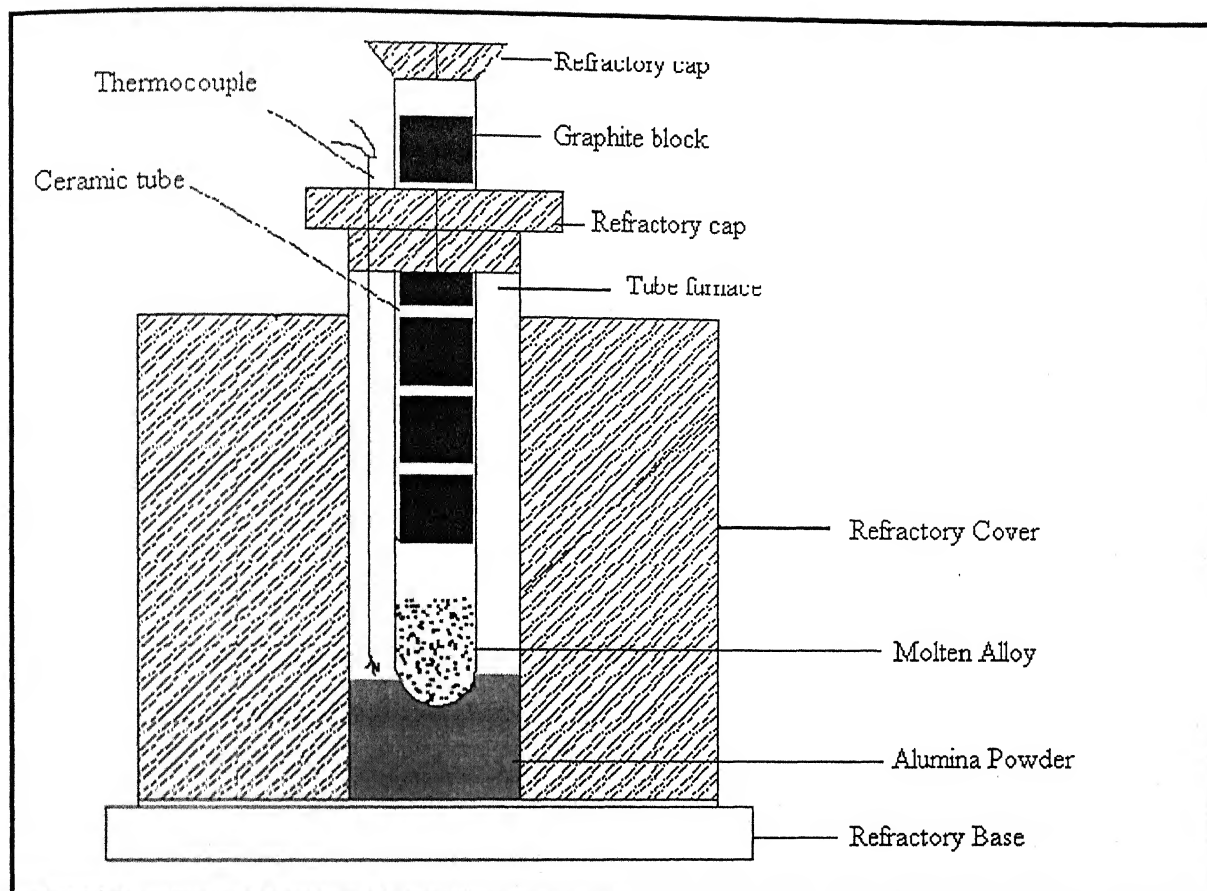


Fig. 4.1: Silicon carbide tube furnace.

(2) Box Furnace –

Box furnace with opening 125 mm wide x 150 mm high x 250 mm deep was used only for sintering of alumina ceramic pellets. The furnace supplied by Bysakh & Co. had the ability to be heated at 1700°C using 8 heating elements of molybdenum disilicate i.e. Kanthal Super 33, type 'U'.

(3) Stainless Steel Tube –

A stainless steel tube of inner diameter 50.8 mm, length 500 mm and thickness 3mm was used to create vacuum inside it. Its one end was closed by welding a 2 mm thick stainless steel plate. The brazing assembly was kept inside a ceramic tube and then, the ceramic tube was gently placed inside this stainless steel tube. The schematic of the assembly is shown in Fig. 4.2. The tube was given a refractory coating to protect the oxidation during each heat.

(4) Digital Balance –

A digital balance, supplied by the Mettler, Germany, was used to determine the weight up to the accuracy of 0.1 mg for fabrication of brazing alloys and alumina ceramic pellets.

(5) Diamond Cutter –

The diamond cutter supplied by Buehler was a low speed saw used for cutting of the titanium, brazing alloys into discs. This was also used to obtain sections from the assembly after bond formation.

(6) Hot Mounting Instrument –

It was used to mount the samples in plastic resin for microstructural characterization purposes.

(7) Grinding Wheel –

A 20 tones (200 kN) hydraulic press on 65.09 mm diameter Ram was used for fabrication of the ceramic pellets. This press was manufactured by Apex Construction Ltd., Gravesend, England.

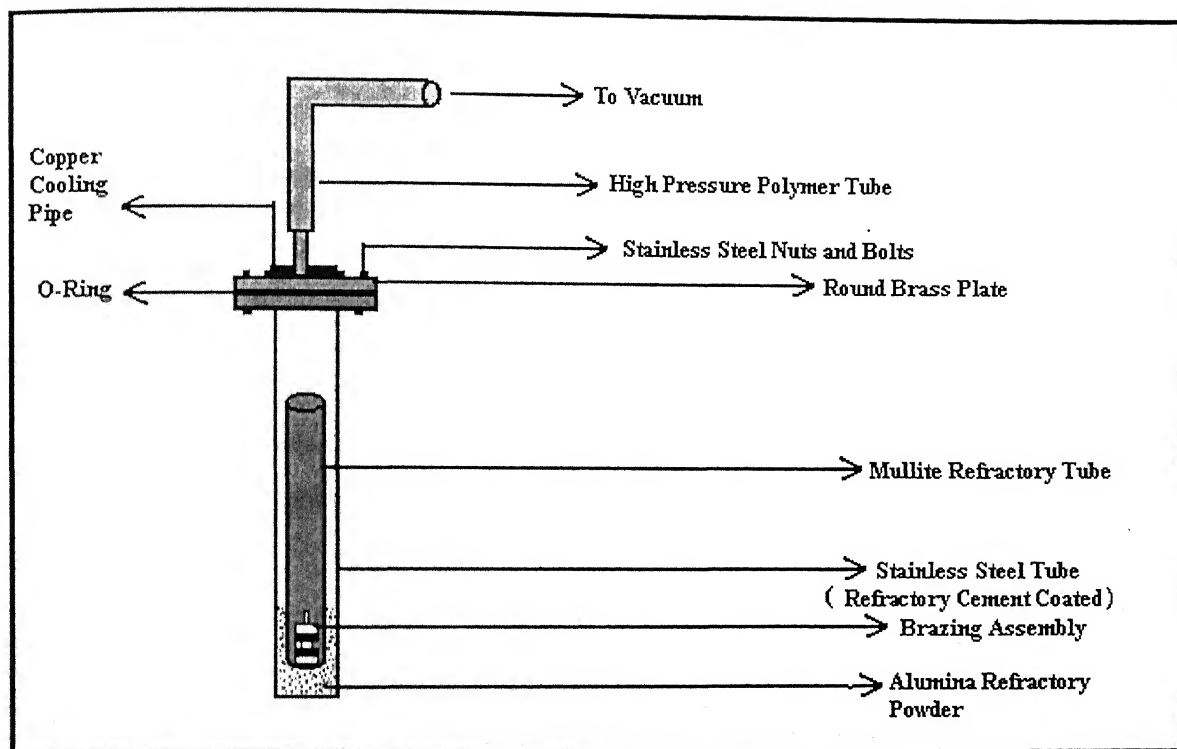


Fig. 4.2: Stainless steel pipe used for creating vacuum.

(8) Polishing Wheel –

Rotating disc polisher was used for mechanical polishing of mounted samples with Alumina powder (1μ size) suspended in distilled water.

(9) Ultrasonic Cleaner –

This was used for further cleaning of the metals' surface, which was to be brazed. The ultrasonic cleaner was supplied by Vibronics Ltd.

(10) Fritsch Particle Sizer –

Fritsch Particle Sizer machine was used to measure the particle size of the alumina powder which was used for making ceramic pellets.

(11) P/M Press –

A 20 tones (200 kN) hydraulic press on 65.09 mm diameter Ram was used for fabrication of the ceramic pellets. This press was manufactured by Apex Construction Ltd., Gravesend, England.

(12) Die –

Diameter of the die used for fabrication of the alumina ceramic pellets was 10 mm. It was made of high carbon high chromium steel.

(13) Sample Holder –

The sample holder of stainless steel was manufactured in the laboratory to hold the sample in the furnace. The sample holder assembly is shown in Fig. 4.3.

(14) Vacuum Pump –

The required vacuum was supplied to the system with the help of rotary type vacuum pump. AC mains supplied the power to this. The pump was manufactured by Hind High Vacuum Co. (Pvt.) Ltd.

(15) Vernier Scale –

One vernier scale was used for accurately measuring the diameter and length of the alumina ceramic pellets before and after sintering at 1600°C for 9 hours.

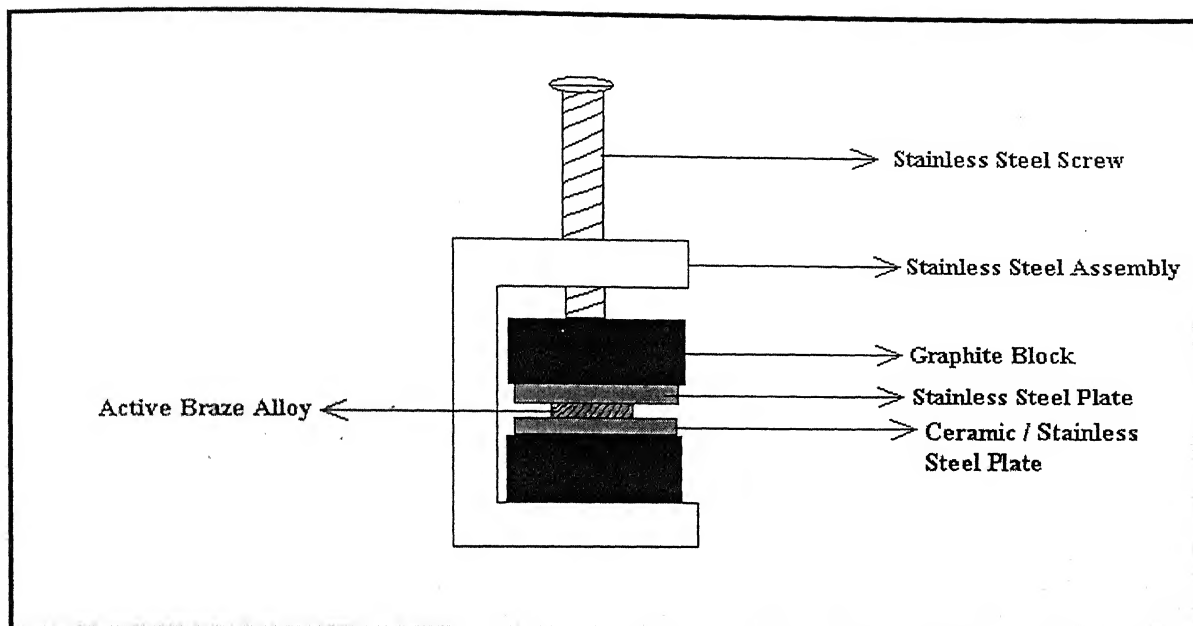


Fig. 4.3: The sample holder assembly with sample.

(16) Torch Brazing Equipment –

For industrially brazing two stainless steel rods one brazing torch was used. The flame used was the oxyacetylene flame.

(17) Silver Brazing Flux and Filler Metal –

Silver brazing flux and Ruptum silver filler metal were used for industrially brazing two stainless steel rods. A.V.S. Products Ltd. supplied these materials.

(18) Universal Testing Machine –

The strength of the alloys as well as the brazed joints was measured using one Instron 1195 Universal Testing Machine.

(19) Metallurgical Microscope –

A Leitz Metallux-3 metallurgical microscope is used for microstructural studies of the alloys as well as the interface of the brazed joints.

(20) Image Analyzer –

Image – Pro Plus, image analyzer version 4.1, is used for scanning of the microstructures.

(21) Electron Probe Micro Analyzer and Scanning Electron Microscope –

Both of these instruments were supplied by JEOL, Japan. These instruments were used for taking photomicrograph of the brazing alloys as well as the interface of the brazed joints.

4.2 Procedures.

Details of the experimental procedure adopted to achieve the goal are given below sequentially.

4.2.1 Fabrication of the Master Eutectic Alloy and Active Braze Alloys.

Eutectic alloy contains 72 wt% Ag and 28 wt% Cu was prepared in the laboratory by melting the required mass in a one end closed mullite tube at around 1100°C in a silicon carbide tube furnace. Graphite blocks were placed inside the mullite tube to minimize the oxidation as shown in the Fig. 4.4. 6 mm diameter rod was obtained from the melt by sucking the liquid metal in a silica quartz tube with using an aspirator. The rod was then cut into small pieces by using a diamond cutter.

For preparing Ag – Cu – 2 Ti, the master eutectic alloy was melt at 1100°C in a one end closed mullite tube. Ti sheet was precleaned in a freshly prepared acid solution, consisting of 5 vol% HF, 5 vol% H_2SO_4 and 90 vol % water. Precleaned and weighed Ti sheet was dipped well inside the molten alloy for 6 hours. The arrangement shown in Fig. 4.5 helped to minimize the oxidation of Ti. The melt was well stirred using Mo wire to homogenize the melt. For preparing other alloys, the same procedure was taken, only the master alloy was changed.

4.2.2 Melting Range Determination.

A Pt – Pt, 10% Rh thermocouple was connected to a temperature-measuring device and the hot junction was dipped inside the melt. A particular alloy was heated up to around 1200°C and then the thermocouple was dipped in the melt as shown in Fig. 4.6. Temperatures were recorded as a function of time during cooling at an interval of 1 minute.

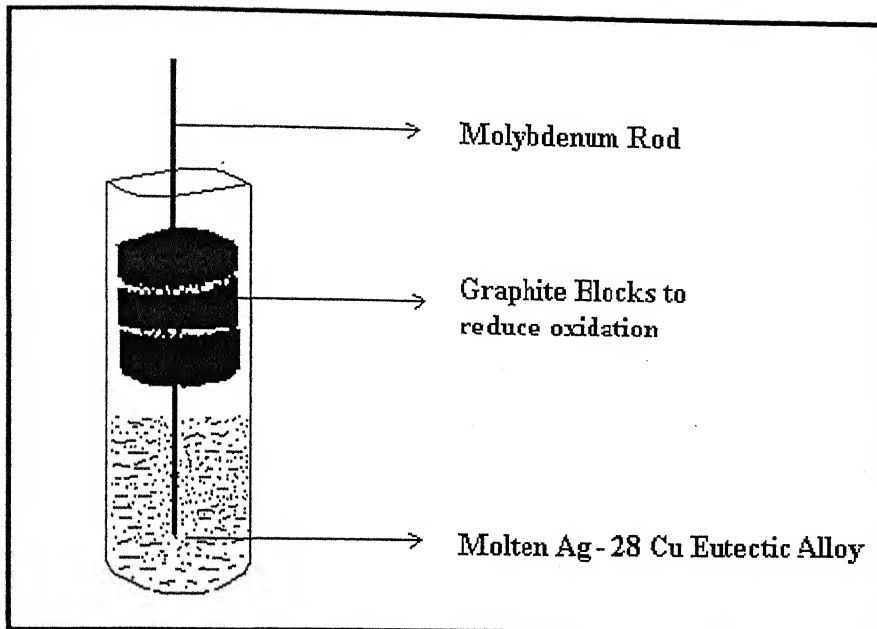


Fig. 4.4: Formation of master eutectic alloy.

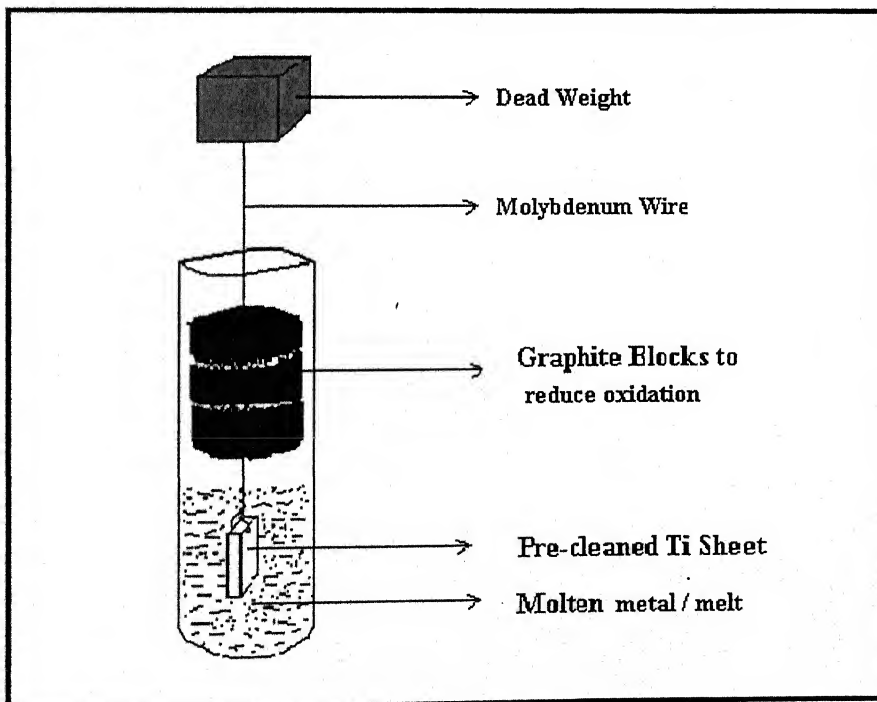


Fig. 4.5: Experimental set up for active braze alloy fabrication.

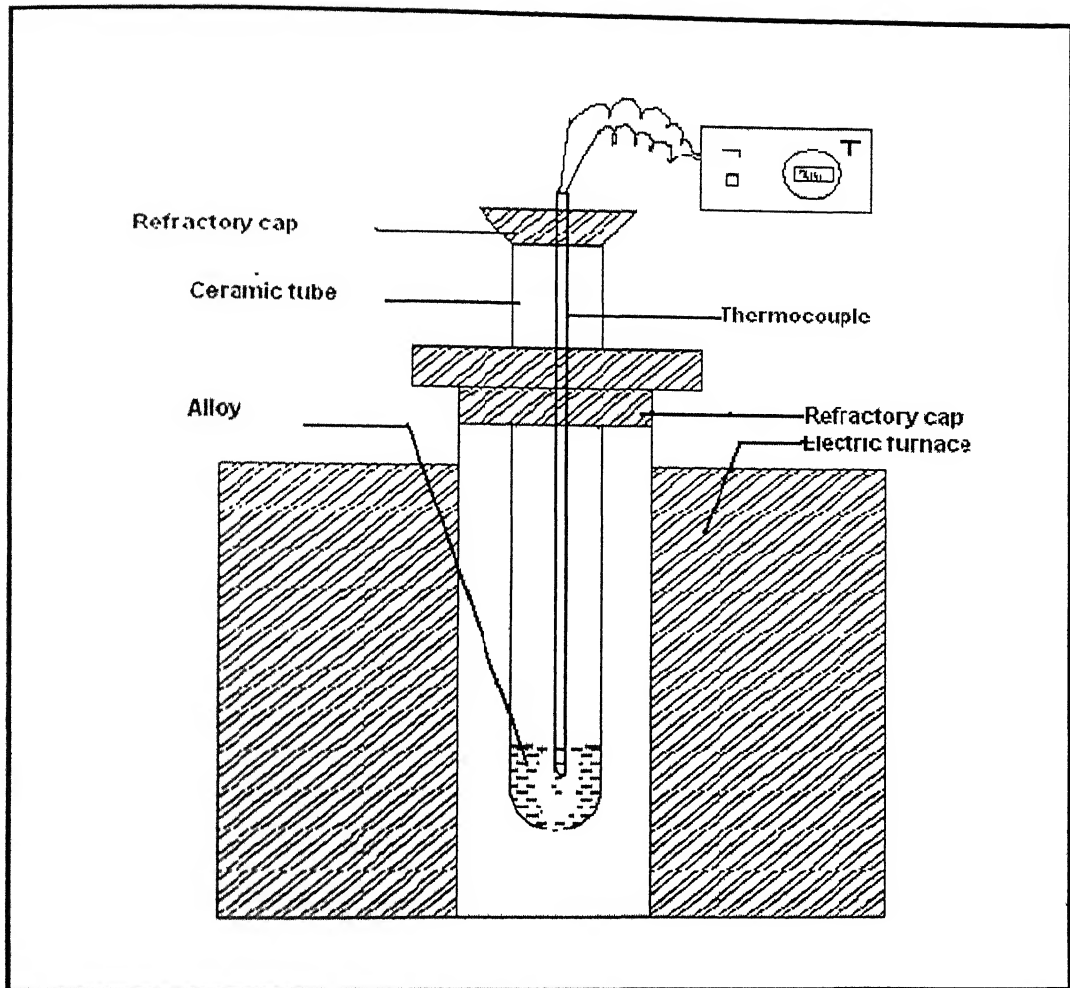


Fig. 4.6: Experimental set up for measuring melting range of the alloys.

4.2.3 Fabrication of Green Alumina Ceramic Pellets.

The green pellets of alumina were fabricated using 99.99% pure alumina powder of size 99% of the total less than $96.14\ \mu\text{m}$ and 50% of the total less than $39.74\ \mu\text{m}$. The pure alumina powder and 4.5 wt% of polyvinyl alcohol and dextrin *weiß* acting as binder was well mixed manually in a porcelain pot. Calculated amount of this mixture was poured into the high carbon high chromium steel die of diameter 10 mm. The die was kept under the hydraulic press and 8 tons of pressure was applied for 5 minutes. After applying pressure, green pellet was carefully brought out of the die and kept in a cotton bed with due care. The whole process was carried out at room temperature. The height and diameter of each green alumina ceramic pellet prepared were measured using a vernier scale.

4.2.4 Sintering of Green Pellets.

The green alumina pellets were sintered at 1600°C for 9 hours in the box furnace. The pellets were furnace-cooled to room temperature and again, the height and diameter of each ceramic pellet were measured using the vernier scale to observe the shrinkage after sintering.

4.2.5 Dipping and Bonding Experiments.

Dipping of Stainless Steel Plates. For observing the wetting phenomena in joining of stainless steel to stainless steel, Ag – 28 Cu, Ag – Cu – 2 Ti and Ag – Cu – 5 Ti brazing alloys were used. Wetting of stainless steel was studied by dipping the stainless steel plate (with or without flux coating) of dimensions 10 mm x 5 mm x 2 mm in the molten alloy in air. Experimental set up is shown in Fig. 4.7. Bonding experiments were also carried out by dipping two stainless steel plates, tied to each other by kanthal wire, in molten Ag – 28 Cu and Ag – Cu – 5 Ti brazing alloys in air atmosphere.

Dipping of Ceramic Pellets. For observing wetting phenomena in joining of ceramic-to-ceramic Ag – 28 Cu and Ag – Cu – 5 Ti brazing alloys were used. Wetting of ceramic was studied by dipping the sintered ceramic pellet in the molten alloy. Experimental set up is shown in Fig. 4.8.

The schemes of experiments carried out in the present work are given in Table 4.1 – Table 4.6.

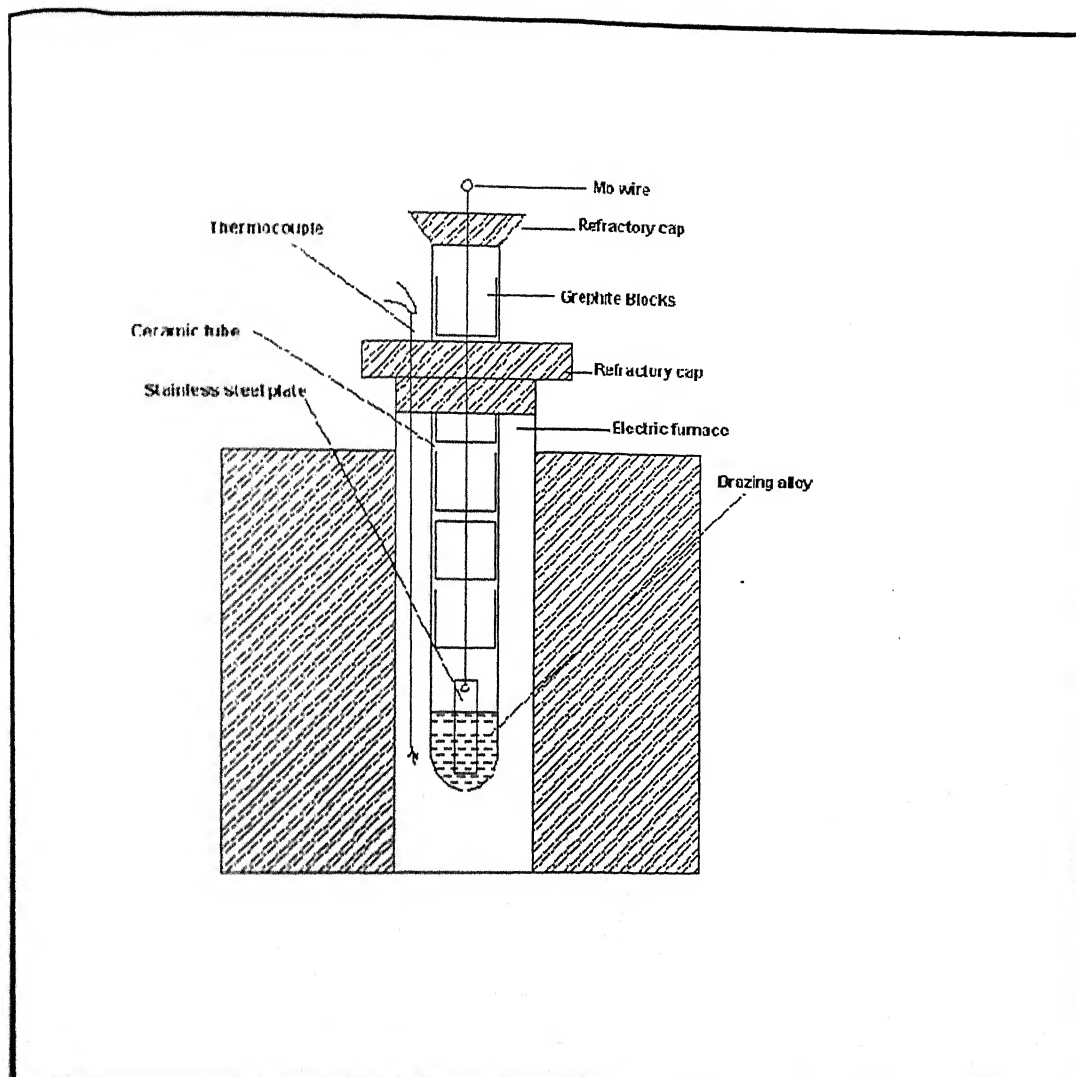


Fig. 4.7: Experimental set up for dipping of stainless steel.

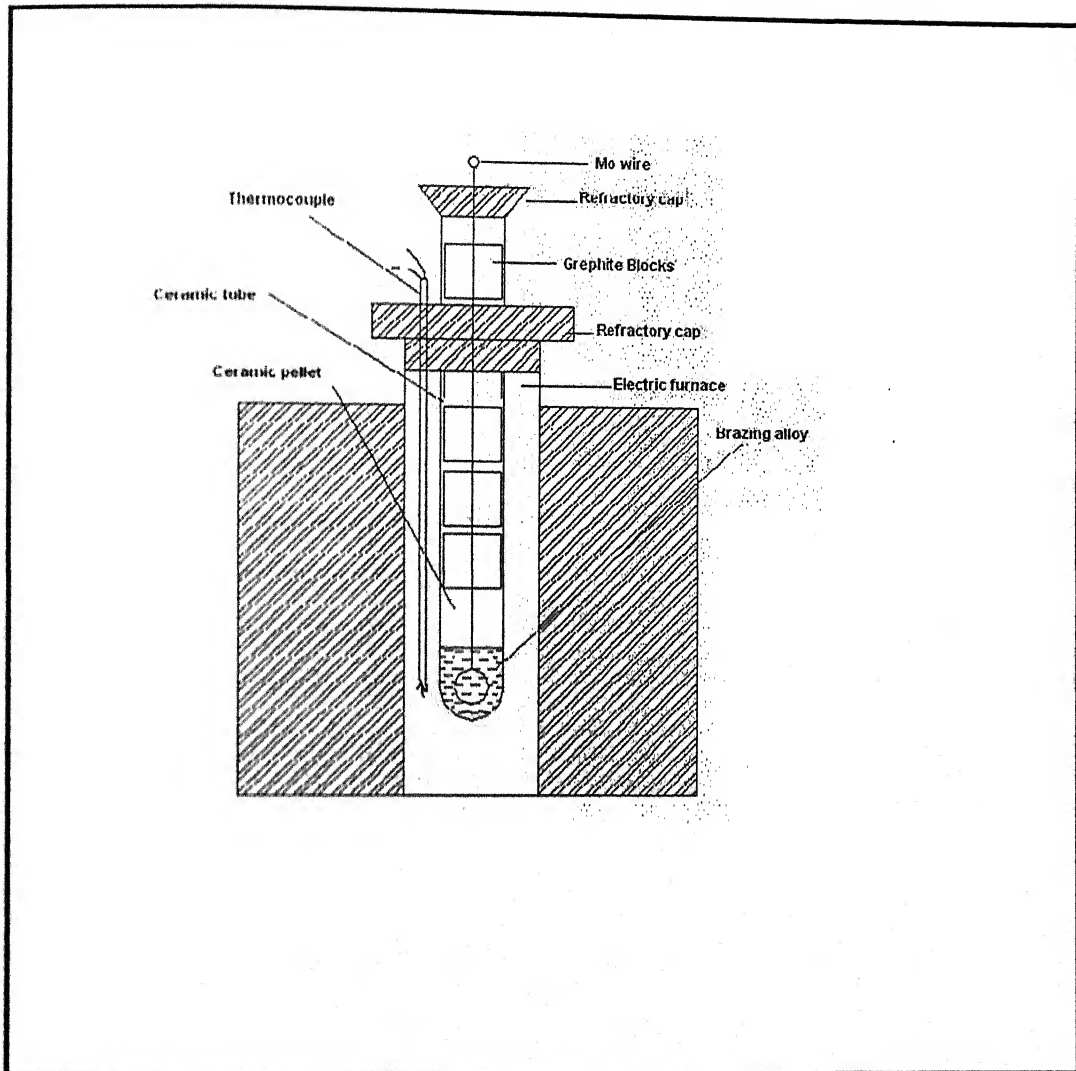


Fig. 4.8: Experimental set up for dipping of alumina ceramic pellet.

Brazing of Stainless Steel to Stainless Steel, Stainless Steel to Ceramic and Ceramic to Ceramic. For brazing stainless steel to stainless steel 10 mm x 5 mm x 2 mm plates were grinded using the grinding wheel to remove the surface oxide layer. After that, the plates were polished using emery papers of grade 1/0, 2/0, 3/0 and 4/0. Polishing in the wheel was also done. The same procedure was followed for polishing the braze filler metal discs (6 mm diameter and 1.5 mm thick). After the polishing was over, these plates and the alloy discs were cleaned in ultrasonic cleaner to make sure that no loose particles remain in the surface.

The samples were then held in the stainless steel sample holder. For brazing of stainless steel to stainless steel, the sequence of the samples was as follows: one stainless steel plate was kept at the lowest position, above which the brazing alloy disc was placed and finally, the other stainless steel plate at the topmost position. For brazing stainless steel to alumina, the sequence of the samples was slightly different: the alumina ceramic part was kept at the lowest position, above which the brazing alloy was placed and finally, the stainless steel plate at the topmost position. Graphite blocks were kept one below the first stainless steel plate/alumina ceramic and the other at the top of the other stainless steel plate/alumina ceramic to be brazed. Graphite blocks were used because it lowered the oxygen potential and made it easy to separate the sample from the holder. The assembly was tightened with a stainless steel screw.

The assembly was then kept in the stainless steel pipe which could be connected to a rotary vacuum pump. Vacuum of around 0.01 atm. was obtained to control high temperature oxidation of stainless steels as well as the brazing filler metals. The stainless steel pipe was gently lowered inside the silicon carbide vertical furnace. The set up for the brazing experiments is shown schematically in Fig. 4.9. The assembly was allowed to cool in the furnace under vacuum. The vacuum was removed after the experiment.

The brazed joints were then cut by the diamond cutter to expose the interface region. The cutting line of the interface region is shown in Fig. 4.10.

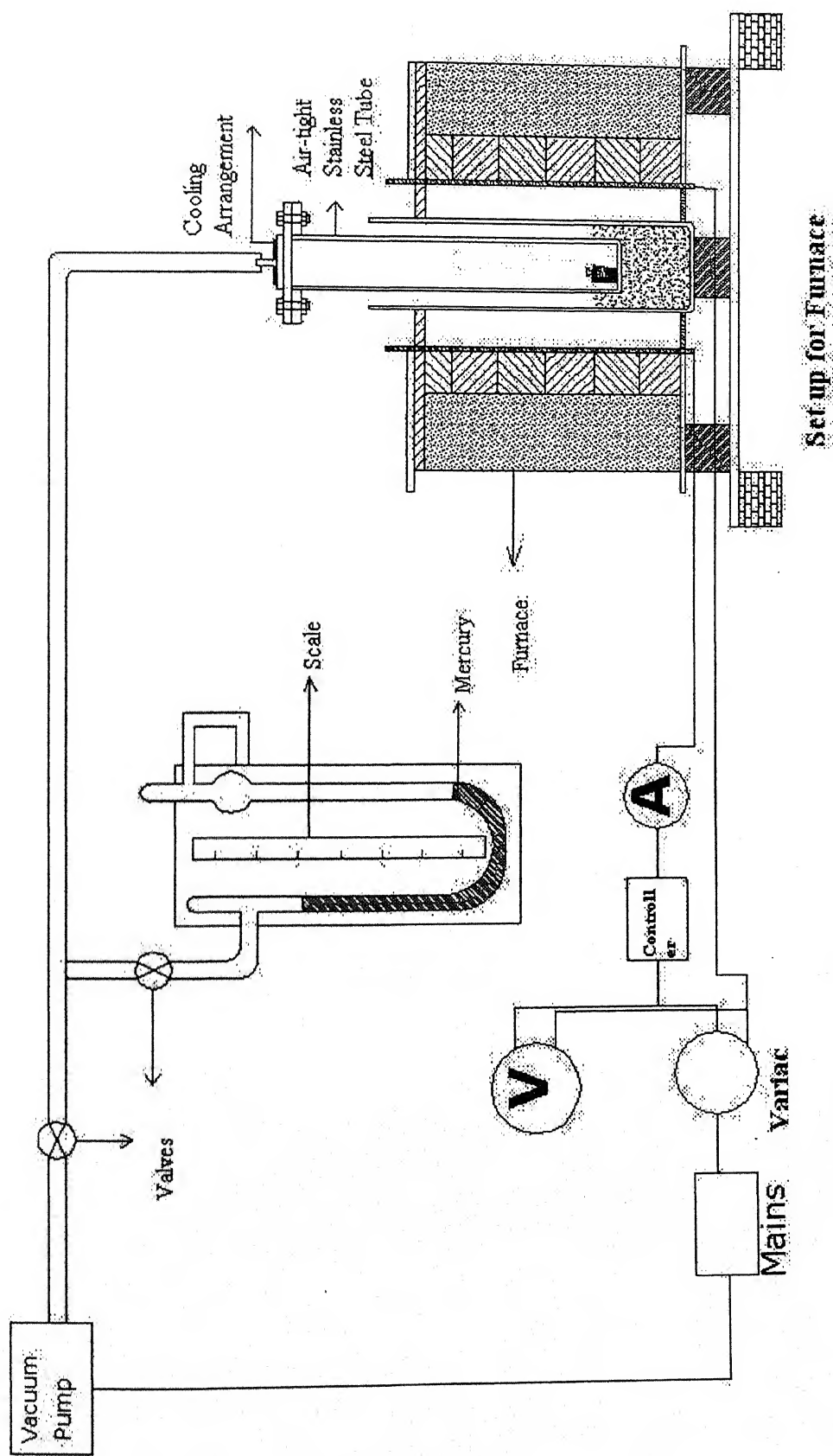


Fig. 4.9: Experimental set up for brazing experiments.

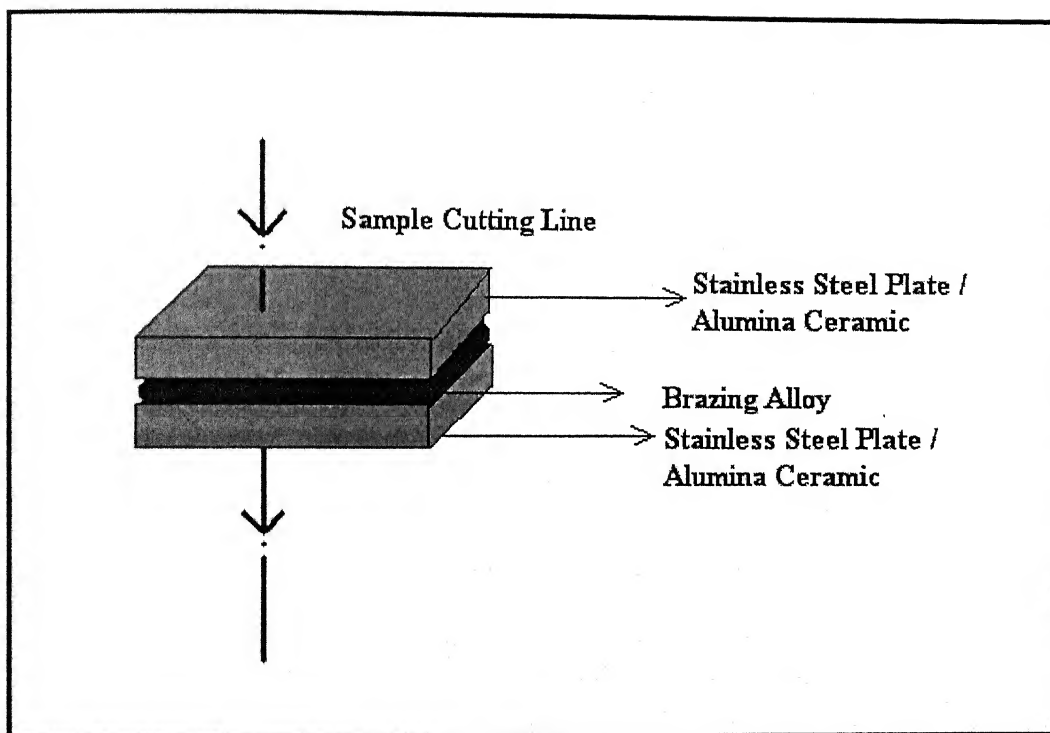


Fig. 4.10: The line along which the brazed joint was cut to expose the interface.

Table 4.1: Dipping experiments with stainless steel plates. (in air)

| Exp. No. | Brazing Alloy Used | Flux Used (Yes/No) | Temperature ($^{\circ}\text{C}$) | Time (Minutes) |
|----------|--------------------|--------------------|------------------------------------|----------------|
| EDSS 1 | Ag - 28 Cu | No | 1050 | 15 |
| EDSS 2 | Ag - 28 Cu | Yes | 1050 | 15 |
| EDSS 3 | Ag - Cu - 2 Ti | No | 1050 | 15 |
| EDSS 4 | Ag - Cu - 2 Ti | Yes | 1050 | 15 |
| EDSS 5 | Ag - Cu - 5 Ti | No | 1050 | 15 |
| EDSS 6 | Ag - Cu - 5 Ti | Yes | 1050 | 15 |

Table 4.2: Bonding experiments with stainless steel plates by dipping in molten alloy. (in air)

| Exp. No. | Brazing Alloy Used | Flux Used (Yes/No) | Temperature ($^{\circ}\text{C}$) | Time (Minutes) |
|----------|--------------------|--------------------|------------------------------------|----------------|
| EBDSS 1 | Ag - 28 Cu | No | 1050 | 15 |
| EBDSS 2 | Ag - 28 Cu | Yes | 1050 | 15 |
| EBDSS 3 | Ag - Cu - 5 Ti | No | 1050 | 15 |

Table 4.3: Dipping experiments with sintered alumina ceramic pellets. (in air)

| Exp. No. | Brazing Alloy Used | Temperature ($^{\circ}\text{C}$) | Time (Minutes) |
|----------|--------------------|------------------------------------|----------------|
| EDC 1 | Ag - 28 Cu | 1050 | 15 |
| EDC 2 | Ag - Cu - 5 Ti | 1050 | 15 |

EDSS – Dipping experiments with stainless steel plates, EBDSS – Bonding experiments with stainless steel plates by dipping in molten alloys and EDC – Dipping experiments with sintered alumina ceramic pellets.

Table 4.4: Bonding experiments with stainless steel plates. (in vacuum, without flux)

| Exp. No. | Brazing Alloy Used | Temperature ($^{\circ}\text{C}$) | Time (Minutes) |
|----------|--------------------|------------------------------------|----------------|
| EBSS 1 | Ag – 28 Cu | 1100 | 30 |
| EBSS 2 | Ag – Cu – 2 Ti | 1100 | 30 |
| EBSS 3 | Ag – Cu – 5 Ti | 1100 | 30 |
| EBSS 4 | Ag – 1 Ti | 1100 | 30 |
| EBSS 5 | Ag – 2 Ti | 1100 | 30 |
| EBSS 6 | Cu – 1 Ti | 1250 | 30 |
| EBSS 7 | Cu – 2 Ti | 1250 | 30 |

Table 4.5: Bonding experiments with sintered alumina ceramic pellets and stainless steel plates. (in vacuum)

| Exp. No. | Brazing Alloy Used | Temperature ($^{\circ}\text{C}$) | Time (Minutes) |
|----------|--------------------|------------------------------------|----------------|
| EBCS 1 | Ag – 28 Cu | 1100 | 30 |
| EBCS 2 | Ag – Cu – 2 Ti | 1100 | 30 |
| EBCS 3 | Ag – Cu – 5 Ti | 1100 | 30 |
| EBCS 4 | Ag – 1 Ti | 1100 | 30 |
| EBCS 5 | Ag – 2 Ti | 1100 | 30 |
| EBCS 6 | Cu – 1 Ti | 1250 | 30 |
| EBCS 7 | Cu – 2 Ti | 1250 | 30 |

Table 4.6: Bonding experiments with sintered alumina ceramic pellets. (in vacuum)

| Exp. No. | Brazing Alloy Used | Temperature ($^{\circ}\text{C}$) | Time (Minutes) |
|----------|--------------------|------------------------------------|----------------|
| EBCC 1 | Ag – Cu – 5 Ti | 1100 | 30 |

EBSS – Bonding experiments with stainless steel plates, EBCS – Bonding experiments with stainless steel plate and sintered alumina ceramic pellet and EBCC – Bonding experiments with one sintered alumina ceramic pellet to another.

4.2.6 Mechanical Testing of the Brazing Alloys and Vacuum Brazed and Torch Brazed Stainless Steel Rods.

Stainless steel rods, 5.3 mm diameter and 40 mm long were prepared in workshop for mechanical testing of brazed joints. Both ends of each stainless steel rod were grinded in the grinding machine to make the surface perfectly flat. Then, one end of each stainless steel rod was subsequently polished in emery papers and rotary polishing wheel. Finally, cleaning was done in an ultrasonic cleaner to remove any further unwanted materials from the surface for smooth wetting and bonding.

Vacuum Brazing. The assembly for brazing two stainless steel rods was a simple one. First, one stainless steel rod, with its polished surface upward, was put inside a 6 mm diameter, 120 mm long quartz guide tube and then the polished braze alloy disc (diameter 5 mm) was kept. Finally, the second stainless steel rod was put inside the quartz tube with its polished surface touching the polished surface of the braze alloy disc. The whole assembly was then kept inside a stainless steel pipe in which vacuum of the order of 0.01 atm. was created. The brazing temperature was 1100°C for Ag – 28 Cu, Ag – 27.4 Cu – 2 Ti, Ag – 26.6 Cu – 5 Ti, Ag – 1 Ti, Ag – 2 Ti and 1250°C for Cu – 1 Ti and Cu – 2 Ti. The time of brazing was 30 minutes in each case. The heating and cooling, both, were done in vacuum to avoid any oxidation and air entrapment in the liquid.

Torch Brazing.

Torch brazing of two stainless steel rods was done by using oxyacetylene flame. Ruptum silver brazing filler metal, in form of wire, and Ruptum silver brazing flux, in form of powder, were used. Polished and cleaned surfaces of two stainless steel rods were kept in close contact above a refractory brick. Flux was applied in the joint and then the filler metal was melted by the heat of the oxyacetylene flame. Finally, after air cooling of the brazed joint, cold water was rinsed in order to remove the excess flux.

Mechanical Testing of the Brazing Alloys and the Brazed Joints. Strengths of the brazing alloys as well as the brazed joints were measured using the Instron 1195 Universal Testing Machine in tensile mode. The load at which the sample failed was noticed from the chart. Full scale load used were 2 kN, 5 kN, 10 kN and 20 kN in different cases, crosshead speed was 1 mm/min and chart speed was 10 mm/min.

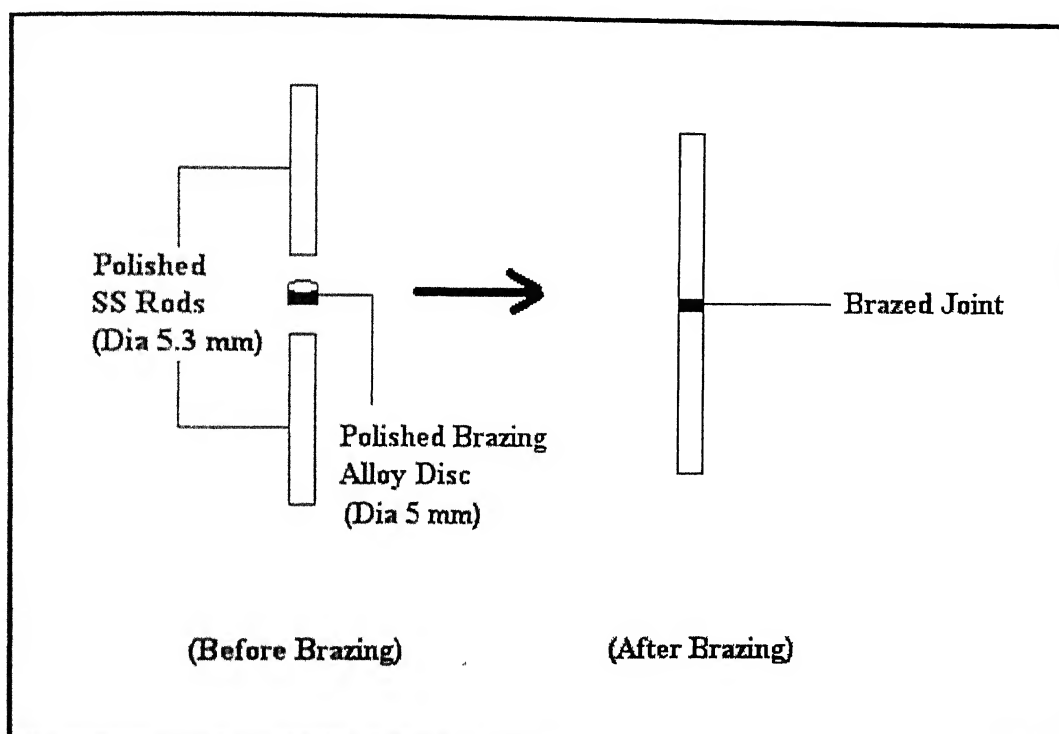


Fig.4.11: Two stainless steel rods, before and after brazing.

5.1 Fabrication and Melting Range Determination of Brazing Alloys and Fabrication and Sintering of Ceramic Pellets.

Results of preparation of eutectic alloy and active braze alloys are included in Table 5.1. Metallographs of the prepared alloys are shown in Fig. 5.1 – 5.5. Temperature – time plots during cooling the alloys Ag – 28 Cu and Ag – 26.6 Cu – 2 Ti, Ag – 2 Ti and Cu – 2 Ti are shown in Fig. 5.6 – 5.8.

Sintering Analysis.

Sintering is used to strengthen the pellets and to reduce the porosity by densification of the pellets. Porosity can be calculated using the follow method:

$$\epsilon = (V - V_{\text{actual}}) / V$$

$$\epsilon = 1 - (\rho / \rho_{\text{actual}})$$

Where, ϵ = Porosity and V = Volume

V_{actual} = Volume of zero porosity pellet

ρ = Density of alumina pellet

ρ_{actual} = Density of alumina powder = 3.97 gm. /cc.

The compacted alumina pellets were sintered at 1600°C for 9 hours. The results before and after sintering are given in Table 5.2 and Table 5.3.

The average porosity before sintering was 0.518 and after sintering it was reduced to 0.436. Scanning electron micrograph of the sintered alumina ceramic pellet at 5000 X magnification is shown below in Fig. 5.9.

Table 5.1: Results of preparation of eutectic alloy and active braze alloys.

| | Unit | Eutectic Alloy, Ag - 28 Cu | Ag-27.4 Cu-2 Ti | Ag-26.6 Cu-5 Ti | Ag - 1 Ti | Ag - 2 Ti | Cu - 1 Ti | Cu - 2 Ti |
|--------------|-------|----------------------------|-----------------|-----------------|-----------|-----------|-----------|-----------|
| Temperature | °C | 1100 | 1100 | 1100 | 1100 | 1100 | 1200 | 1200 |
| Holding Time | hours | 0.5 | 6 | 6 | 6 | 6 | 6 | 6 |
| Ag | gm. | 71.97 | ----- | ----- | 76.23 | ----- | ----- | ----- |
| Cu | gm. | 28.03 | ----- | ----- | ----- | ----- | 113.15 | ----- |
| Ti | gm. | ----- | 1.67 | 0.87 | 0.77 | 0.48 | 1.13 | 0.48 |
| Master Alloy | gm. | ----- | 82.03 | 27.99 | ----- | 47.43 | ----- | 48.34 |
| Total Alloy | gm. | 100.00 | 83.70 | 28.86 | 77.00 | 47.91 | 114.28 | 48.82 |
| % Ag | ----- | 71.97 | ----- | ----- | ----- | ----- | ----- | ----- |
| % Cu | ----- | 28.03 | ----- | ----- | ----- | ----- | ----- | ----- |
| % Ti | ----- | ----- | 2.00 | 3.00 | 1.00 | 1.00 | 1.00 | 1.00 |
| Sucked | gm | 17.34 | 28.88 | 10.54 | 20.86 | 22.53 | 61.89 | 26.18 |
| Residue Melt | gm. | 82.03 | 54.19 | 18.06 | 55.43 | 24.98 | 50.79 | 21.83 |
| Loss | gm. | 0.63 | 0.63 | 0.26 | 0.71 | 0.40 | 1.60 | 0.81 |
| % Loss | ----- | 0.63 | 0.75 | 0.90 | 0.92 | 0.83 | 1.40 | 1.66 |

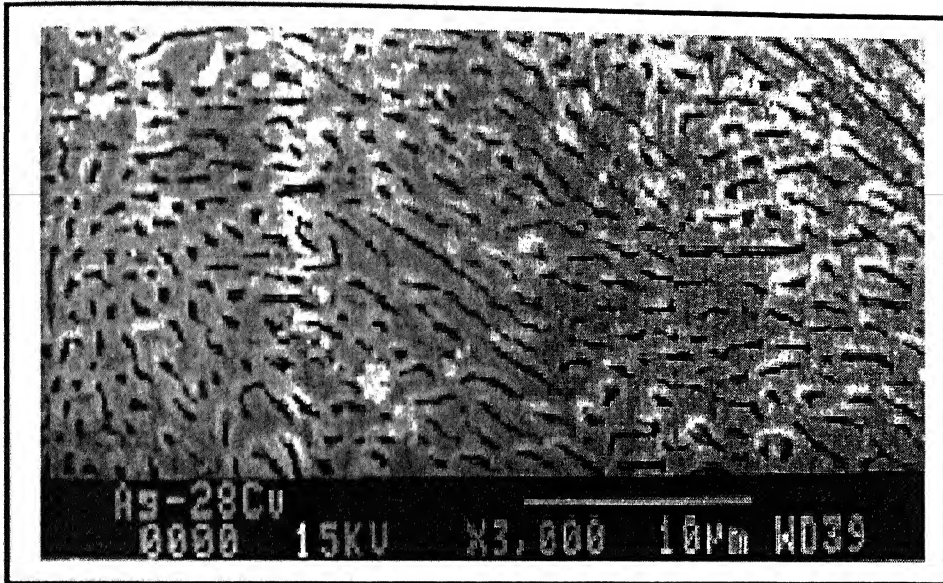


Fig. 5.1 – Photomicrograph of Ag – 28 Cu at 3000 X (Aq. FeCl₃ etch).

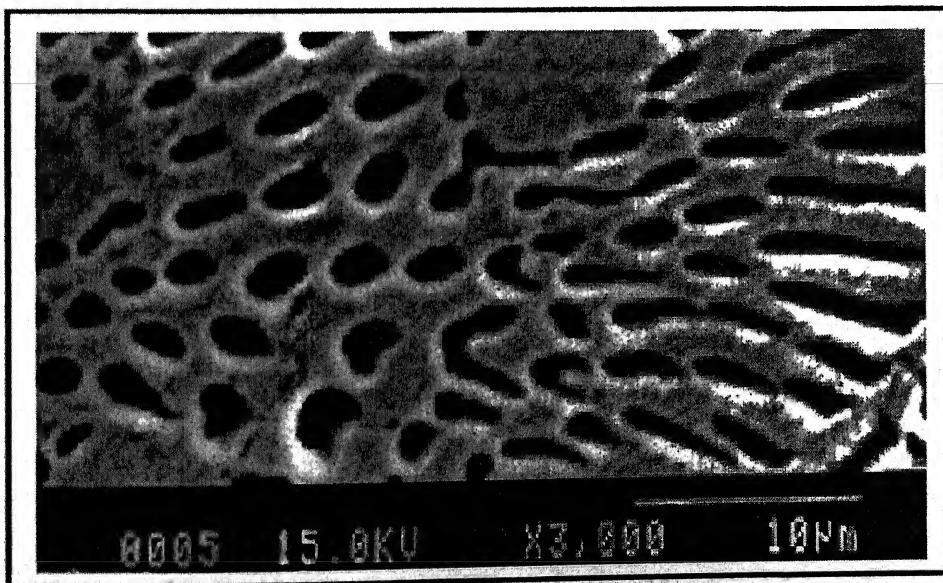


Fig. 5.2 – Photomicrograph of Ag – 27.4 Cu – 2 Ti at 3000 X (Aq. FeCl₃ etch).

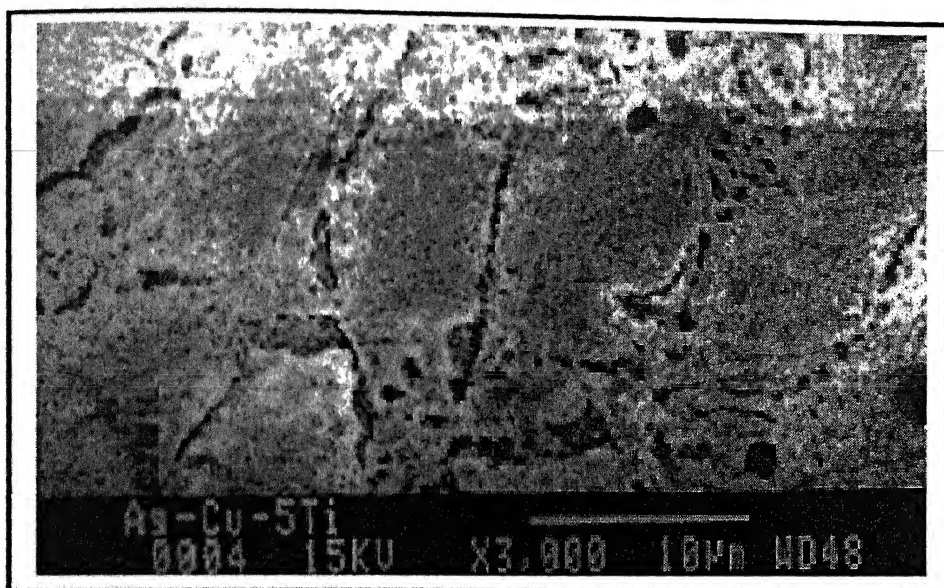


Fig. 5.3 – Photomicrograph of Ag – 26.6 Cu – 5 Ti at 3000 X (Aq. FeCl₃ etch).

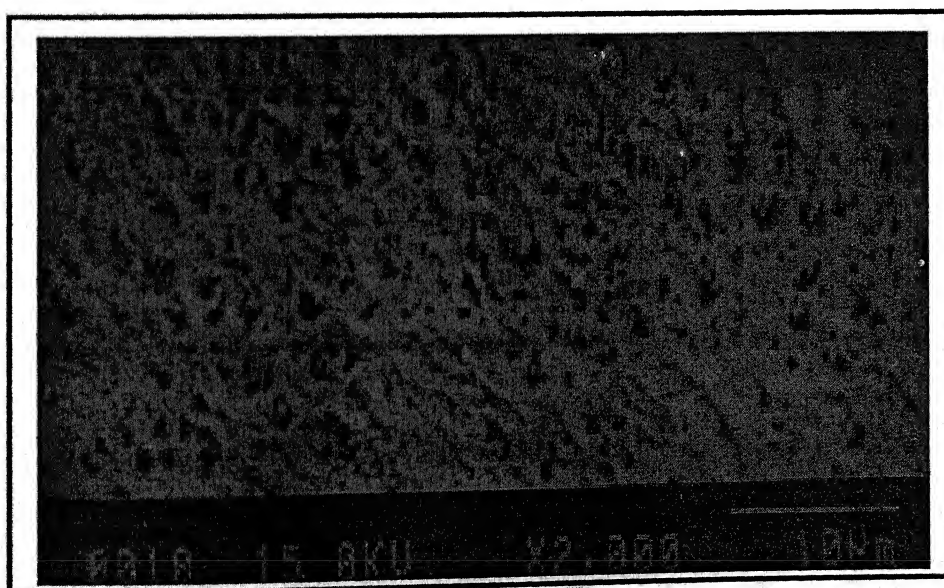


Fig. 5.4 – Photomicrograph of Cu – 1 Ti at 2000 X (Aq. FeCl₃ etch).

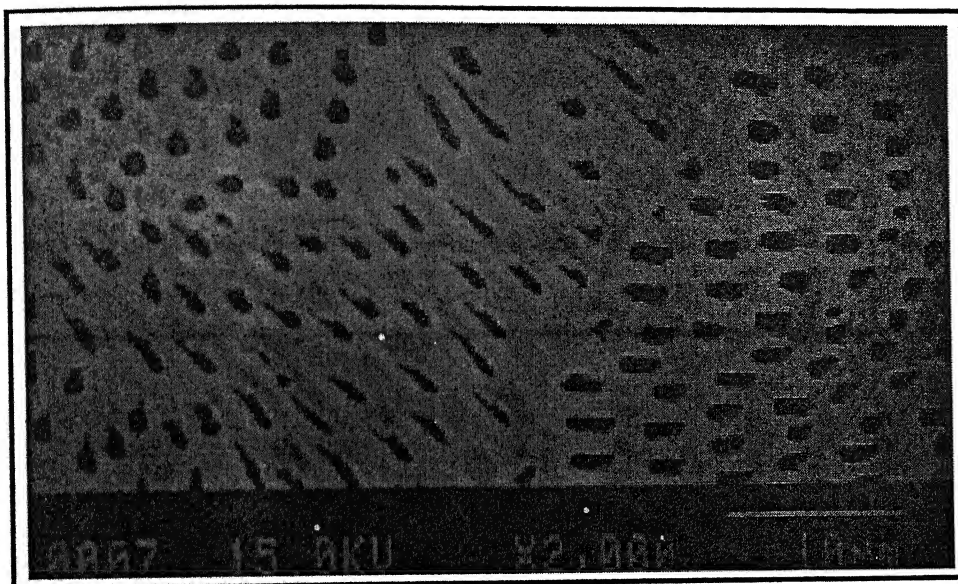


Fig. 5.5 – Photomicrograph of Cu – 2 Ti at 2000 X (Aq. FeCl₃ etch).

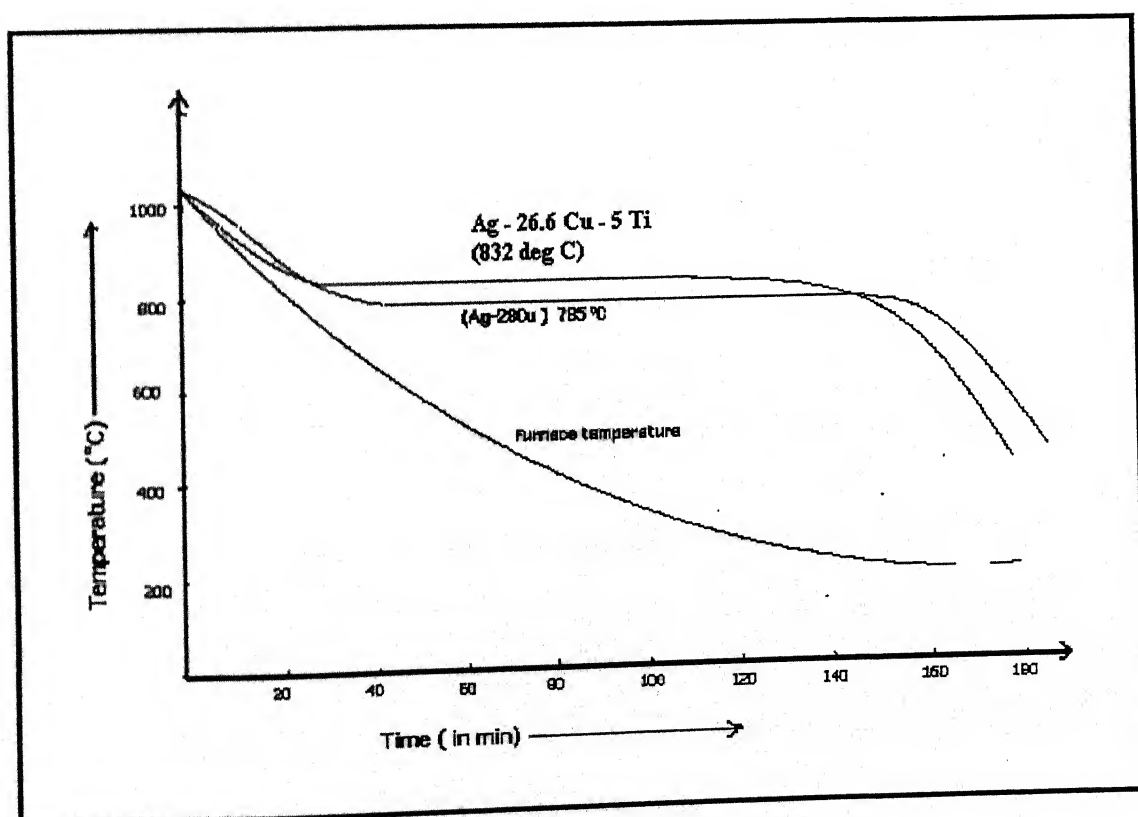


Fig. 5.6 – Temperature – time plots of Ag – 28 Cu and Ag – 26.6 Cu – 5 Ti during cooling.

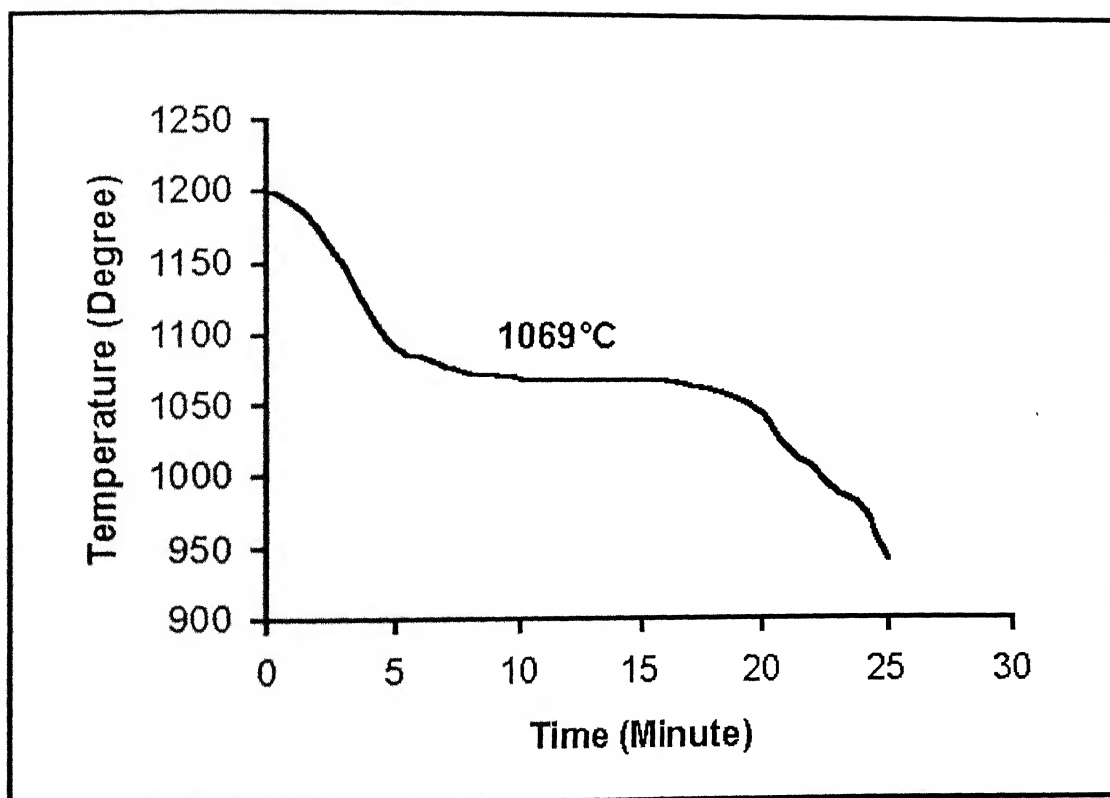


Fig. 5.7 – Temperature – time plot of Cu – 2 Ti during cooling.

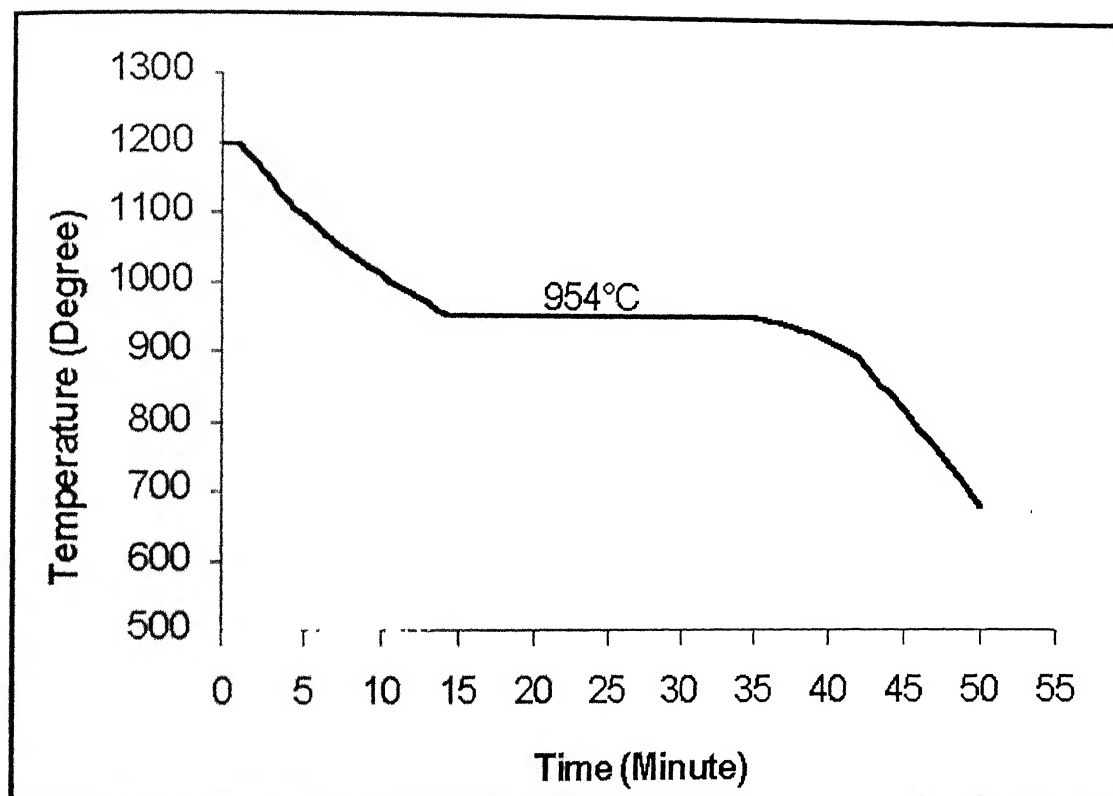


Fig. 5.8 – Temperature – time plot of Ag – 2 Ti during cooling.

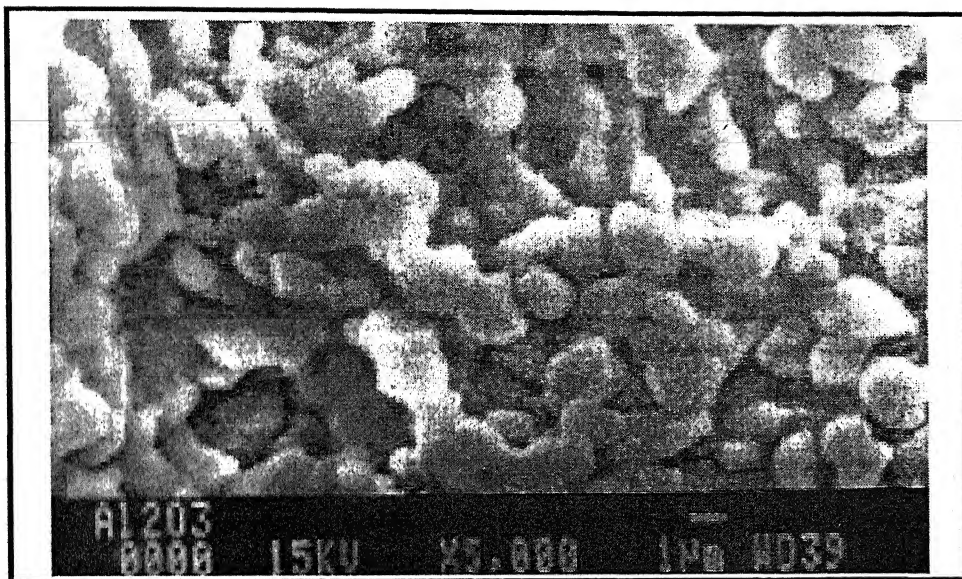


Fig. 5.9 – Photomicrograph of the sintered ceramic pellet at 5000 X.

Table 5.2: Data Analysis of Green Pellets before Sintering at 1600°C for 9 hours.

| SERIAL NO. | DIAMETER (cm) | HEIGHT (cm) | WEIGHT (gm) | DENSITY (gm/cc) | CALCULATED POROSITY |
|------------|---------------|-------------|-------------|-----------------|---------------------|
| P1 | 1.022 | 0.344 | 0.564 | 1.997 | 0.497 |
| P2 | 1.020 | 0.544 | 0.863 | 1.942 | 0.511 |
| P3 | 1.022 | 0.710 | 1.125 | 1.932 | 0.513 |
| P4 | 1.022 | 0.472 | 0.719 | 1.857 | 0.532 |
| P5 | 1.024 | 0.318 | 0.478 | 1.824 | 0.541 |
| P6 | 1.020 | 0.290 | 0.445 | 1.877 | 0.527 |
| P7 | 1.022 | 0.464 | 0.721 | 1.895 | 0.523 |
| P8 | 1.020 | 0.434 | 0.681 | 1.921 | 0.516 |
| P9 | 1.022 | 0.342 | 0.530 | 1.889 | 0.524 |
| P10 | 1.020 | 0.504 | 0.796 | 1.932 | 0.513 |
| P11 | 1.020 | 0.442 | 0.702 | 1.945 | 0.510 |
| P12 | 1.024 | 0.440 | 0.700 | 1.932 | 0.513 |
| P13 | 1.020 | 0.388 | 0.599 | 1.889 | 0.524 |
| P14 | 1.024 | 0.382 | 0.590 | 1.876 | 0.527 |
| P15 | 1.022 | 0.342 | 0.536 | 1.912 | 0.518 |
| P16 | 1.022 | 0.344 | 0.562 | 1.992 | 0.498 |
| P17 | 1.020 | 0.362 | 0.562 | 1.899 | 0.524 |
| P18 | 1.024 | 0.366 | 0.595 | 1.975 | 0.503 |
| P19 | 1.022 | 0.364 | 0.563 | 1.886 | 0.525 |
| P20 | 1.024 | 0.316 | 0.487 | 1.872 | 0.528 |
| P21 | 1.022 | 0.412 | 0.650 | 1.922 | 0.516 |
| P22 | 1.020 | 0.382 | 0.589 | 1.888 | 0.524 |
| P23 | 1.022 | 0.366 | 0.580 | 1.932 | 0.513 |

* P stands for Pellet

Table 5.2 (Contd.): Data Analysis of Green Pellets before Sintering at 1600°C for 9 hours.

| SERIAL NO. | DIAMETER (cm) | HEIGHT (cm) | WEIGHT (gm) | DENSITY (gm/cc) | CALCULATED POROSITY |
|-----------------------|--------------------------|------------------------|------------------------|----------------------------|--------------------------------|
| P24 | 1.024 | 0.318 | 0.491 | 1.875 | 0.528 |
| P25 | 1.020 | 0.414 | 0.637 | 1.883 | 0.526 |
| P26 | 1.020 | 0.382 | 0.600 | 1.922 | 0.516 |
| P27 | 1.022 | 0.436 | 0.677 | 1.892 | 0.523 |
| P28 | 1.024 | 0.434 | 0.694 | 1.943 | 0.511 |
| P29 | 1.022 | 0.462 | 0.740 | 1.952 | 0.508 |
| P30 | 1.020 | 0.320 | 0.503 | 1.922 | 0.516 |

*** P stands for Pellet**

Table 5.3: Data Analysis of Pellets after Sintering at 1600°C for 9 hours.

| SERIAL NO. | DIAMETER (cm) | HEIGHT (cm) | WEIGHT (gm) | DENSITY (gm/cc) | CALCULATED POROSITY |
|------------|---------------|-------------|-------------|-----------------|---------------------|
| P1 | 1.012 | 0.286 | 0.536 | 2.330 | 0.413 |
| P2 | 1.010 | 0.462 | 0.842 | 2.275 | 0.427 |
| P3 | 1.002 | 0.586 | 1.012 | 2.190 | 0.448 |
| P4 | 1.000 | 0.366 | 0.668 | 2.324 | 0.415 |
| P5 | 1.006 | 0.236 | 0.432 | 2.303 | 0.420 |
| P6 | 1.012 | 0.238 | 0.422 | 2.204 | 0.445 |
| P7 | 1.000 | 0.378 | 0.658 | 2.216 | 0.442 |
| P8 | 1.004 | 0.362 | 0.638 | 2.226 | 0.439 |
| P9 | 1.010 | 0.288 | 0.503 | 2.180 | 0.451 |
| P10 | 1.000 | 0.444 | 0.762 | 2.185 | 0.450 |
| P11 | 1.010 | 0.386 | 0.699 | 2.260 | 0.431 |
| P12 | 1.014 | 0.382 | 0.672 | 2.178 | 0.451 |
| P13 | 1.000 | 0.328 | 0.559 | 2.170 | 0.453 |
| P14 | 1.000 | 0.330 | 0.557 | 2.149 | 0.459 |
| P15 | 1.000 | 0.268 | 0.488 | 2.318 | 0.416 |
| P16 | 1.012 | 0.292 | 0.546 | 2.325 | 0.414 |
| P17 | 1.010 | 0.302 | 0.548 | 2.265 | 0.430 |
| P18 | 1.012 | 0.306 | 0.572 | 2.324 | 0.415 |
| P19 | 1.014 | 0.302 | 0.538 | 2.206 | 0.444 |
| P20 | 1.014 | 0.254 | 0.461 | 2.248 | 0.434 |
| P21 | 1.010 | 0.356 | 0.634 | 2.223 | 0.440 |
| P22 | 1.000 | 0.330 | 0.559 | 2.157 | 0.457 |
| P23 | 1.012 | 0.302 | 0.559 | 2.301 | 0.420 |

*** P stands for Pellet**

Table 5.3 (Contd.): Data Analysis of Pellets after Sintering at 1600°C for 9 hours.

| SERIAL NO. | DIAMETER (cm) | HEIGHT (cm) | WEIGHT (gm) | DENSITY (gm/cc) | CALCULATED POROSITY |
|---------------|------------------|----------------|----------------|--------------------|------------------------|
| P24 | 1.014 | 0.256 | 0.471 | 2.278 | 0.426 |
| P25 | 1.010 | 0.352 | 0.617 | 2.188 | 0.449 |
| P26 | 1.000 | 0.336 | 0.570 | 2.160 | 0.456 |
| P27 | 1.010 | 0.376 | 0.659 | 2.188 | 0.449 |
| P28 | 1.012 | 0.368 | 0.671 | 2.226 | 0.439 |
| P29 | 1.010 | 0.398 | 0.729 | 2.286 | 0.424 |
| P30 | 1.010 | 0.268 | 0.481 | 2.24 | 0.436 |

* P stands for Pellet

5.2 Results of Dipping and Bonding Experiments.

Results of the dipping experiments carried out to study wetting of stainless steel plates in air with or without any flux coating are given in Table 5.4. The results show that in absence of fluxes wetting did not occur for stainless steel when using Ag – Cu eutectic as a brazing filler metal, but there were some degree of wetting when active braze filler metals Ag – Cu – 2 Ti and Ag – Cu – 5 Ti were used.

Results of the experiments in bonding one stainless steel plate to another by dipping in molten Ag – Cu eutectic and Ag – Cu – 5 Ti active brazing alloy are summarized in Table 5.5. Photomicrographs of bonded stainless steel plates are shown in Fig. 5.20 and 5.21.

Results of the dipping experiments carried out for sintered alumina ceramic pellets are given in Table 5.6. The experiments were done for two brazing alloys, Ag – Cu and Ag – Cu – 5 Ti. There was no wetting when using Ag – Cu eutectic as brazing filler metal, but some degree of non-uniform wetting took place when active braze filler metal Ag – Cu – 5 Ti was used.

Results of the experiments in bonding stainless steel plate to stainless steel plate with different brazing alloys are summarized in Table 5.7. Cu – 2 Ti. In general, good bonding between two stainless steel plates occurred when active brazing filler metals containing Ti were used. Photomicrographs of bonded stainless steel plates are shown in Fig. 5.11 – 5.19.

Results of the experiments in bonding sintered alumina ceramic pellet to stainless steel plate are shown in Table 5.8. The experiments were done using seven types of brazing filler metals, namely, Ag – 28 Cu, Ag – Cu – 2 Ti, Ag – Cu – 5 Ti, Ag – 1 Ti, Ag – 2 Ti, Cu – 1 Ti and Cu – 2 Ti. Out of these seven alloys, only Ag – Cu – 5 Ti active braze alloy was able to wet both the stainless steel and the ceramic surfaces. But the wetting was non-uniform and the joint strength obtained was not very good. The filler metal was able to wet completely the stainless steel surface but not completely the ceramic surface.

Result of the experiment in bonding one sintered alumina ceramic pellet to another is shown in Table 5.9. The experiment was done using only Ag – Cu – 5 Ti active braze filler metal because other alloys except this alloy were unable to wet the ceramic surface.

Table 5.4: Results of dipping experiments with stainless steel plates. (in air atmosphere)

| Exp. No. | Brazing Alloy Used | Flux Used Yes/No | Temperature ($^{\circ}\text{C}$) | Time (Minutes) | Observations |
|----------|--------------------|------------------|------------------------------------|----------------|---|
| EDSS 1 | Ag – 28 Cu | No | 1050 | 15 | Poor wetting, wetting occurred at few spots on the surface. |
| EDSS 2 | Ag – 28 Cu | Yes | 1050 | 15 | Good wetting. |
| EDSS 3 | Ag – Cu – 2 Ti | No | 1050 | 15 | Non-uniform wetting took place. |
| EDSS 4 | Ag – Cu – 2 Ti | Yes | 1050 | 15 | Excellent uniform wetting. |
| EDSS 5 | Ag – Cu – 5 Ti | No | 1050 | 15 | Good wetting, but in some places it was non-uniform. |
| EDSS 6 | Ag – Cu – 5 Ti | Yes | 1050 | 15 | Excellent uniform wetting. |

Table 5.5: Results of bonding experiments with stainless steel plates by dipping in molten alloys. (in air atmosphere)

| Exp. No. | Brazing Alloy Used | Flux Used Yes/No | Temperature (°C) | Time (Minutes) | Observations |
|----------|--------------------|------------------|------------------|----------------|--|
| EBDSS 1 | Ag – 28 Cu | No | 1050 | 15 | Poor wetting, wetting occurred at few spots on the surface. No bonding between the two plates. |
| EBDSS 2 | Ag – 28 Cu | Yes | 1050 | 15 | Good wetting on the surface but poor bonding between the two plates. |
| EBDSS 3 | Ag – Cu – 5 Ti | No | 1050 | 15 | Excellent wetting on the surface. Good bonding between the two plates. |

Table 5.6: Results of dipping experiments with sintered alumina ceramic pellets (in air atmosphere).

| Exp. No. | Brazing Alloy Used | Temperature (°C) | Time (Minutes) | Observations |
|----------|--------------------|------------------|----------------|---------------|
| EDC 1 | Ag – 28 Cu | 1050 | 15 | No wetting. |
| EDC 2 | Ag – Cu – 5 Ti | 1050 | 15 | Poor wetting, |

Table 5.7: Results of bonding experiments with stainless steel plates. (in vacuum atmosphere, without flux)

| Exp. No. | Brazing Alloy Used | Temperature (°C) | Time (Minutes) | Observations |
|----------|--------------------|------------------|----------------|---|
| EBSS 1 | Ag – 28 Cu | 1100 | 30 | Good wetting and bonding on one plate. |
| EBSS 2 | Ag – Cu – 2 Ti | 1100 | 30 | Good wetting and bonding on both plates. |
| EBSS 3 | Ag – Cu – 5 Ti | 1100 | 30 | Excellent wetting and bonding on both plates. |
| EBSS 4 | Ag – 1 Ti | 1100 | 30 | Good wetting and bonding on one plate. |
| EBSS 5 | Ag – 2 Ti | 1100 | 30 | Excellent wetting and bonding on both plates. |
| EBSS 6 | Cu – 1 Ti | 1250 | 30 | Good wetting and bonding on one plate. |
| EBSS 7 | Cu – 2 Ti | 1250 | 30 | Excellent wetting and bonding on both plates. |

Table 5.8: Results of bonding experiments with sintered alumina ceramic pellets and stainless steel plates. (in vacuum atmosphere)

| Exp. No. | Brazing Alloy Used | Temperature (°C) | Time (Minutes) | Observations |
|----------|--------------------|------------------|----------------|---------------------------------------|
| EBCS 1 | Ag – 28 Cu | 1100 | 30 | No bonding |
| EBCS 2 | Ag – Cu – 2 Ti | 1100 | 30 | No bonding |
| EBCS 3 | Ag – Cu – 5 Ti | 1100 | 30 | Good bonding but non-uniform wetting. |
| EBCS 4 | Ag – 1 Ti | 1100 | 30 | No bonding. |
| EBCS 5 | Ag – 2 Ti | 1100 | 30 | No bonding. |
| EBCS 6 | Cu – 1 Ti | 1250 | 30 | No bonding. |
| EBCS 7 | Cu – 2 Ti | 1250 | 30 | No bonding. |

Table 5.9: Results of bonding experiments with sintered alumina ceramic pellets. (in vacuum atmosphere)

| Exp. No. | Brazing Alloy Used | Temperature (°C) | Time (Minutes) | Observations |
|----------|--------------------|------------------|----------------|---|
| EBCC 1 | Ag – Cu – 5 Ti | 1100 | 30 | Poor bonding, non-uniform wetting on the ceramic surface. |

Photomicrograph of the as received specimen:

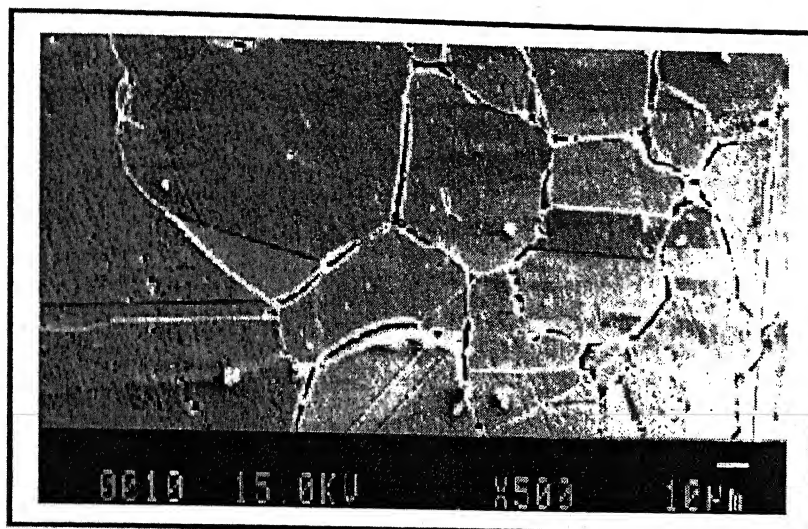


Fig. 5.10: Photomicrograph of the as received stainless steel at 500 X (Marble's etch).

Photomicrographs of the bonded stainless steel plates:

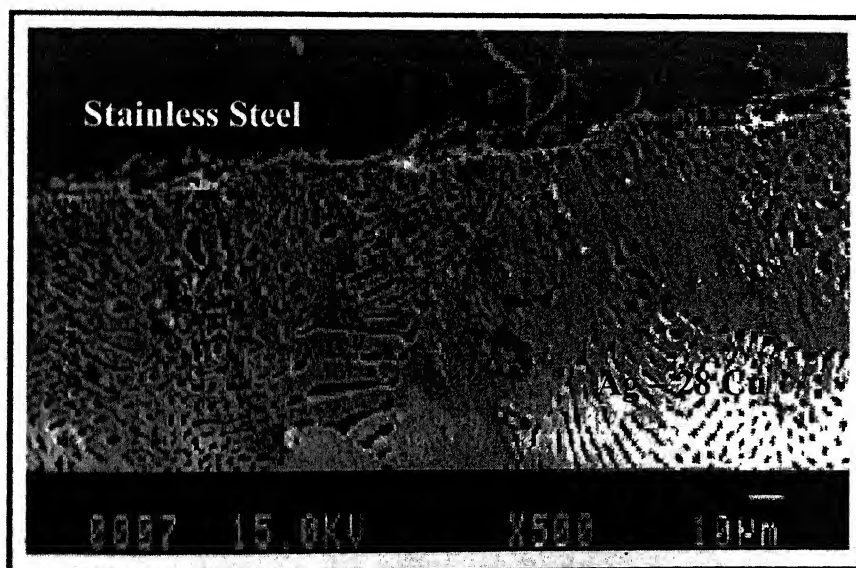


Fig. 5.11 – Photomicrograph of the interface of stainless steel and Ag – 28 Cu at 500 X (Marble's etch). (EBSS – 1)

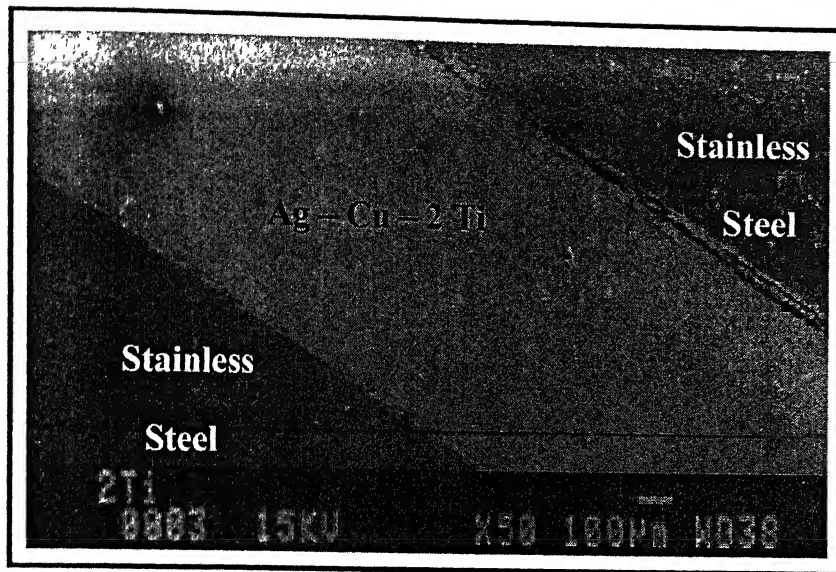


Fig. 5.12 – Photomicrograph of stainless steel to stainless steel brazed joint by Ag – Cu – 2 Ti at 50 X (Marble's etch). (EBSS – 2)

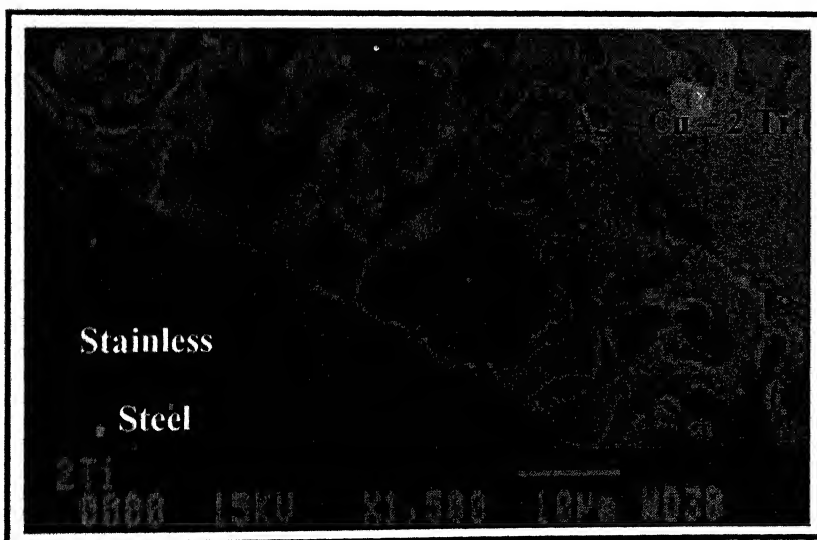


Fig. 5.13 – Photomicrograph of the interface of stainless steel and Ag – Cu – 2 Ti at 1500 X (Marble's etch). (EBSS – 2)

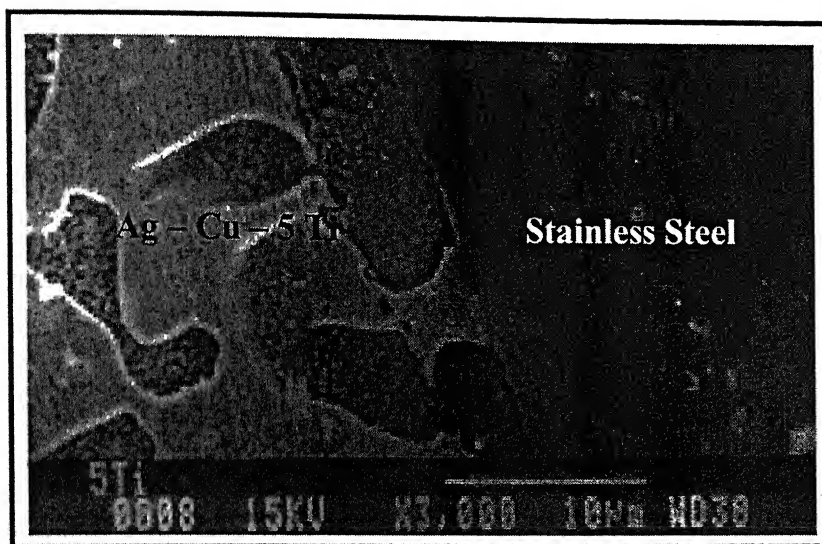


Fig. 5.14 – Photomicrograph of the interface of stainless steel and Ag – Cu – 5 Ti at 3000 X (Marble's etch). (EBSS – 3)

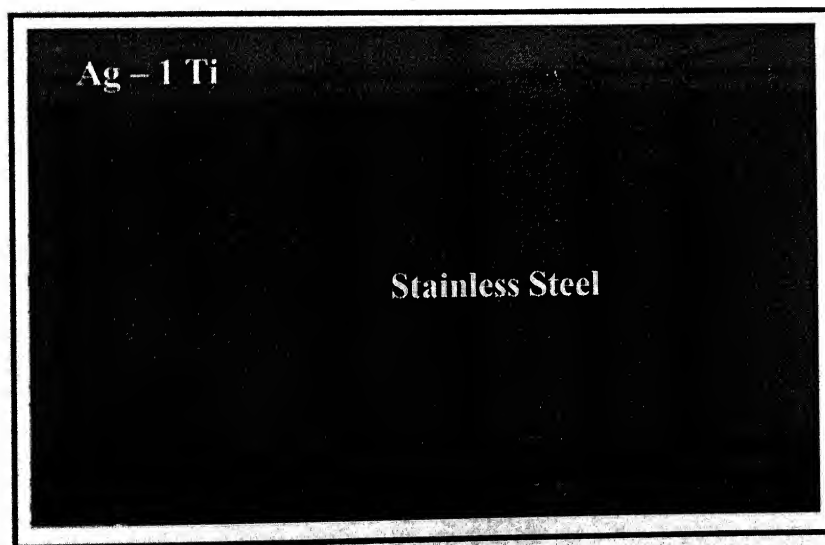


Fig. 5.15 – Photomicrograph of the interface of stainless steel and Ag – 1 Ti at 1000 X (Marble's etch). (EBSS – 4)

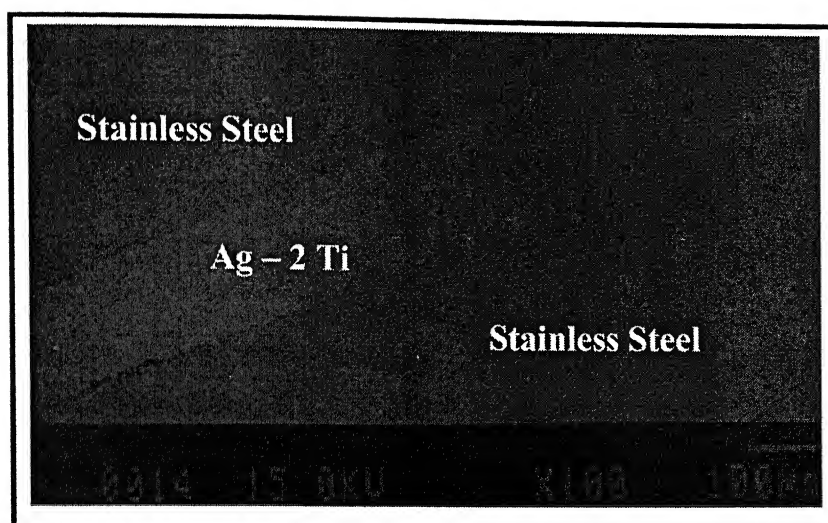


Fig. 5.16 – Photomicrograph of the stainless steel to stainless steel brazed joint by Ag - 2 Ti at 100 X (Marble's etch). (EBSS - 5)

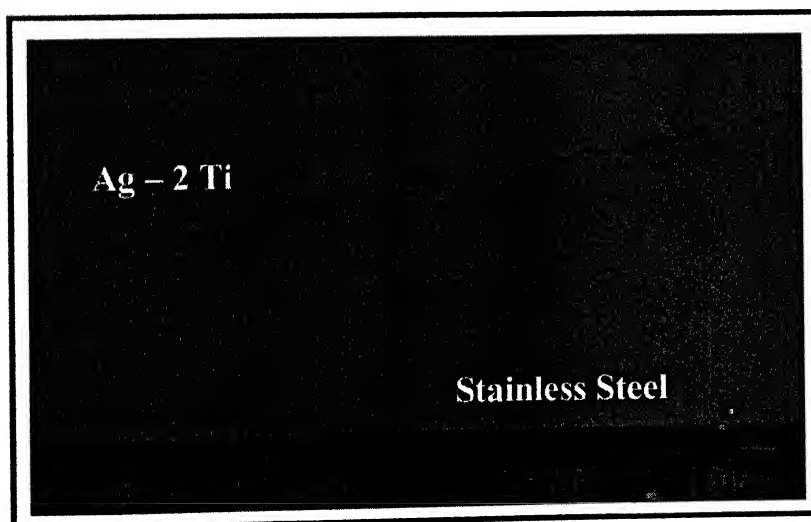


Fig. 5.17 – Photomicrograph of the interface of stainless steel and Ag - 2 Ti at 500 X (Marble's etch). (EBSS - 5)

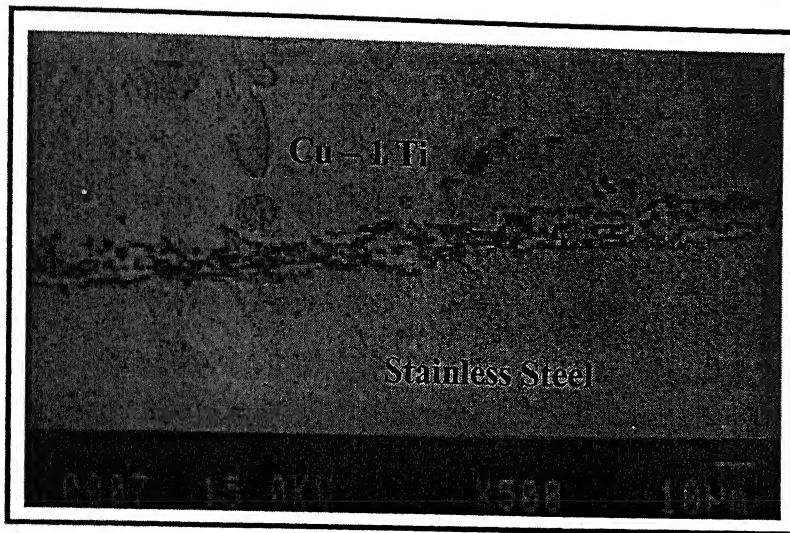


Fig. 5.18 – Photomicrograph of the interface of stainless steel and Cu – 1 Ti at 500 X (Marble's etch). (EBSS – 6)

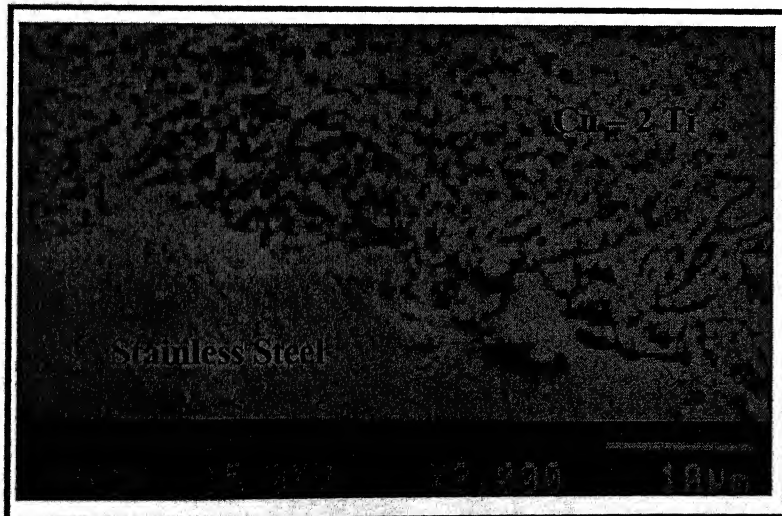


Fig. 5.19 – Photomicrograph of the interface of stainless steel and Cu – 2 Ti at 2000 X (Marble's etch). (EBSS – 7)

Photomicrographs of the bonded stainless steel plates:

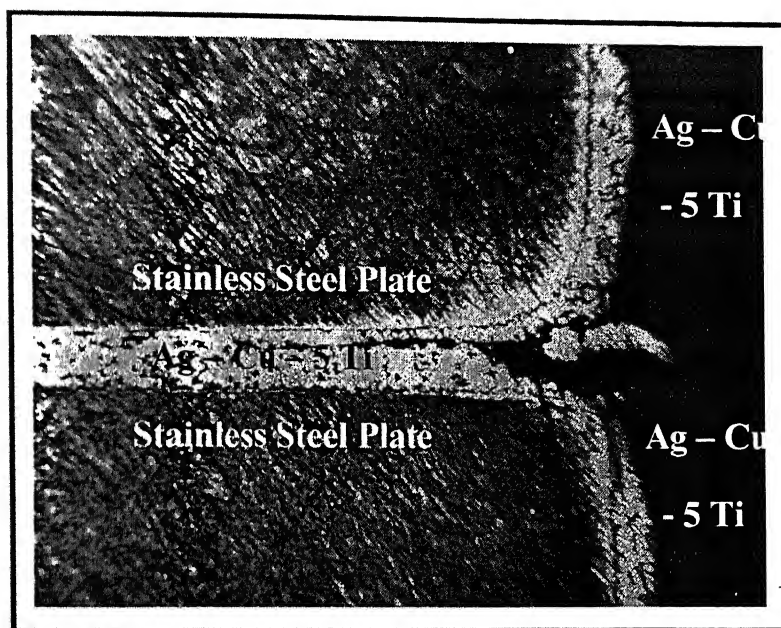


Fig. 5.20 – Photomicrograph showing wetting as well as bonding of two stainless steel plates by Ag – Cu – 5 Ti at 50 X. (EBDSS – 3)

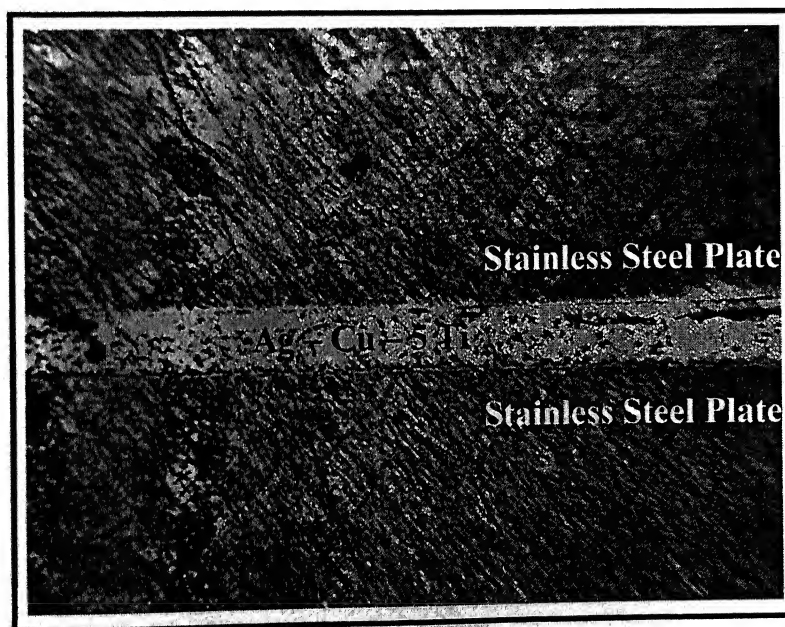


Fig. 5.21 – Photomicrograph showing bonding of two stainless steel plates by Ag – Cu – 5 Ti at 50 X. (EBDSS – 3)

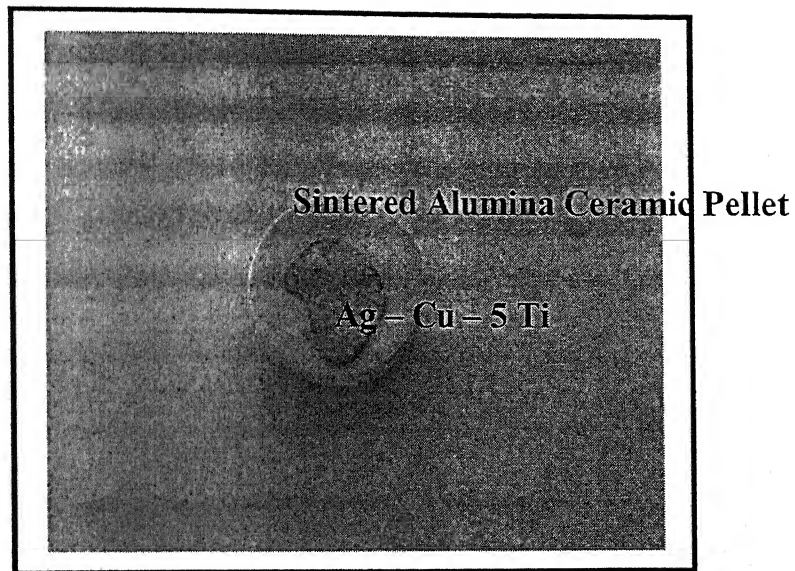


Fig. 5.22 – Photograph showing wetting of alumina ceramic surface by the active braze filler metal Ag - Cu - 5 Ti. (EBCC - 1)

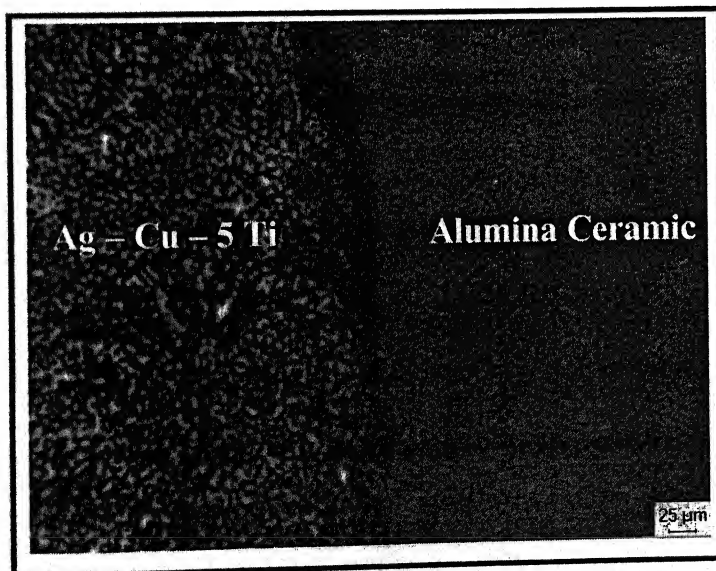


Fig. 5.23 – Photomicrograph showing wetting of alumina ceramic surface by the active braze filler metal Ag - Cu - 5 Ti at 100 X. (EBCC - 1)

5.3 Results of Mechanical Testing of the Brazing Alloys and the Brazed Stainless Steel Rods.

Results of mechanical testing of the brazing alloys and the brazed joints made by them are shown in Table 5.10. It shows that Ag – 28 Cu – 5 Ti braze filler metal has the best strength among the seven filler metals. The joints made by Ag – 2 Ti and Ag – Cu – 5 Ti have the best strength values than the other alloys. In general, an increase in Ti content of the filler metal resulted in an increase in the alloy strength as well as the in the joint strength.

Results of mechanical testing of the torch brazed stainless steel rods are given in Table 5.11.

Table 5.10: Strength values of the brazing alloys and the vacuum brazed stainless steel rods.

| Brazing Alloy | Strength of the Alloy (MPa) | Strength of the SS Rods after Brazing (MPa) |
|-------------------|-----------------------------|---|
| Ag – 1 Ti | 117.14 | 81.13 |
| Ag – 2 Ti | 136.24 | 102.34 |
| Cu – 1 Ti | 110.52 | 49.78 |
| Cu – 2 Ti | 151.20 | 87.56 |
| Ag – 28 Cu | 101.45 | 60.87 |
| Ag – 28 Cu – 2 Ti | 107.87 | 66.21 |
| Ag – 28 Cu – 5 Ti | 170.61 | 98.45 |

Table 5.11: Strength values of the torch brazed stainless steel rods.

| Sample No. | Strength (MPa) |
|------------|----------------|
| 1. | 199.44 |
| 2. | 611.92 |
| 3. | 417.34 |
| 4. | 362.57 |

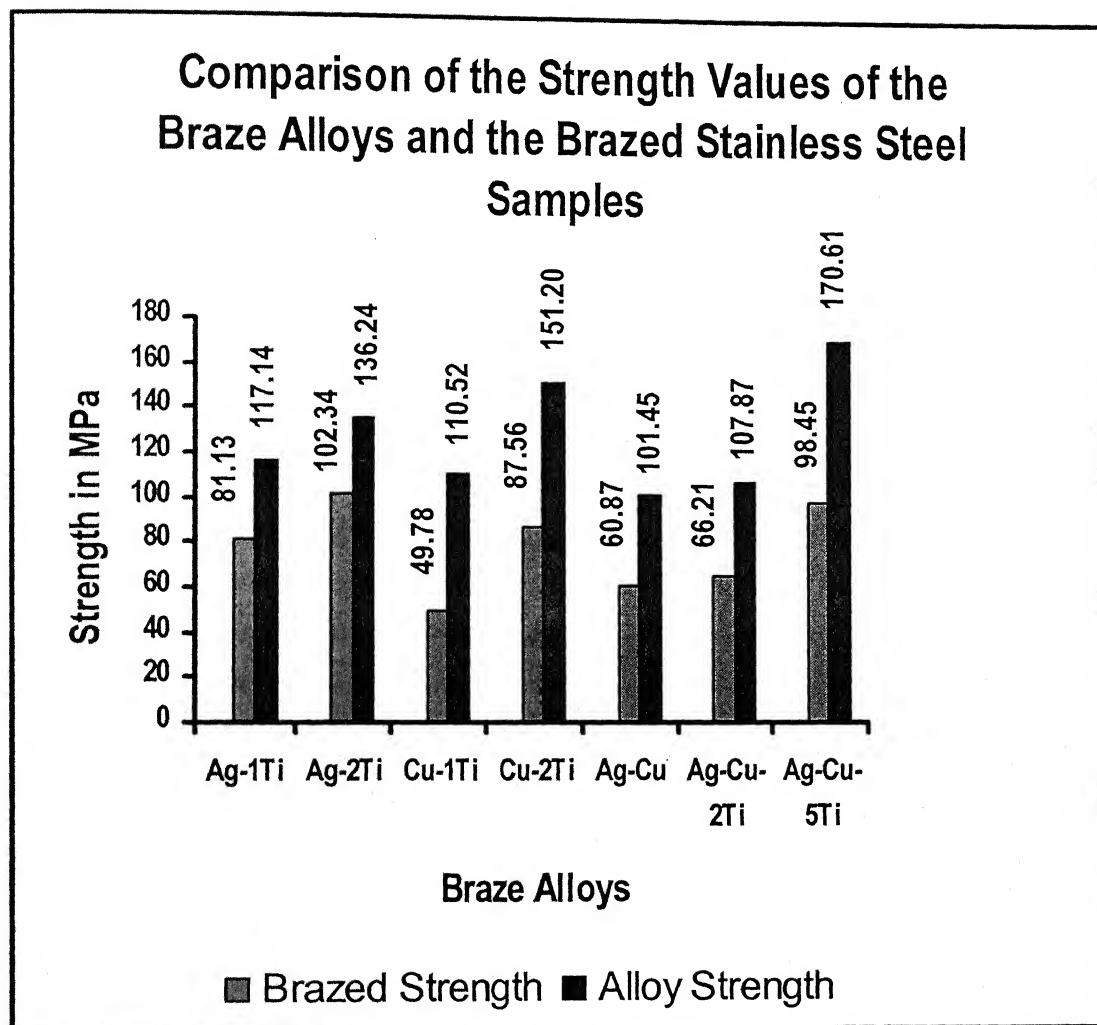


Fig.5.24: Comparison of the strength values of the brazing alloys and the vacuum brazed stainless steel rods.

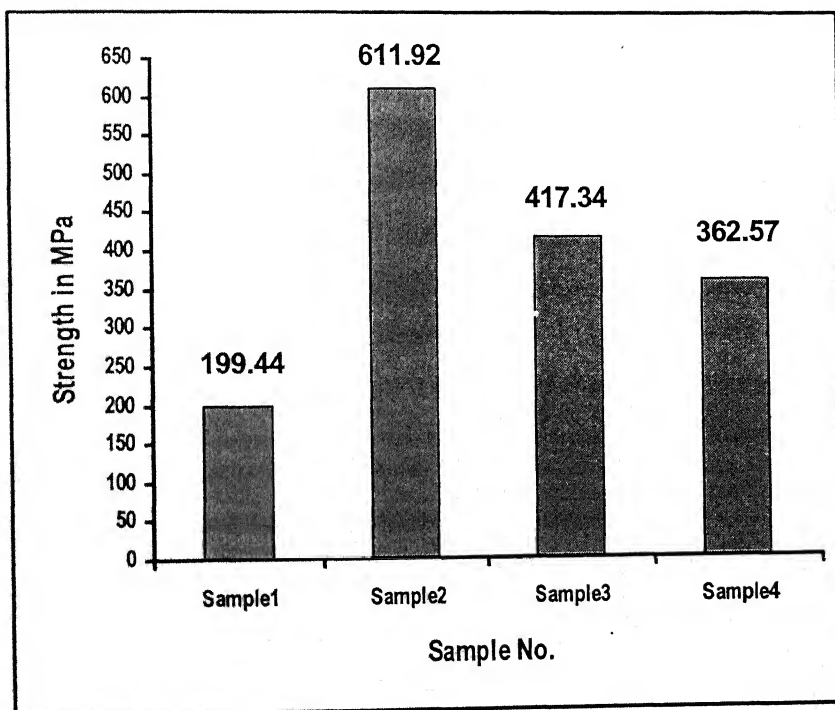


Fig.5.25: Strength values of the torch brazed stainless steel rods.

CHAPTER 6

DISCUSSIONS

Results of experiments on measurement of temperatures during cooling of the melt show that melting point of the eutectic 72 Ag – 28 Cu alloy is increased by about 50°C from around 785°C to 832°C by addition of around 5 wt. pct. titanium (Fig. 5.6). Melting point of copper is decreased from 1083°C to around 1069°C by adding 2 wt. pct. titanium (Fig. 5.7) while that of silver falls from reported value of 962°C to around 954°C (Fig. 5.8). It was not possible to analyze titanium content of the alloys but it could be estimated by the amount of titanium dissolved in the alloys after the experiments. Photomicrograph of Ag – 26.6 Cu – 5 Ti (Fig. 5.3) corresponds mainly to eutectic Ag – Cu alloy. Part of titanium may be present in solid solution in both silver and copper rich phases, while a part as intermetallics such as Cu₂Ti, CuTi and CuTi₂, as reported by Prasad.^[29] Dark spots in Ag – 26.6 Cu – 5 Ti, Cu – 1 Ti and Cu – 2 Ti in Fig. 5.3 to Fig. 5.5 may be attributed to formation of intermetallics on solidification.

It was possible to increase the bulk density of alumina pellets from around 1.9 to between 2.2 and 2.3 on firing at 1600°C for 9 hours in air. This is much less than the true density of alumina of around 3.8 to 4.0. Poor wettability of sintered alumina pellets by Ag – Cu eutectic as well as Ag – 26.6 Cu – 5 Ti alloy may be attributed to large porosity (around 41% to 45%) in the sintered alumina pellets. In one experiment (EBCC 1), good wetting could be obtained when the assembly of two sintered alumina ceramic pellets with disc of Ag – 26.6 Cu – 5 Ti between them was heated in vacuum of around 0.013 atmospheres or 10 mm of Hg at 1100°C. The stainless steel screw could not apply proper pressure at such a high temperature to keep the parts intact. Ag – 26.6 Cu – 5 Ti alloy could wet the bottom pellet but not the upper one. Experiment on wetting of sintered alumina pellet by dipping it inside Ag – 26.6 Cu – 5 Ti brazing alloy in air atmosphere (EDC 2) did not meet success. Metal type Ti-O film could not be formed at the ceramic interface which is reported^[13] to enhance wetting characteristics. This could be attributed to high porosity of the pellets and not so high degree of vacuum achieved in the experiment.

Results of experiments on dipping of stainless steel plate (EDSS 1 to EDSS 6) show that it can be wetted easily by the eutectic Ag – Cu alloy at 1050°C if the plate is precoated

with a flux layer of KCl. In absence of flux covering, wetting could be achieved only in the bath of Ag – 26.6 Cu – 5 Ti and not in 72 Ag – 28 Cu (EDSS 5). Titanium plays an important role in overcoming the problem due to presence of chromium oxide film on the surface of stainless steel substrate. Such an oxide film could be formed, while the plate, even after due cleaning, is being lowered into the bath to study wetting characteristics. Though the oxide film enhances the corrosion resistance properties of the stainless steel but it is well known to be detrimental to wetting by liquid brazing filler metal. The formation of the oxide film is retarded when the stainless steel plate is precoated with a layer of flux such as KCl. The flux becomes molten at high temperature of 1050°C and is easily replaced by the braze filler metal.

Experiments on bonding of stainless steel plates together using different braze filler metal highlighted the importance of titanium in the braze filler metal. In the present work, experiments could be carried out in vacuum of 10 mm of Hg level while the recommended range of vacuum for stainless steel brazing is 0.01 mm of Hg or less. Good bonding could be obtained when the assembly containing two stainless steel plates and disc of braze filler metal sandwiched between them was heated in vacuum of 10 mm of Hg whenever the braze filler metal contained 2 to 5 wt. pct. of titanium (EBSS 1 to EBSS 7). Thus, the problem due to slight oxidation of the stainless steel could be taken care of by the presence of titanium in the braze filler alloy. No bonding occurs when the heating of assembly is carried out in air. This is attributed to excessive oxidation of the base material i.e. stainless steel as well as that of titanium in the active braze filler metal. In dipping experiments, the problem of oxidation of the substrate is minimized even when the experiment is carried out in air (EDSS 5 and EBDSS 3).

Experiments on mechanical testing of the laboratory prepared brazing alloys and the bonded stainless steel rods in vacuum revealed the following:

- (i) Measured tensile strength of the braze filler metals lied in the range of 100 to 170 MPa. In general, the tensile strength increased with an increase in the titanium content in the filler. This may be compared with reported strength of copper metal after annealing.

- (ii) The strength of the bonded assembly lied in the range of 50 to 100 MPa. In general, strength of the bonded stainless steel rods increased with an increase in the titanium content of the braze filler metal.

Strength of the stainless steel rods after torch brazing using conventional braze filler metal and flux lied in the range of 200 to 600 MPa. This lied closer to the tensile strength of the stainless steel of around 600 to 650 MPa.

The poorer strength of the stainless steel rods bonded in vacuum as compared to torch brazing may be attributed to the following:

- (i) There is lack of proper alignment and clearance when two stainless steel rods are heated in vacuum.
- (ii) There is oxidation of the faying surface due to low degree of vacuum achieved during the experiments.

One may thus expect better results on wetting of stainless steel and ceramic pellet if the experiments are designed in the temperature range of $1000^{\circ}\text{C} - 1200^{\circ}\text{C}$ in much higher degree of vacuum of 0.01 mm of Hg or less. Higher densification of the pellets will be another factor to be looked into while carrying out such a study further.

SUMMARY AND CONCLUSIONS

1. Active brazing alloys containing 1 – 5 wt. pct. of titanium were prepared in the laboratory by forcing the duly cleaned titanium plate in silver copper melt for 6 hours or so.
2. Melting range of the brazing alloys was determined by recording the temperature – time plots, during cooling of the melt. Melting points of 72 Ag – 28 Cu eutectic and Ag – 26.6 Cu – 5 Ti, Ag – 2 Ti and Cu – 2 Ti active brazing filler alloys were found to be 785°C, 832°C, 954°C and 1069°C respectively.
3. Strength of the active braze alloys lied in the range of 100 – 170 MPa. There was an increase in the strength with an increase in the titanium content of the alloys.
4. Stainless steel rod of around 5 mm diameter could be bonded to another rod of same diameter by placing the active braze filler alloy between them and heating the assembly together to a high temperature in vacuum of 0.013 atmosphere. The strength of the bonded assembly lied in the range of 50 – 100 MPa.
5. Strength of the stainless steel rods joined together by the conventional method of torch brazing was found to be in the range of 200 to 600 MPa.
6. Porosity of the alumina pellets decreased from 52 % to around 44 % on firing at 1600°C for 9 hours. Fired pellets could be wetted by the active braze alloy. However, experiments on bonding of two such pieces together using the active brazing alloy Ag – 26.6 Cu – 5 Ti at 1100°C in vacuum of 0.013 atmosphere did not meet success.
7. Lack of bonding between two sintered alumina pellets was attributed to high porosity of the pellet, low degree of vacuum and improper clearance between the two pieces to be bonded together.
8. Wetting of stainless steel plate occurred when it was dipped in the active brazing alloy Ag – 26.6 Cu – 5 Ti. There was no wetting when it was dipped inside the silver copper eutectic alloy.
9. Stainless steel plate, precoated with KCl, could be wetted both by the silver copper eutectic alloy and the active brazing alloys Ag – 27.4 Cu – 2 Ti and Ag – 26.6 Cu – 5 Ti.

10. Good bonding occurred when two stainless steel plates were dipped together into the Ag - 26.6 Cu - 5 Ti melt.
11. Stainless steel plates could be bonded together by preplacing the active braze filler metal Ag - 26.6 Cu - 5 Ti disc in between them and heating the assembly in vacuum of around 0.013 atmospheres.

RECOMMENDATIONS FOR FURTHER WORK

Further work in this field can be recommended as below:

1. Stainless steel can be replaced by other reactive metal members like alloys of titanium or aluminium etc.
2. Instead of alumina, other ceramic members can be used for brazing stainless steel to ceramic by using active braze alloys, for example ZrO_2 , SiC , Si_3N_4 etc.
3. The active brazing filler metal may contain other reactive metal instead of titanium, such as Zr, Hf etc.
4. The interface structures of the joints made can be studied using Electron Probe Micro Analyzer.
5. The measurement of joint strength of the brazed stainless steel plates as well as ceramic pellets may be an excellent work for future study. A set up for measuring the joint strength can be devised.
6. The variation of joint strength with the thickness of the filler metals can be measured.
7. The variation of joint strength with brazing time and brazing temperature can also be noticed.
8. The variation of joint strength with the amount of vacuum created during the experiment can also be studied.
9. The effect of insertion of interlayer of soft materials can be measured.

LIST OF REFERENCES

- [1] "Brazing Handbook", American Welding Society, Fourth Edition, AWS Committee on Brazing and Soldering, 1991.
- [2] Schwartz, Mel M. "Brazing", ASM International, Metals Park, Ohio, 1987.
- [3] Cannon, R. M., Saiz, E., Tomsia, A. P. and Carter W. C. "Reactive wetting taxonomy" [Structure and properties of interface in ceramics], Mat. Res. Soc. Proc., Vol. 357, 1995, pp. 279 - 291.
- [4] "Brazing of Stainless Steels", "ASM Handbook", "Welding, Brazing and Soldering", ASM International, Vol. 6, 1993, pp. 911 - 923.
- [5] Suganuma, K., Okamoto, T., Shimada, M. and Koizumi, M. "New method for solid state bonding between ceramic and metals", Journal of American Ceramic Society, July 1983, pp. C117 - C 118.
- [6] Xien, A. P. and Si, Z. Y. "Interlayer design joining pressureless sintered Sialon ceramic and 40Cr steel brazing with $Ag_{57}Cu_{38}Ti_5$ filler metal", Journal of Materials Science, Vol. 27, 1992, pp. 1560 - 1566.
- [7] Jeffus, L. and Johnson, H.V. "Welding principle and applications", Second Edition, Delmer Publishers Inc., 1988, pp. 401 - 428.
- [8] Schwartz, Mel M. and Sikorsky Aircraft "Fundamental of Brazing", ASM Handbook, 1987, pp. 114 - 125.
- [9] Singh, J.P., B.Tech. Project Report, MME Department, IIT Kanpur, May 2002.
- [10] Badirujjaman, S., M.Tech. Thesis Report, MME Department, IIT Kanpur, December 1998.
- [11] Chakravarty, I., M. Tech. Thesis Report, MME Department, IIT Kanpur, April 2002.
- [12] Feduska, W. "High temperature brazing alloy - base metal wetting reaction", Welding Journal, Vol. 38, No. 3, March, pp. 122 - 130.
- [13] Lancaster, J. F. "Metallurgy of Welding, Soldering and Brazing", 1965, pp. 126 - 127.

- [14] Schwartz, Mel M. "Brazing: For the engineering technologist", Chapman and Hall, 1995.
- [15] Mizuhara, H. and Oyama, T. "Ceramic/Metal Seals", Reprinted from ASM Handbook, Vol. 4, Ceramic and Glass, 1993.
- [16] Humpston, G. and Jacobson, D. M. "Principles of Soldering and Brazing", ASM International, First Printing, March 1993.
- [17] Sheward, G. "High temperature brazing in controlled atmospheres (UKAEA)", Springfields Laboratories, Preton, UK, 1989, pp. 35 – 36.
- [18] Smith, R. W. "Active solder joining of metals, ceramics and composites", Welding Journal, Vol. 80, No. 10, October 2001, pp. 30 – 35.
- [19] Xien, A. P. and Z. Y. S. "Wetting of tin based active solder on sialon ceramic", Journal of Materials Science Letters, Vol. 10, No. 22, 1990, pp. 1315 – 1317.
- [20] Valentine, T. M., Nicholus, M. G. and Waite, M. J. "The wetting of alumina by copper alloyed with titanium and other elements", Journal of Materials Science, Vol. 15, No. 7 – 9, 1980, pp. 2197 – 2206.
- [21] Nicholus, M. G. "Ceramic metal interfaces", Surfaces and interfaces of ceramic material, Series E, Applied Science, Vol. 173, Kluwer Academic Publishers, London, 1989, pp. 393 – 417.
- [22] Lochman, R., Tomsia, A. P., Pask, J. A. and Johnson, S. M. "Bonding mechanism in Silicon Nitride Brazing", Journal of American Ceramic Society, Vol. 73, No. 3, 1990, pp. 552 – 558.
- [23] Mizuhara, H. and Huebel, E. "Joining of ceramic to metal with ductile filler metal", Welding Journal, Vol. 65, No. 10, 1986, pp. 43 – 51.
- [24] Murray, J. L. "Binary alloy phase diagrams", ASM International, Materials Park, Ohio, Vol. 1, 1989, pp. 970 – 972.
- [25] Samandi, M., Gudze, M. and Evans, P. "Application of ion implantation to ceramic/metal joining", Nuclear Instrument and Method in Physics Research, Section B,

Beam Interaction with Materials and Atoms, Vol. 127 – 128, May 2, 1997, pp. 669 – 672.

- [26] Xien, A. P., Si, Z. Y., Zhou, L. J., Shen, J. N. and Li, T. F. “Improvement of the oxidation resistance of Ag – Cu eutectic – 5 at.% Ti brazing alloy for metal/ceramic joints”, Materials Letters, Vol. 12, No. 1 – 2, September 1991, pp. 84 – 88.
- [27] Batra, N. K. “Advances in joining processes”, Lecture Notes, Short Term Course, May 23 – 28, 1994, MME Department, IIT Kanpur.
- [28] “Welding Handbook”, “Materials and applications, Part – 1”, Chapter 8, Eighth Edition, Vol. 3, American Welding Society, pp. 390 – 416.
- [29] Prasad, N. K., M.Tech. Thesis Report, MME Department, IIT Kanpur, May 2000.

Date **11** p[illegible]

A143516